A Synthetic Biodegradable Oriented Scaffold for Skeletal Muscle Tissue Engineering

A thesis submitted to the University of Manchester for the degree of Doctor of Philosophy in the Faculty of Engineering and Physical Sciences.

2010

Kathryn Jane Aviss

School of Materials

Table Of Contents

Final word count: 36,393

List of Figures

List of Tables

List of abbreviations

ADP – Adenosine di-phosphate

ATP – Adenosine tri-phosphate

DAPI – 4’6-diamidino-2-phenylindole

DCF – Dicholorofluorescein

DCF-DA - Dicholorofluorescein diacetate

DMEM – Dulbecco’s Modified Eagles Medium

DSC – Differential Scanning Calorimetry

ECM – Extracellular Matrix

ELISA – Enzyme-Linked Immunosorbent Assay

FAC – Focal Adhesion Complex

FAK – Focal Adhesion Kinase

FBS – Foetal Bovine Serum

FITC – Fluorescein Isothiocyanate

FTIR – Fourier Transfer Infrared spectroscopy

GAPDH – Glyceradehyde 3-phosphate Dehydrogenase

HFIP – Hexafluoroisopropanol

HGF – Hepatocyte Growth Factor

ICC – Immunocyto Chemistry

MMP – Matrix Metalloproteinase

MyHC – Myosin Heavy Chain

PCL – Polycaprolactone

PCR – Polymerase Chain Reaction

PDMS – Polydimethylsiloxane

PGA – Poly-glycolic acid

PGS – Poly(glycerol-sebacate)

PLA – Poly-lactic acid

PLGA – Poly(lactide-*co*-glycolide)

SEM – Scanning Electron Microscopy

TCP – Tissue Culture Plastic

TE – Tissue Engineering

TgA – Thermogravimetric Analysis

Abstract

The aim of this project was to create a novel biodegradable, synthetic scaffold that will provide the correct topographical cues for myoblast alignment and efficient differentiation into myotubes.

Skeletal muscle repair after major surgery or serious burns is often overlooked leading to poor healing and consequent loss of power in movements of affected limbs. In order to overcome this problem a tissue engineered construct could be utilised as a grafting patch to encourage further regeneration and enhance possible power to the limb. Using a biodegradable polymer can provide structural support until the tissue is established, and will be excreted by the body's natural processes as it degrades. A synthetic polymer is desirable as it can reduce the risk of immunogenic responses thus reduce risk of graft rejection. For successful *in vitro* growth of skeletal muscle, the cells must be encouraged to arrange themselves into parallel arrays in order for efficient fusion and consequent contraction. By incorporating the correct topographical cues into the scaffold to promote contact guidance for cellular alignment this can be achieved. Electrospinning is a reliable technique which yields highly reproducible aligned fibres from the micro- to the nanoscale.

This project focuses upon creating and characterising the electrospun scaffold, checking biocompatibility with myoblasts by monitoring the topography, residual solvent within the scaffold, the mechanical properties of the scaffold, and a brief investigation into the degradation profile of the electrospun fibres. The immunogenicity of the scaffold was investigated by monitoring cytokine release from macrophages. Myoblast morphology was monitored, as was the efficiency of the cells to differentiate and their potential to become contractile myofibres. Cellular adhesion to the scaffold was also looked into by measuring the expression of integrins during early and late adhesion and on substrates with different topographies.

It was found that the electrospun scaffold did not contain a significant amount of residual solvent, and macrophages were not activated any more than on tissue culture plastic. Myoblasts responded to the topography of the aligned fibres by aligning along the length of the fibres, showing elongation and bi-axial cytoskeletal arrangement after just 30 minutes culture on the aligned fibres. This elongation prompted fusion and differentiation of the myoblasts to occur faster than cells which were not exposed to the aligned topography, and this global alignment was maintained in long term culture.

COPYRIGHT STATEMENT and DECLARATION

i. The author of this thesis (including any appendices and/or schedules to this thesis) owns any copyright in it (the "Copyright") and s/he has given The University of Manchester the right to use such Copyright for any administrative, promotional, educational and/or teaching purposes.

ii. Copies of this thesis, either in full or in extracts, may be made **only** in accordance with the regulations of the John Rylands University Library of Manchester. Details of these regulations may be obtained from the Librarian. This page must form part of any such copies made.

iii. The ownership of any patents, designs, trade marks and any and all other intellectual property rights except for the Copyright (the "Intellectual Property Rights") and any reproductions of copyright works, for example graphs and tables ("Reproductions"), which may be described in this thesis, may not be owned by the author and may be owned by third parties. Such Intellectual Property Rights and Reproductions cannot and must not be made available for use without the prior written permission of the owner(s) of the relevant Intellectual Property Rights and/or Reproductions.

iv. Further information on the conditions under which disclosure, publication and exploitation of this thesis, the Copyright and any Intellectual Property Rights and/or Reproductions described in it may take place is available from the Head of School of Materials (or the Vice-President) and the Dean of the Faculty of Life Sciences, for Faculty of Life Sciences' candidates.

No portion of the work referred to in the thesis has been submitted in support of an application for another degree or qualification of this or any other university or other institute of learning.

Acknowledgements

What a journey! I would like to thank all my friends on both sides of the Pennines for all their help and support when things got stressful! Special thanks to Simon P., Adam and Alastair for fun times. Also special thanks to Jim and Kate, without whom I'm not sure what's left of my sanity would've survived, and thanks for all your help and advice you've always given me, scientific and otherwise – long may it continue!

I am also very grateful to Julie Gough and Cathy Merry for all their support and helping me out of situations where I thought I may be stuck!

Of course I thank my parents for starting my academic career at Huddersfield, continuing it at Leeds until I finally earned some of my own money! And thanks to my wonderful fiancé Simon W. You are my rock and this thesis wouldn't have happened without you. I now look forward to actually have a life to share with you now this is done!

Kathryn J. Aviss

Chapter 1: Introduction

Introducing skeletal muscle and the areas of biomaterials and tissue engineering

The University of Manchester

1. Introduction

1.1 Tissue engineering

The area of tissue engineering (TE) is a rapidly emerging research field with great promise for clinical applications. Being able to regenerate tissues outside the body could provide solutions to a plethora of diseases affecting many tissues throughout the body. To date work has been done to progress creation of engineered skin (Kumbar et al., 2008), blood vessels (Xu et al., 2004), cardiac tissue (Engelmyr et al., 2008), bladder (Tian et al., 2010), nerve (Sun and Downes, 2009), and ligament tissue (Cooper et al., 2007) to name a few. The application of biomaterials in the research into TE is important with the ability to produce a suitable scaffold with characteristics tailored to the specific tissue. Materials can be biodegradable polymers e.g. PCL (polycaprolactone), PLA (poly-lactic acid), PGA (poly-glycolic acid), PLGA (poly-lactide-co-glycolide); also natural materials can be processed to form polymeric scaffolds e.g. collagen. Degradable polymers, such as these, are optimal for soft tissue engineering.

The ability to mimic the natural environment of a tissue is essential in biomaterials for TE. Polymer processing techniques dictate the architectural and mechanical properties of the scaffold. Electrospinning is a flexible polymer processing technique that can be used to create fibrous meshes with defined and controlled characteristics (Aviss et al., 2010; Bian and Bursac, 2009; Blackwood et al., 2008; Choi et al., 2008; Huang et al., 2006), depending on the choice of polymer and the parameters employed for electrospinning.

Where prolonged high mechanical strength is required for the application, e.g. bone replacements (Niinomi, 2008) or for medical devices e.g. pacemakers, a non-degradable,

non-corrosive material is required. Titanium is the main metallic biomaterial used in hip and knee replacements, and dental implants, and is the material used for medical devices due to its biocompatibility and reliable mechanical properties (Niinomi, 2008).

Skeletal muscle is responsible for movement of limbs, and is also involved in respiration. Any serious injury to skeletal muscle, e.g. large tumour excision from skeletal muscle area or 4^{th} degree burns, is currently treated by grafting muscle from another part of the body to the affected area (autografting) (Vindigni et al., 2004), taking healthy tissue from a donor patient (allografting) (Vargas et al., 2009), or using tissue harvested from an animal e.g. pig (xenografting) (Rotherburger et al., 2002). Autografting and allografting can be unsatisfactory because these methods would produce two areas of damaged muscle: the area already damaged, and the area from which the graft material was taken, neither of which will return to its pre-injury strength. Xenografting would seem like an attractive alternative, but through researching this it has been found that xenografts of pig heart valves do not maintain mechanical structure (Rotherburger et al., 2002). Also with any three of these types of graft the tissue used can be troublesome for younger patients as none of them will grow with the patient so repeat surgeries will be required to maintain functionality as the patient grows (Rotherburger et al., 2002).

An ideal solution to this problem would be to use an grafting material seeded with cells e.g. tissue engineered skeletal muscle or heart valve, so as not to damage any other muscles within the patient. Using a cellularized scaffold or a scaffold which contains specific biological cues e.g. glycosaminoglycans or proteins, to encourage natural cell growth and repair whilst also minimising scar tissue formation so functionality is maintained. There

are of course serious problems concerning this; the main one being the immunological effects of artificial muscle in the recipient, but another would be the time frame in which a surgeon has to graft any type of muscle onto the damaged area. An artificial muscle, made via TE, could provide grafting material for some skeletal muscle traumas.

1.2 Structure and function of skeletal muscle

For movement to take place, bones must be moved. Skeletal muscle initiates this movement via contraction, which then transfers energy to the bone mover via tendons. Tendons are made of compact bundles of collagen and join skeletal muscles to bones. Skeletal muscle is a highly hierarchical tissue from the microfilaments responsible for contraction, up to the myofibers and fibrils that build the bulk of skeletal muscle tissue (see figure 1). There is very little ECM within the tissue as this leaves more space for functional tissue, ECM is mainly found as the sarcoplasm between myofibres which provide anchorage and support for myofibres and satellite cells.

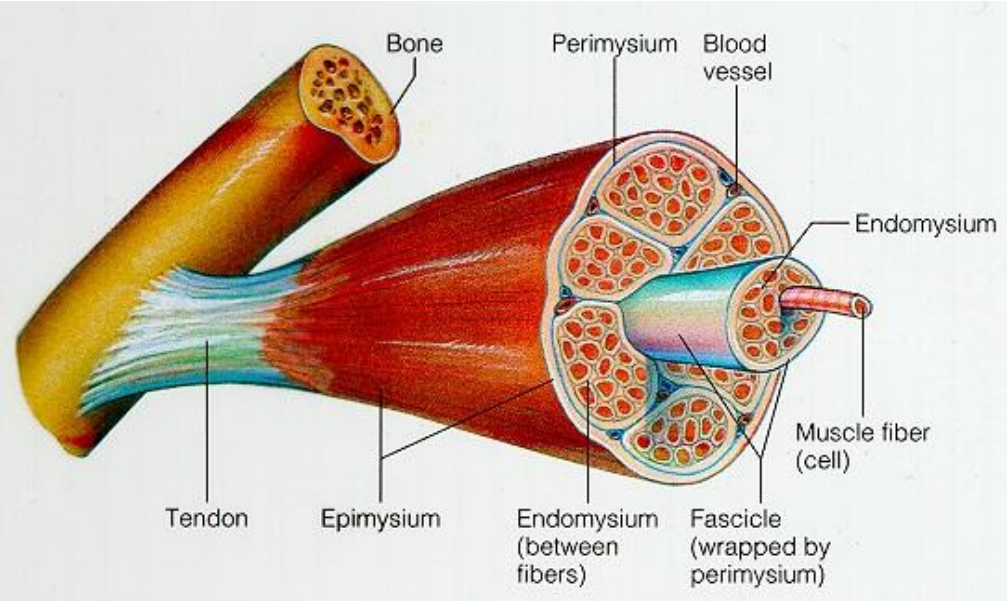

Figure 1: *Hierarchy of skeletal muscle tissue showing progression from muscle body surrounded by the epimysium, to the bundles of muscle fibres encapsulated by the endomysium and collected into fascicles by the perimysium. Taken from figure 9.1 (a) in Marieb Human Anatomy and Physiology 5th Edition (Marieb, 2001).*

The precise hierarchy allows for efficient contraction as the bundles of fibres (myofibrils) are arranged in parallel so force can be produced and transmitted unilaterally. The development of this precise hierarchy can be observed *in vitro* using myoblastic cell lines e.g. C2C12 murine myoblasts. Myoblast cells (or satellite cells – see section 1.4) are myogenic stem cells which, at the correct trigger, can multiply, align themselves and fuse to form mulitnucleated myotubes and ultimately myofibrils (Wakelam, 1985). *In vitro* myoblast cells are stimulated to fuse and form myotubes by reducing the mitogen content in the growth medium. Fusion is a multifaceted and complex event with the main events being cell alignment and the myoblasts forming tight, irreversible junctions with neighbouring myoblasts, which are similar to gap junctions (Wakelam, 1985). The reaction of satellite cells to injury is very similar to that of myoblast differentiation, with regards to

transcription factor up-regulation and downstream effects of these changes. Several transcription factors that are part of the MRF (myogenic regulatory factor family) stand out from the plethora of molecular mechanisms involved in these processes: MyoD, and myf5 which are involved in satellite cell/myoblast activation and myogenin and myf4 which are more involved with the terminal differentiation of myoblast cells (Charge and Rudnicki, 2004). These transcription factors are often used as markers for proliferative or differentiated myoblasts. Modulating or maintaining the levels of these transcription factors relies heavily on cell-cell communication and also factors available in the ECM environment. Differentiation is negatively regulated by a host of mitogens and growth factors. These include: hepatocyte growth factor (HGF), fibroblast growth factor (FGF), transforming growth factor-β (TGF-β) and various cytokines, to name a few have profound effects on the expression of transcription factors. HGF was shown to be involved in maintenance of the proliferative state of C2C12 myoblasts and to encourage satellite cells to enter the cell cycle. This was shown by it's prescence in proliferative myoblasts and forced expression of the receptor for HGF (c-met) inhibited differentiation. Also, shown by the same group, when injected in to injured muscle, HGF blocked regeneration but increased the myoblast population by 3-fold (Tatsumi et al., 1998). FGF has been shown to interact with MyoD transcription factor. Yablonka-Reuveni and Rivera have worked with both primary cell lines and cultured immortal cell lines from the C2 lineage. They found that with primary cell lines FGF has no difference on MyoD expression, but the cells maintain proliferation (Yablonka-Reuveni and Rivera, 1997). In immortalised cell lines FGF only effects cells not expressing MyoD to maintain the proliferative state (Graves and Yablonka-Reuveni, 2000). These growth factors are found in serum that cells are cultured in. In order to induce differentiation of myoblast cells, serum (often foetal bovine serum)

content is either reduced to lower the concentration of these growth factors circulating, or an adult serum e.g. horse serum can be used. An adult serum will have a lower concentration of these growth factors as the adult will not need to grow de-novo tissue like a foetus.

1.3 Physiology of skeletal muscle

Two main proteins are responsible for contraction within skeletal muscle. These two proteins create a striated tissue in appearance: the thin filament actin creating light bands (I bands), and the thick filament myosin creating dark bands (A bands). These bands were initially found using high angle x-ray diffraction by W. T. Astbury at The University of Leeds (Astbury, 1947). The I bands had a low refractive index, so were termed light bands, whereas the A bands had a higher refractive index so were termed dark bands (Astbury, 1947). These filaments, along with other contractile elements form the contractile unit known as the sarcomere (see figure 2).

A sarcomere is measured from I band to I band. There are many proteins within the sarcomere to complement the contractile elements and some will respond to calcium ion influx to control contraction-excitation coupling. In the cartoon shown below, there are three more of the proteins present in a sarcomere labelled. These are titin, tropomyosin and the troponin complex both situated along the length of the actin filament. Titin is an elastic protein found in the z discs which aids in maintaining the sarcomeric structure during contraction and relaxation cycles. The troponin complex lies at intervals along the length of tropomyosin, their functions are intertwined as the troponin complex hides the myosin

binding sites on tropomyosin until excitation-contraction coupling is initiated, then it moves away from these sites to allow myosin binding (see figure 3).

Hugh E. Huxley was a forerunner in the research into muscle contraction, and was one of the first people to realise the sliding filament theory which is taken for granted now. He combined x-ray diffraction and electron microscopy in rigor and relaxed frog muscles to find out more about how the actin and myosin filaments interact to produce shortening of the sarcomere. (Huxley, 1974) Huxley was the first to suggest that the A band of the sarcomere remained a constant length, and that it is the I band which shortens during contraction, and that the filaments increasingly overlap as contraction occurs (Huxley and Neidergerke, 1958). Prior to this it was thought that the A band (myosin filaments) shortened (Huxley, 1974).

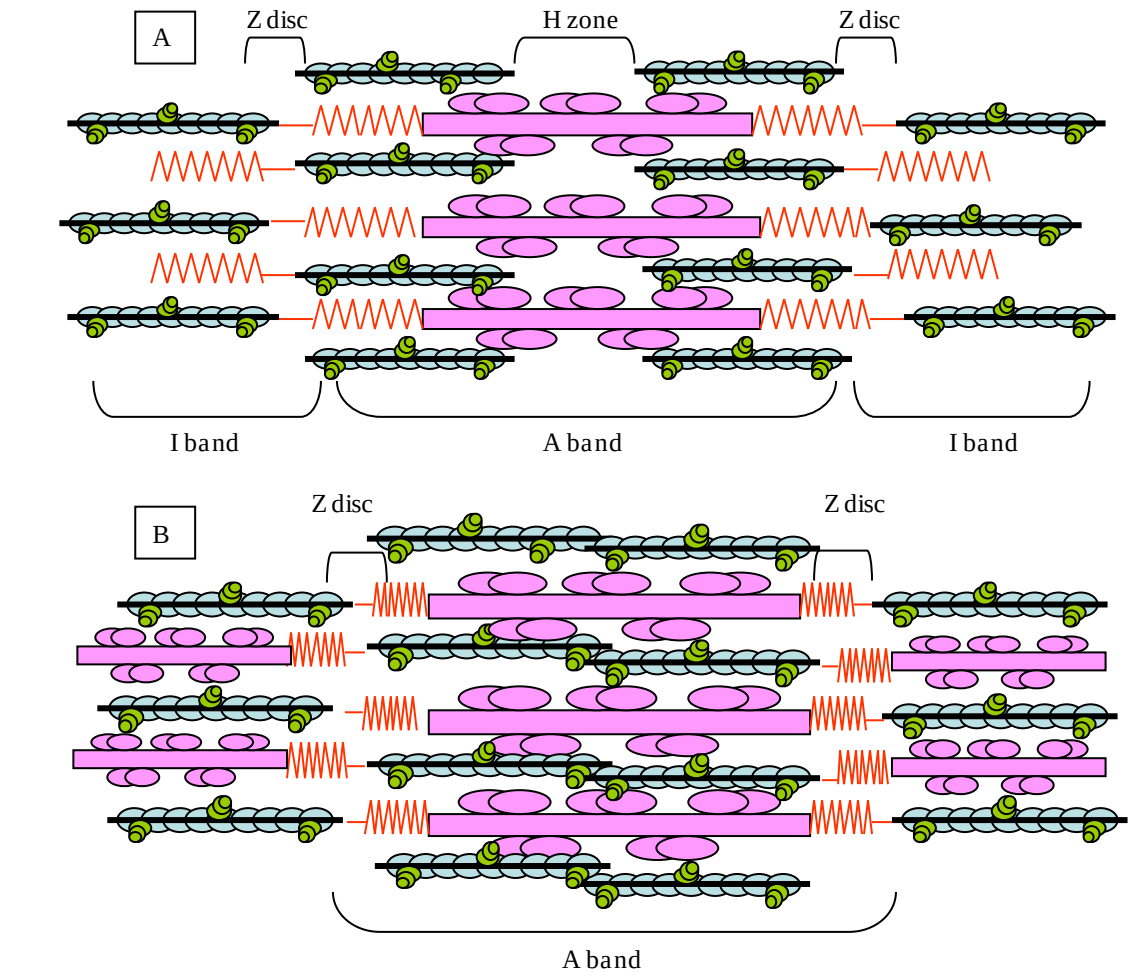

Figure 2: *Diagrammatic representation of a sarcomere. A depicts a relaxed sarcomere, B depicts a contracted sarcomere.*

The intricate control of the sliding filament theory of skeletal muscle contraction is done by carefully controlled release of calcium ions in response to a change in the membrane potential generated from a neuromuscular synapse. Release of calcium ions into the

sarcolemma occurs through a process known as excitation-contraction coupling. Calcium ions released into the sarcolemma from a neuromuscular excitation bind to sites upon the troponin complex. As this occurs, more free binding sites on the troponin complex become available for more calcium ions to bind, which then moves tropomyosin away from actin's active sites for myosin head cross linking with actin.

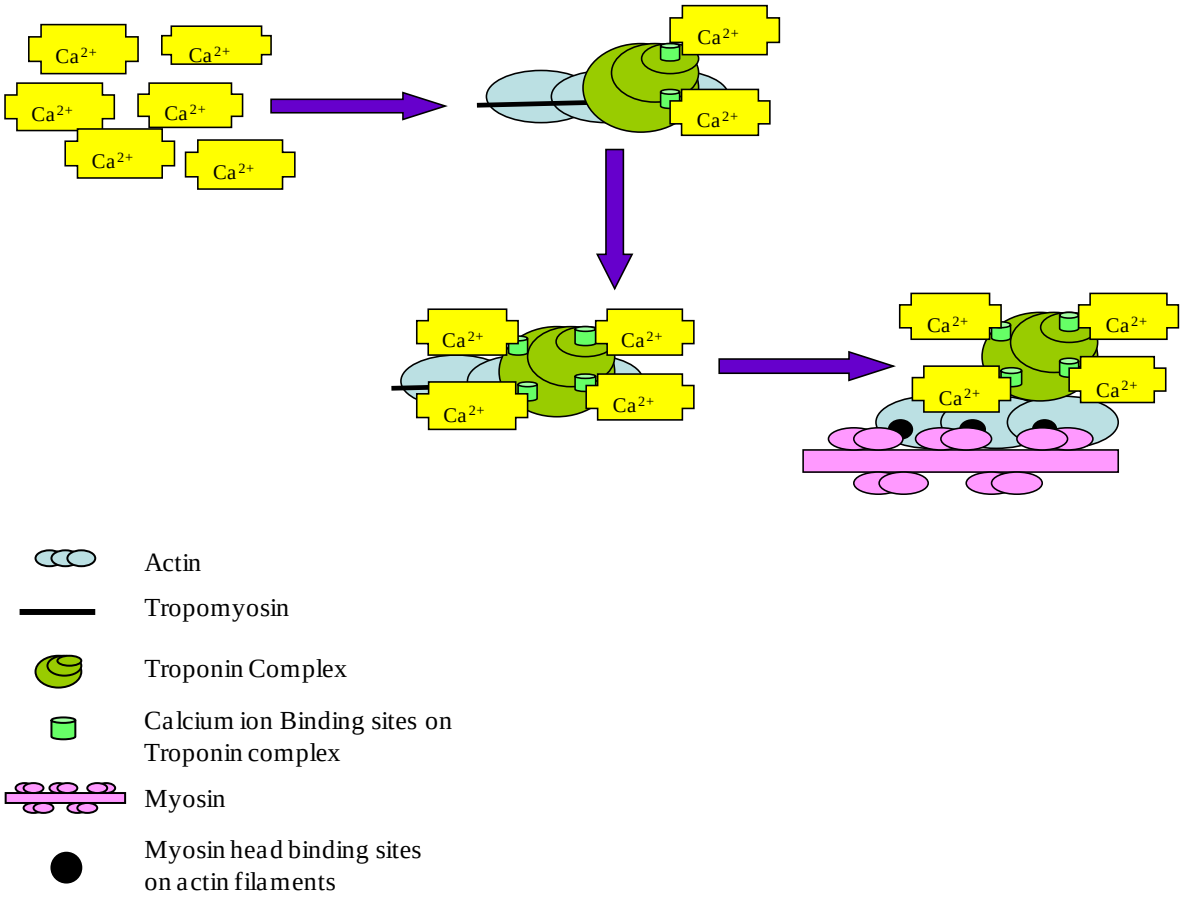

Figure 3: *Diagrammatic representation of the role of calcium ions in revealing myosin head binding sites on actin filaments during contraction.*

ADP (adenosine di-phosphate) and an inorganic phosphate (P_i) bound to myosin in its high energy state is used to power the sliding of the filaments together, producing a contraction of the sarcomere, and releasing the ADP and P_i. The cross bridge can only be

released for a new contraction in the presence of ATP (adenosine tri-phosphate). ATP is used to take the myosin head back to its high energy state with ADP and P_i, and the contraction cycle can begin again with the introduction of a new neuromuscular stimulation (Marieb, 2001).

1.4 Satellite cells

Satellite cells procure their nomenclature from their positioning on the outer surface of the myofibre within the sarcolemmal basement membrane (Bischoff, 1975; Mauro, 1961; Nag and Foster, 1981). This positioning is illustrated in figure 4.

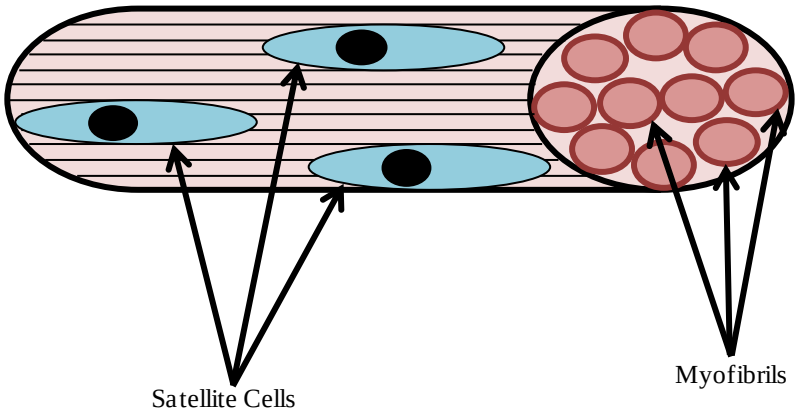

Figure 4: *Diagram of a myofibre to illustrate the positioning of satellite cells around the perimeter of the myofibre containing the contractile myofibrils.*

Currently the hypothesis for the origins of satellite cells in mammals and birds is that they are derived from somites, which differentiate into the dermomyotome and sclerotome then mesodermal cells specify as skeletal muscle precursors in the myotome (Zammit et al.,

2006); although more recent research suggests some head muscles are derived from the prechordal mesoderm as opposed to the somites.

How a satellite cell differentiates into a mature myofibre has distinct stages that can be monitored by tracking specific markers that are expressed by the cells. Some of these markers overlap expression as the cells progress through differentiation; the transcription factor Pax7 is expressed by both quiescent and activated satellite cells and in proliferative myoblasts, fading as the myoblasts commit to differentiation. MyoD, another transcription factor which is often used as a marker for initiation of differentiation, is expressed in an activated satellite cell, right through until fusion into myotubes occurs. Myogenin is a marker showing commitment to differentiation and is expressed in commited myoblasts until full maturation into myofibres (Zammit et al., 2006).

A satellite cell becomes activated in response to damage; satellite cells that are activated include those local to the trauma, and those along the length of the myofibre, although satellite cells from adjacent muscles is not seen (Schultz et al., 1985). As early as 1986, Bischoff identified a mitogen present in crushed muscle extract which had an activation effect on quiescent satellite cells, but had no effect on the proliferation of muscle fibroblasts (Bischoff, 1986). He initially saw a proliferative effect in satellite cells in single fibres with many dead fibres present, compared to those with more healthy fibres. By incorporating crushed muscle extract into the basal media, Bischoff found myoblasts to proliferate more than fibroblasts (Bischoff, 1986).

It is now known that hepatocyte growth factor (HGF) can bind to the c-met receptor on satellite cells to induce activation of them (Tatsumi and Allen, 2004; Tatsumi et al., 1998). Tatsumi et al 2004, showed that HGF is present in the active form in satellite cells and that this triggers a cascade towards proliferation.

Satellite cells are responsible for post natal muscle growth and regeneration of skeletal muscle (Jejurikar et al., 2006), as they are able to fuse to damaged myofibrils and initiate regrowth. These specialised cells may be of limited supply, although this point is highly controversial; whether they expire through apoptosis (Jejurikar et al., 2006), or whether they are not able to respond to trauma as rapidly as host ages (Conboy et al., 2003), the result is a reduction in the regenerative capacity of skeletal muscle.

When muscle is damaged and the satellite cell population is low, more collagenous scar tissue can form and the muscle may not return to its former contractility. Jejurikar et al (2006) suggest that skeletal muscle satellite cell population may be more inclined to apoptosis as the age of the host increases (Jejurikar et al., 2006). If this is the case, older animals may be at an increased risk of irreversible or poor regeneration of muscle post-trauma.

Apoptosis is a check-point controlled series of events leading to the programmed destruction, or death, of a cell. It is a natural occurrence as it is involved in the natural turnover of cells throughout the body. Each event in apoptosis has a marker that can be followed to monitor the progression of apoptosis; Jejurikar et al (2006) used these check point proteins along with destruction proteins to investigate the susceptibility of satellite cells to apoptosis (Jejurikar et al., 2006). Conboy et al (2003) looked into how age changes the responsiveness of satellite cells to trauma. They investigated number of satellite cells present in young and old muscle and found no significant difference in CD34 and M-cadherin positive cells (found by FACS (fluorescent analysis cell sorting)) in young and old muscle. From this they concluded that it cannot be the lack of satellite cells present, but how they respond to injury. To investigate this further they looked at Notch-1 signalling, which is necessary for cell proliferation and differentiation. They found that a reversible

lack of Notch-1 signalling in the older satellite cells could be responsible for the slower responding time in older cells (Conboy et al., 2003). Satellite cell population in the artificial muscle can be investigated in tissue engineered muscle as it is imperative for the artificial muscle to behave in the same way as natural muscle with regards satellite cell population. If the artificial muscle has an unstable satellite cell population, repair of this muscle will be impaired. Genetic manipulation of the myoblasts may enable us to enhance the satellite cell population therefore enhancing the artificial muscle's capacity to heal itself.

1.5 Natural skeletal muscle repair

Skeletal muscle heals via fibrosis repair rather than regeneration like other tissues e.g. skin, cardiac muscle and lungs (Gurtner et al., 2008). This repair mechanism is not totally efficient as the collagenous fibrotic scar tissue which forms, especially in the elderly (Jejurikar et al., 2006), does not have the same mechanical properties as skeletal muscle; which can lead to swift re-injury (Chan et al., 2003). As discussed, satellite cells are responsible for naturally healing damaged skeletal muscle. Muscle tissue itself is unable to regenerate; it has a population of specialised cells present in the sarcolemma called satellite cells.

Repair via satellite cells leads to the by-product of scar tissue in the form of collagen III. This scar tissue is essential during the healing and regenerating process as it provides a support mechanism for the novel cells to grow upon, but it remains as scar tissue, compromising the integrity of the regenerated skeletal muscle. Hany Bedair et al (2007) investigated matrix metalloproteinase one (MMP-1) that is involved in the destruction of collagen III, which is the main collagen in scar tissue produced during skeletal muscle

repair and regeneration. MMPs are normally involved in the maintenance of the ECM (Alberts et al., 2002), but can also be used, by satellite cells, to degrade the basement membrane in order to migrate to sites of injury by releasing MMP-2 or 9, which are gelatinases (Bedair et al., 2007). Because they are specific, each MMP carries out a specific job. MMPs 1, 8, 13, and 18 are specific to cleave collagen types I, II, and III; MMP-1 is specific to collagens I, and III. Bedair et al chose MMP-1 because of its specificity to these collagens and they hypothesised that it would aid in removing the collagen III that is put down as scar tissue after the regenerative process. In order to carry out this investigation, Bedair et al made lacerations in the gastrocnemius muscles of immunodeficient mice and injected myoblasts (C2C12) transduced with the reporter gene LacZ, and exogenous MMP-1 at the site of injury in one leg. The other leg was used as a control injected with C2C12 cells with the LacZ reporter and just PBS with no MMP-1. They found that the mice exposed to MMP-1 had much less fibrotic tissue compared to the control group, indicating that MMP-1 presence can remove the scar tissue that may compromise skeletal muscle integrity (Bedair et al., 2007).

Another group in the same laboratory as Bedair et al also investigated MMP-1 in skeletal muscle regeneration. Based on the previous publication by Bedair et al in 2007, Wang et al (2009) demonstrated that MMP-1 also enhances myoblast (C2C12) migration after disrupting the monolayer of cells with a sterile pipette tip. The found that cells on surfaces coated with fibronectin or type-1 collagen, the cells responded better to the MMP-1 treatment with regards migration to the wounded area. Wang et al also investigated the effect of MMP-1 treatment on myoblast differentiation, they found that MMP-1 treatment accelerated myogenin, MRF4, and MyoD within 3 hours of treatment induction (W. Wang, 2009). These two groups have shown that MMP-1 introduction to damaged skeletal muscle

or myoblast cells has a positive effect by either reducing scar tissue, or by inducing differentiation of migrated myoblasts into myotubes and accelerating the healing process of a monolayer of cells.

By introducing MMP-1 to the tissue engineered muscle, as per Bedair et al and Wang et al's research, it may provide a mechanism to improve the regenerative capacity of the artificial muscle, or may aid in clinical applications by alleviating scar tissue formation, and encouraging native cellular migration and differentiation to the site of grafting.

1.6 Cellular Adhesion

There are different methods of cellular adhesion depending on whether cells are forming cell-cell contacts, or cell-matrix contacts. In this project the focus is on cell-matrix adhesion in order to create an artificial matrix for myoblast adhesion for muscle repair.

The ECM provides structural support for the cells, providing the relevant mechanical cues for the specific tissue/cell type and functions as a growth factor and cytokine reservoir in order to elicit specific responses to cells relevant to any external stimulation e.g. hypoxia, trauma etc. Collagen fibrils in the ECM provide structural integrity and mechanical strength to the cellular environment. Various types of collagens have an array of biochemical functions, as they have active domains along their length that can interact with, and store, growth factors such as transforming growth factor-β (TGF-β) (Schiffino and Partridge, 2008).

The ECM is rich in glycoproteins such as laminin, fibronectin, vitronectin, and tenascins. Most of these glycoproteins contain a cell recognition amino acid sequence: RGD (Arginine – Glycine – Aspartate).

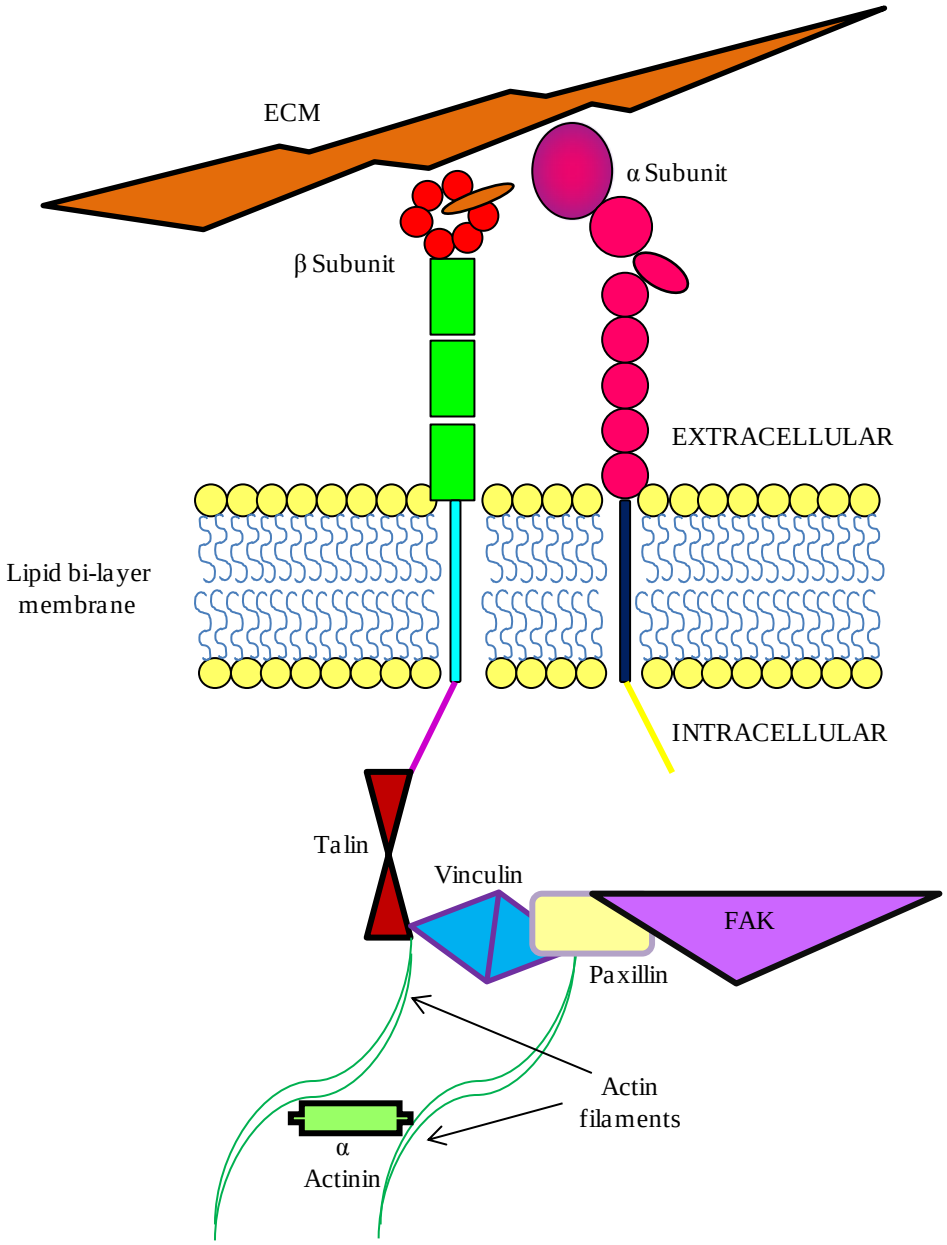

Figure 5: *Diagrammatic representation of a focal adhesion using an integrin to interact with the ECM on the outside of the cell and four of the many proteins involved in anchoring the cell at the adhesion point as well as influencing the actin cytoskeleton.*

Integrins are transmembrane glycoproteins which interact directly with the ECM components to provide outside-in signalling to cells. Integrins are responsible for the majority of cell-matrix adhesions (see figure 5). Integrins belong to a large family with

various subgroups depending on subunit constitution. Each amalgamation of subunits yields different binding properties which can be specific to cell types (Hynes, 1987) or initialise different intracellular cascades (Hynes, 1992; Hynes, 2002). Once an integrin is bound to its substrate focal adhesion kinase is phosphorylated. This culminates in the creation of a focal adhesion complex (FAC) which comprises of a multitude of proteins involved in adhesion of cells to their substrate (ECM). Common components of the FAC include phosphorylated focal adhesion kinase (pFAK), vinculin, and talin. Using monoclonal antibodies to target both the integrin, either of its subunits or the matrix ligand, it has been possible to determine which ligand is matched with which integrin. The majority of integrins bind fibronectin; laminin and collagen are also widely recognised by a variety of integrins. Several integrins are involved in cell-cell contacts via VCAMs (vascular cell adhesion molecules), ADAMs (a disintegrin and metalloprotease), or ICAMs (intercellular cell adhesion molecules).

Integrin clustering is an important event to progress focal adhesion evolution from a focal contact. Ren et al (2010) investigated substrate stiffness and its effect on myoblast adhesion and integrin expression. They found that integrin clustering occurred on soft and stiff surfaces but only on stiffer surfaces did the integrin clustering from the focal contact evolve into a focal adhesion (Ren et al., 2010).

Skeletal muscle cells use FACs as a means to adhere to a substrate. As myoblastic cells differentiate into myofibres however, the FACs appear to congregate along the length of the fibre anchoring the fibre under the Z disc striations (Danowski et al., 1992; Pardo et al., 1983a; Pardo et al., 1983b; Senetar et al., 2007). These organised FACs are termed costameres from the Latin costa, meaning rib, and meros, meaning part (Pardo et al., 1983a) due to their rib-like appearance over the cortex of the muscle fibres. Pardo et al

(1983a,b) used purified anti-vinculin antibodies to immunostain contracted and stretched whole muscle segments. They found that vinculin staining localised to distinct areas over the surface of the sarcolemma; and that this staining was absent inside the myofibres. From this they concluded that vinculin is involved in anchoring the myofibre to the sarcolemma via the I bands, specifically the Z discs (Pardo et al., 1983a; Pardo et al., 1983b).

1.7 Biomaterial Selection

The relevant biomaterial for skeletal muscle tissue engineering needs to be able to provide an elastomeric substrate for myofibre contractions. Along with this necessity, the scaffold will provide the template for alignment of the myoblasts. An elongated morphology of fibroblast cells (Bashur et al., 2006), and also myoblast cells (Choi et al., 2008) has been shown to occur when cells are seeded on oriented electrospun scaffolds.

Michelle Peckham researched the importance of aligned actin stress fibres in myoblasts for efficient myotube fusion leading to correct sarcomeric arrangement (Peckham, 2008). She found that myoblasts which reorganised their actin cytoskeleton as they started to differentiate were more successful in fusing into myotubes (Peckham, 2008). There are a number of techniques that can be performed to create the alignment template: electrospinning of aligned fibres via water tension (Smit et al., 2005), using a rotating mandrel as a collector plate (Theron et al., 2001), uniaxial stretching (Huang et al., 2006); or micropatterning (Huang et al., 2006) of an electrospun polymer mat.

Electrospinning has many advantages such as the flexibility in what characteristics the resulting scaffold will have. By changing the parameters, the scaffold can have larger or smaller diameter fibres and therefore larger or smaller pores, variation of fibre orientation from random to aligned. All electrospun scaffolds have an inherent porosity as they are

meshes, changing parameters can allow for creation of pores large enough for cellular infiltration, or enough for nutrient flow but not for cellular infiltration.

1.8 Material for Skeletal Muscle

As mentioned above, it is essential that the scaffold for the tissue engineering of skeletal muscle has the capability to stretch and be stretched by the contractions of myoblasts differentiating into myofibres. Yen-Chih Huang et al (2004) used a similar method to Vandenburgh et al (1988), who were the pioneers of *in vitro* skeletal muscle modelling; by using a gel as the substrate for skeletal muscle tissue engineering (Vandenberg et al., 1988). Huang et al (2004) used a fibrin gel as the muscle cells within the gel will degrade the fibrin in three to four weeks as they make and maintain their own ECM (Huang et al., 2005). When the 3D engineered fibrin gel constructs were measured for force transduction, the specific force measured was around 40 kN/m^2; which is similar to the soleus (44 kN/m^2) muscle in 1-day-old Wistar rats (Huang et al., 2005). Specific force represents how much intrinsic force a muscle can produce in relation to its area (Reeves et al., 2004). Fibrin gels are a useful tool in tissue engineering as they are easy to make and are both biodegradable in a short amount of time, and biocompatible. The only drawback of using fibrin gels as a scaffold for skeletal muscle tissue engineering is that they convey no template for alignment.

Lam et al (2009) (from the same group as Huang et al 2005) utilised a PDMS (polydimethylsiloxane) aligned scaffold coated with 2 µg/ml laminin to encourage initial myoblast attachment and alignment. When 80-90% of the myoblasts had differentiated into myotubes, a fibrin gel was applied over the PDMS scaffold. The fibrin gel was used as a 3D scaffold for myotubes to interact with and migrate through while making their own

ECM. The cells in the gel formed a cylindrical construct which could be anchored at either end via artificial silk tendons pinned down using pins. This construct was then tested for contractility using a method developed by Dennis and Kosnik (2000). They found that myotubes that started as myoblasts seeded on aligned PDMS scaffolds prior to fibrin gel introduction produced greater twitch, tetanus, and specific forces compared to those on non-aligned PDMS scaffolds (Lam et al., 2009). This group acknowledged that the constructs, especially the aligned constructs contained more gel, which would not contribute to force transduction, so modified the specific force calculation to account for this.

The idea of using the synthetic polymer as a temporary scaffold for myoblast attachment and arrangement then using a fibrin gel to encourage 3D cell expansion could be utilised in this project. The electrospun scaffold would perform as the template scaffold for the initial stage of cellular attachment and alignment then the fibrin gel could be encorporated to encourage 3D myotube expansion. The electrospun scaffold need not be removed as it will also degrade. The only drawback to this would be the extra material present i.e. both the fibrin gel and the electrospun PLGA would decrease contractility until both had fully degraded. Inclusion of fibrin gel may introduce the issue of immunogenicity with regards clinical applications, but for proof of concept and further *in vitro* studies it could be a very valuable technique.

A study by Engler et al (2004) showed that the flexibility of the scaffold has an impact on how myoblasts differentiate. They report that myoblast cells differentiated into myotubes more frequently, and resembled natural muscle much more on more elastic scaffolds, e.g. they compared glass with different types of collagen coated poly-acrylamide gels or collagen gels, with similar stiffness to natural muscle (around 12 kPa), and found that

myoblasts differentiate preferentially on the softer, more elastic scaffolds (Engler et al., 2004). A study by Ren et al (2008) also investigated the influence of scaffold stiffness on myoblast differentiation (Ren et al., 2008). This study used polyelectrolyte multilayer films made from poly(l-lysine)/hyaluronan with varying crosslinks to modify the stiffness of the films. The Young's modulus of these films ranged from a more elastic 3 kPa for native, non crosslinked films, to 100 kPa for low crosslinking, and up to 400 kPa for highly crosslinked films. They found that C2C12 myoblasts detached earlier on the soft gels tested here, perhaps because they found the cells formed fewer focal adhesions on the flexible softer surfaces. On the stiffer substrates, myoblasts differentiated into longer multinucleated myotubes, with more striations (Ren et al., 2008).

Another study, by Levy-Mishali et al (2009) looked at PLGA foams with varying LA:GA ratios. They found that scaffolds with a Young's modulus of greater than 200 kPa, with a greater lactic acid content, were better for differentiation than scaffolds with a greater glycolic acid content, which were softer (Levi-Mishali et al., 2009).

The research from these groups has an impact on this research as it further proves that an elastomer should be used for the scaffold, so the scaffold will not collapse under the contractions of the myofibre and will also aid differentiation of myoblast cells into myotubes (Engler et al., 2004).

Electrospinning has been used for skeletal muscle tissue engineering by Choi et al (2008) (Choi et al., 2008). Choi et al blended PCL with collagen to improve the biocompatibility of the scaffold. Aligned fibres were made using a rotating collector plate. They also investigated how the increase in speed of rotation increased the alignment within the fibres; an increase in rotation speed lead to an increase in the degree of alignment within the fibre meshes collected. When these PCL-collagen fibres were tested for their tensile strength,

there was around 1 MPa difference between random fibres and aligned fibres tested with the load being applied along the length of the aligned fibres. Random fibres had a tensile strength of 4 MPa, aligned fibres had a tensile strength of 5 MPa (Choi et al., 2008). This result indicates that randomly oriented fibres are more elastic than random fibres, which could be due to the randomly oriented fibres being pulled to align parallel as the load is applied before the load is really taken by the fibres. Xin et al (2006) used AFM (atomic force microscopy) to look at the Young's modulus of a single electrospun PL85GA15 fibre. To transform the displacement data acquired from the AFM, they used the Hertz model which:

"Defines a relationship between contact radius, the nanoindentation load, and the central displacement." (Xin et al., 2006)

They found that the Young's modulus of single electrospun PLGA fibres was 42 ±26 kPa. They follow this with evidence of human mesenchymal stem cells growing and differentiating into osteoblasts and chondrocytes; showing the mechanical properties of the scaffold were suitable for cell culture and differentiation (Xin et al., 2006).

1.9 Controlled Architecture to control Cellular Morphology

The organisation of the myofibres within the contractile unit is vital for the correct function of skeletal muscle. A major problem within tissue engineering of skeletal muscle has been how to recreate such fine control over the architecture of the myofibres. Tissue engineering of skeletal muscle fibres in vitro leads to myotubes arranging themselves in random patterns thus not recreating a fully functioning muscle as the fine architecture is

lost (Huang et al., 2006). This research aims to utilize electrospinning of elastomeric polymers to generate aligned nanofibres which could create a template or scaffold for the correct architecture of skeletal muscle. Huang et al (2006) used a biodegradable elastomer, poly(L-lactide) (PLLA) as a scaffold for skeletal muscle growth and differentiation. Results from this study undertaken in 2006 are very relevant as it provides a study to base ideas upon and also proves two items: 1) Generating aligned elastomer fibres is possible, and 2) These aligned fibres do allow aligned growth and differentiation of myoblast cells (Huang et al., 2006). Huber et al (2007) electrospun Nylon 6/6 for directional myofibre growth. They showed that using highly aligned nylon microfilaments they could show consequent myotube alignment (Huber et al., 2007). They did this without the use of a fibroblast feeder layer to minimise myofibre detachment from the scaffold during differentiation contractions, but they did put a layer of Matrigel™ on the scaffold prior to cell seeding. This matrigel may have encouraged cellular attachment in the first instance, but it may have influenced cellular behaviour during differentiation, with regards contractile detachment.

Recent research has shown nanofibres made with different polymers allow growth of aligned muscle fibres. Riboldi et al (2005) used a commercially available degradable block polyesterurethane called DegraPol®. This polymer was chosen because it has elastomeric properties and has been shown to be biocompatible, and is also able to be electrospun which increases the chance of creating aligned microfibrous membranes (Riboldi et al., 2005). Wan-Ju Li's research group used poly-ε-caprolactone (PCL) to create a three-dimensional micro-patterned scaffold with similar structural anisotropy (directionality) of skeletal muscle (Li et al., 2007). PCL is a relevant polymer as it is biodegradable and biocompatible and is already used in clinics for implants and drug delivery.

Another group (Huang et al., 2006) used the elastomer poly(L-lactide) (PLLA) with electrospinning and uniaxially stretching to create an aligned nanofibrous scaffold for myoblast seeding. They found that myoblasts seeded on aligned micropatterned substrates (grooves were 10 μm wide, 10 μm apart, and 2.8 μm deep) did not elongate as much as those seeded on aligned nanofibrous scaffolds. Comparing the dimensions of the grooves to the electrospun aligned fibrous PLGA scaffolds fabricated in this project the diameter of the fibre compared to the groove is an order of magnitude larger – the average electrospun fibre diameter in aligned PLGA is 700 nm, and spaces between fibres range from <1-5 μm (Huang et al., 2006). This work demonstrated that aligned nanofibres encourage directional growth of myoblasts compared to randomly oriented fibres after 3 days and 7 days in culture, and provides a background hypothesis on which to base the author's research upon.

1.10 Choice of Polymer

The polymer characteristics are an important consideration for the application; each polymer has its own signature DSC trace to illustrate the crystallinity of the polymer which indicates elasticity. Reduced crystallinity in a polymer causes a decrease in brittleness and an increased elasticity. The mechanism by which a polymer degrades is also important as it may be necessary for the polymer to degrade in a manner so it retains its mechanical properties, or that the degradation products must be non-toxic to cells and tissues, or that the degradation time is rapid or slow. All these features must be examined and made relevant to the application for the scaffold.

A group led by Robert Langer and Yadong Wang have synthesised a novel biocompatible, biodegradable elastomer. This elastomer appears to have great potential for

all forms of tissue engineering, including skeletal muscle regeneration. The polymer consists of glycerol as it is the basic building block for lipids (Wang et al., 2002), and sebacic acid because it is the natural metabolic intermediate in oxidation of medium to long fatty acid chains, due to these two components the biodegradable elastomer is called poly(glycerol-sebacate) (PGS) (Wang et al., 2002). When synthesising this novel elastomer, the research group aimed to include five criteria their polymer required: hydrolysable bonds to minimise enzymatic effects, a low density of crosslinking to reduce brittleness – for this they used an ester bond, minimisation of heterogeneous degradation by using crosslink chemical bonds similar to those in the backbone, and finally, use of non-toxic monomers which are tri-functional with one providing hydroxyl groups for hydrogen bonding (Wang et al., 2002). Their research proved that PGS is a tough bidegradable elastomer and that it has properties that can rival if not beat those of another elastomer PLGA (poly(DL-lactide-co-glycolide)). The Young's modulus of PGS is around 0.3MPa which indicates the formation of a soft material and the ultimate tensile strength was measured at >0.5MPa, with a strain to failure value similar to large blood vessels – up to 260% (Wang et al., 2002). 3T3 fibroblast cells proliferate faster over 6 days on the PGS substrate compared to one made from PLGA, as measured via the MTT assay. Light microscopy of the fibroblasts was also undertaken with cells from which Wang et al concluded that PGS is as biocompatible as PLGA. PLGA and PGS discs were implanted sub-cutaneously in rats. PGS produced a lower inflammatory response than PLGA, and the fibrous capsule of scar tissue produced was identical over 35 days in both polymers (Wang et al., 2002). Along with this low inflammatory response, PGS has also been shown to degrade via surface erosion which means its mechanical properties remain stable throughout the degradation process as the geometry is maintained (Wang et al., 2002),

therefore the scaffold will preserve its structure without deforming. Any deformation in the scaffold may cause the scaffold to collapse. A 3D scaffold that has the potential to collapse seriously impedes the mechanical properties of said scaffold. The reports about this elastomer from the group in USA appear to make it a great option for tissue engineering of soft or elastic tissue. This is because of its elasticity, the way it degrades, and the low inflammatory response it receives post-implantation. A controlled inflammatory response is thought to aid healing of the damaged tissue (Wang et al., 2002). This group went on to use PGS as a nerve conduit by seeding Schwann cells on the polymer (Sundback et al., 2005), and also used the PGS for vascular engineering by making biphasic tubes out of PGS and a porous POC (poly(1,8-octanediol citrate) outer layer (Motlagh et al., 2006).

1.11 Poly-(lactide-co-glycolide); PLGA

PLGA was chosen for this research as it is a biodegradable polymer that can be electrospun, and previous groups have shows cell attachment upon this polymer (Aviss et al., 2010; Kumbar et al., 2008; Pan et al., 2008; Xin et al., 2006). This polymer is biodegradable and has been shown to generate nanofibres when electrospun and is an elastomer. PLGA is a random co-polymer of lactide and glycolide, and has already been used for various medical procedures e.g. sutures and drug delivery systems (Gilding and Reed, 1979; Lee et al., 2007).

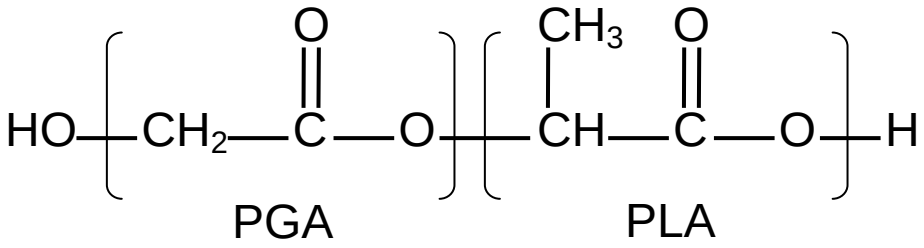

Figure 6: *Chemical structure of PLGA made up of PGA and PLA repeat units.*

Figure 6 illustrates the linear structure of PLGA, made up of glycolide and lactide. Glycolide and lactide are cyclic anhydrous di-esters of the hydroxy-acids glycolic acid and lactic acid respecively. Polymerization of these anhydrous di-esters yields higher molecular weight polymers than can be achieved using the hydroxy acids. The condensation polymerization of hydroxy acids gives water as a by-product which unless removed would prevent further polymerization. This problem is avoided by using the anhydrous di-esters glycolide and lactide (see figure 7) and high molecular weight polymers can be achieved via a ring opening polymerization.

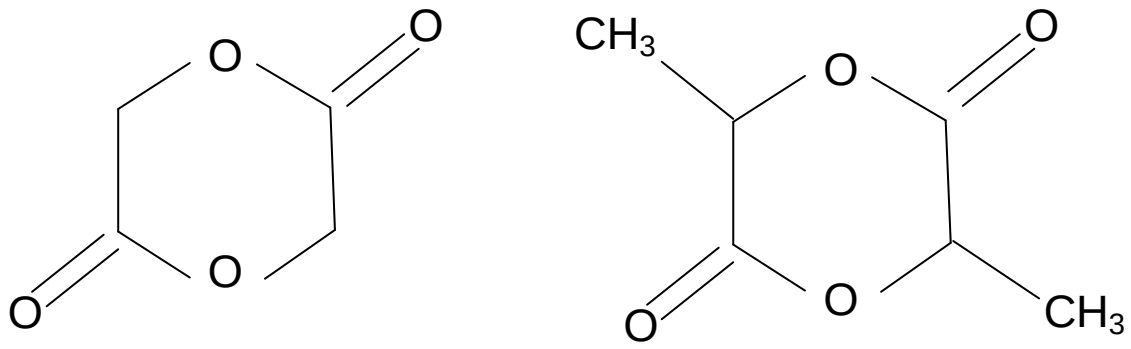

Figure 7: *Chemical ring structures of anhydrous di-esters; glycolide and lactide.*

In order to form the random co-polymer PGLA, a catalyst, often tin chloride (Gilding and Reed, 1979), is used to speed up the opening of the di-ester ring structures to promote further polymerization between the two di-esters by forming new ester bonds between them. This process produces a co-polymer with blocks of glycolide interspersed randomly with lactide. Gliding and Reed (1979) showed that a growing glycolide chain has a 3:1 preference for adding another glycolide, and a growing lactide chain has a 5:1 preference to add a glycolide. A co-polymer of lactide and glycolide provides a useful method to combine the different properties of the two components. Because poly-lactide (PLA) has a hydrophobic methyl group its degradation rate is much slower than that of poly-glycolide (PGA). PGA (Dexon®) has a 46-53% crystallinity (Gilding and Reed, 1979) thus processing this polymer alone using systems that require dissolving the polymer in solvents can be difficult; in contrast PDLLA is amorphous so dissolving in solvents is not a problem. By combining the two polymers to form a co-polymer it is possible to tailor the end product by controlling the ratio of the polymers.

Zong et al (2003) have shown that electrospun PLGA is flexible and less hydrophobic than the solvent cast film with an increased surface area to volume ratio and the membrane density was decreased (Zong et al., 2003). The decrease in hydrophobicity in the electrospun fibres compared to flat solvent cast films of PLGA could be due to water wicking through the fibres creating a false water contact angle measure. PLGA degrades in a way similar to PGS in that it is hydrolysed via ester bonds, and the byproducts of this degradation are lactic acid and glycolic acid. Zong et al (2003) found that PLGA shrinks around 37^{o}C, but the higher molecular weight PLGA had much less shrinkage than the lower molecular weight. Shrinkage at the temperature indicated is not appropriate for uses in biomedical procedures as this is body temperature. How a polymer's mechanical

properties alter as it degrades depends on the method of degradation for that polymer e.g. PLGA degrades via hydrolysis of ester bonds, due to its amorphous nature, water molecules can easily access the ester bonds which starts a cascade of low molecular weight chains being released autocatalysing more ester bond breakage via acidic end blocks (Zong et al., 2003). Zong et al 2003 monitored electrospun PL10GA90 as it degraded in closed bottles containing PBS (phosphate buffered saline pH 7.27) at 37^{o}C. They measured shrinkage within the polymer, used DSC (differential scanning colourimetry) to monitor crystallinity changes within the polymer, and, SEM (scanning electron microscopy), WAXS (wide-angle X-ray diffraction) and SAXS (small-angle X-ray scattering) to monitor morphological and structural changes respectively (Zong et al., 2003). They found that after six days degradation the weight loss decreased rapidly corresponding to an increase in water absorption which could be due to the combined effects of increased porosity and swelling of the degradation products. The DSC showed that the glass transition (Tg) of the PLA10GA90 initially increased after just one day – indicating more crystallinity, this gradually decreased to day 6 when it began to rise again to the final day of the experiment, day 12 (Zong et al., 2003).

1.12 Polymer Processing

As discussed earlier, topographical cues provided by the scaffold to the cells has an influence on cellular morphology. For skeletal muscle, aligned, bi-polar cells are desirable as this is thought to encourage the distinct hierarchy within the tissue from the molecular level, and to allow parallel arrangement of cells for contraction to take place (Riboldi et al., 2005). There are various polymer processing techniques available to create different

topographical cues to cells; e.g. hydrogels for a 3D environment (Jayawarna et al., 2006; Zhou et al., 2009), surfaces can also be modified with adherence motifs or proteoglycans (Shekaran and Garcia, 2010), pillars of polymer made either by replication moulding (Milner and Siedlecki, 2007) exploiting the interesting effect high voltage has on the surface tension within a polymer melt (Goldberg-Oppenheimer and Steiner, 2010), nanogrooves made by nanolithography (Dalby et al., 2008), and fibrous scaffolds made by electrospinning a polymer dissolved in a solvent (Aviss et al., 2010; Choi et al., 2008; Huang et al., 2006; Riboldi et al., 2005; Srouji et al., 2008).

1.13 The technique of electrospinning

Electrospinning is a flexible method to create fibres in the nanometer (<500nm) size from many different polymers. The process of electrospinning was introduced by Formhals and patented in the 1930s (Stankus et al., 2006). It has since been shown to be an excellent choice for tissue engineering, due to its flexibility in collection methods, and by being able to use a wide variety of polymers. This variety means a polymer can be selected to best suit the needs of the electrospun scaffold. The nanofibres create a 3-dimensional mat of fibres which, when introduced to cell media can resemble the ECM (Stankus et al., 2006; Xu et al., 2004; Zong et al., 2005), which is a huge advantage for growing cells upon over flat, smooth surfaces which do not have the capacity to resemble the ECM. Electrospinning of nanofibres can provide a further advantage with the ability to create directional fibers which can control the direction of cell growth.

Electrospinning uses a high voltage to cause phase separation of a polymer solution to form fibres which can be in the micro or nanometer range. The polymer solution – polymer of chosen concentration dissolved in a relevant solvent – is in a syringe attached to a pump

which controls the flow rate of the polymer expulsion from the syringe via the needle at the end of the syringe. The blunted needle at the end of the syringe is connected to the voltage supply, as shown in figure 8.

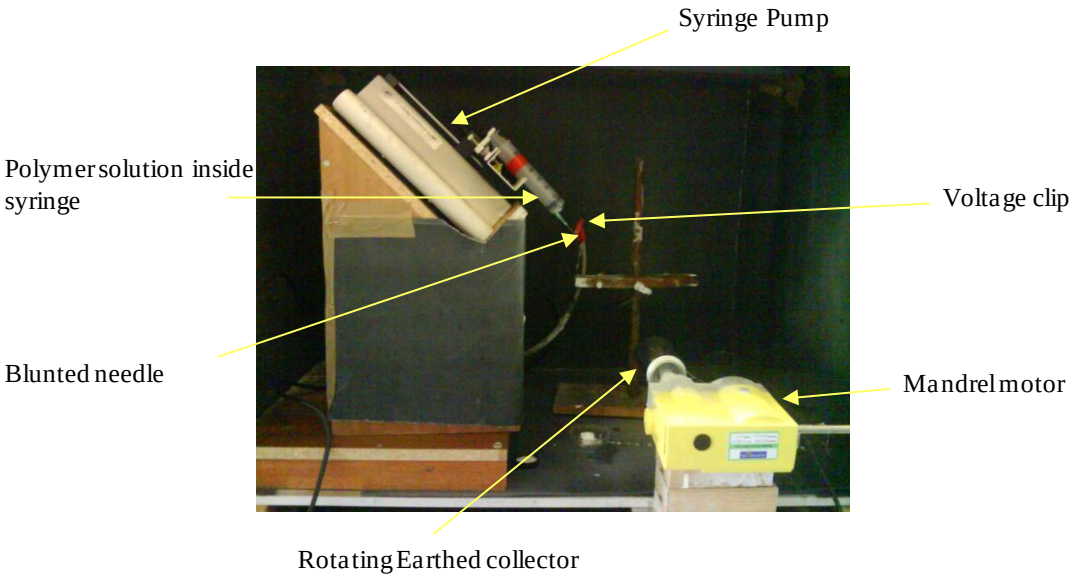

Figure 8: *A photograph of the electrospinning kit used in this study, important components for the electrospinning process are clearly labelled.*

The voltage can be varied depending on the polymer and desired results; the usual voltage range is between 10 kV and 25 kV. Applied voltage introduces free charged ions into the solution which move towards the opposite electrical pole, towards the grounded collector plate. As the charged ions move, they transfer tensile forces to the polymer encouraging polymer expulsion from the needle in the form of fibres (Subbiah et al., 2004). The needle is blunted because a sharp point on it would prevent a droplet to be formed as the voltage is applied. A droplet is necessary in order to form a Taylor cone with the correct angle (49.3 degrees) to balance the electrostatic tension of the polymer with the surface tension of the liquid (Subbiah et al., 2004). The electrostatic forces surrounding the Taylor cone then

make the polymer jet unstable, causing the jet to be arranged in a series of loops which can then be collected on an earthed collector plate (Theron et al., 2001). A rotating mandrel as the collector plate provides the ability to create randomly oriented nanofibres, as well as fibres which are highly aligned, dependent on the speed of the rotation. For randomly oriented fibres, a slow rotational speed is used, typically around 300 rpm, for aligned fibres this speed is increased to 1500 rpm.

The parameters employed during electrospinning can produce a variety of fibre types, e.g. increasing the flow rate will lead to increase in fibre diameter, therefore larger pore formation, but will also lead to highly beaded fibres. Beads form when polymer does not elongate prior to landing on the collector plate. The environment in which electrospinning takes place also has an effect on the products, e.g. high humidity may not allow for efficient solvent evaporation (Subbiah et al., 2004), leading to fibers with a more ribbon-like morphology.

Randomly oriented fibres have been noted to have a structural resemblance to natural ECM (extracellular matrix) (Bian and Bursac, 2009; Christopherson et al., 2009) as the fibres mimic the ECM protein mesh. The type of polymer and how it can be modified can also play a role in ECM mimicking. Incorporating biologic components into the nanofibres can be done using the electrospinning technique. Electrospinning biological materials e.g. collagen and fibrin, has been done and suited the application for the scaffold. Specific amino acid sequences, known to be involved in cellular attachment can also be incorporated into the polymer solution e.g. RGD and YIGSR. This incorporation of amino acids may not be fully controlled, e.g. the sequence could appear on the surface of the fibres or it could be found to be on the interior of the fibres, where the cells will not benefit from its

presence in order to aid attachment. It is also possible to alter the surface chemistry of the polymer to introduce specific groups to the surface to aid binding of ECM proteins or GAGs (glycosaminoglycans) e.g. heparan sulphate and heparin (K. Meade and C. L. R. Merry 2010 unpublished data).

1.14 Project aims

This project aims to utilise electrospinning to create a fibrous scaffold for myoblast growth. Changing the electrospinning parameters allows the creation of oriented fibres to encourage directional cell growth; this project will compare randomly oriented and aligned poly-lactide-co-glycolide (PLGA) fibres to investigate the effect of fibre orientation on cell morphology, proliferation and myoblast differentiation.

- Electrospin an aligned PLGA fibrous mesh to encourage directional cell growth
- Investigate material characteristics of the scaffold relevant to application
- Illustrate cellular morphology using cytoskeletal immunostaining
- Monitor cellular proliferation
- Analyse mechanisms of cellular adhesion via integrins
- Measure temporal differentiation of myoblasts into myotubes using immunostaining and molecular biology techniques.

Kathryn J. Aviss

Chapter 2: Materials and Methods

The University of Manchester

2 Materials and Methods

2.1 Polymer Characterisation

2.1.1 Electrospinning

A 20% solution of poly(lactide-co-glycolide) (Sigma-Aldrich) (PL85GA15) in hexafluoroisopropanol (HFIP) (Apollo Scientific) was electrospun at a flow rate of 1 ml/hour, under 25 kV, at a distance of 15 cm. To create aligned fibres, a high speed rotating mandrel was employed. The collecting area on the mandrel was 11 cm in length, and 3.5 cm in diameter; the rotating speed to form aligned fibres was 1500 rpm. The same mandrel was used to create randomly oriented fibres by decreasing the rotating speed to 300 rpm. For both types of fibre, the collection time was 1-1.5 hours at room temperature (not controlled).

2.1.2 Spin Coating

200 µl of a 20% solution of PL85GA15 in HFIP was applied to a 2 cm/2 cm clean glass slide which was mounted on a spin coater (WS-400B-6NPP/LITE Laurell Technologies Corporation) using a local vacuum. The sample was spun at 2000 rpm for 20 seconds to fully cover the glass slide with a thin film of polymer solution. Samples were then placed in a fume hood overnight before being placed in a vacuum oven for 2 days to aid solvent evaporation and film preparation.

2.1.3 Scanning Electron Microscopy (SEM)

A Topcon SEM and a Zeiss EVO SEM was used to visualise the manufactured polymer surfaces with and without cells. The spot size used was 8, with an accelerating voltage of 5 kV. Samples were mounted on aluminium stubs with carbon tabs and gold sputter coated on an Edwards Sputter Coater E150b under an argon gas atmosphere.

Fibre diameter and alignment were determined from five different 5000 times magnified SEM images using the software ImageJ (National Institute of Health), and the student's-test was used to analyse any statistical difference between random and aligned fibres.

2.1.4 Differential Scanning Calorimetry (DSC)

DSC was performed to investigate any crystallinity within the sample and also provide an accurate measure of melting and glass transition temperatures. Approximately 2 mg sample was added to each DSC pan. For each type of sample 3 pans were tested. Samples were loaded into the DSC machine (Q100 TA Instruments) and run on a heat-cool-heat cycle between 100^{o}C on the heat cycle to -100^{o}C on the cool cycle. Universal Analysis software (version 3.0) was used to analyse the data, i.e. to find the glass transition temperature and the melting temperature. From these two values the total enthalpy change was calculated.

2.1.5 Water Contact Angle

Hydrophobicity of the PLGA scaffolds was measured using a Kruss Drop Shape Analyser (DSA100), and Drop Shape Analysis software (version 1.91.0.2 [HS]). Videos were made of the drop where appropriate with a frame speed of 142 frames per second, and drop analysis undertaken every 5 frames where possible. Where necessary still photos were

taken every minute for 10 minutes and each image was analysed for contact angle measurements.

2.1.6 Fourier Transfer Infrared Spectroscopy (FTIR)

FTIR is a type of vibrational spectroscopy used to identify specific bond vibrations within a sample. The spectrum is obtained via the frequency resonant with the type of vibrational transition obtained through the absorption of radiation. Molecule groupings vibrate within well defined frequency ranges that can be used to create a fingerprint of the sample e.g. hydrogen stretching occurs between 4000-2200 cm^{-1} and double bonds between carbon-oxygen and carbon-carbon occur between 1850-1550 cm^{-1} (Chalmers and Everall, 1993).

FTIR was carried out on a Perkin-Elmer FTIR. Background interference was measured before each sample. Each sample (including background) was read 30 times to produce a clear representative of the types of bonds present. A band around wavenumber 3500 cm^{-1} indicates presence of solvent in a solid sample as it is characteristic of OH banding.

2.1.7 Thermogravimetric Analysis (TgA)

TgA monitors total weight loss during heating to high temperatures. For the PLGA samples, the temperature was ramped up by the TgA (TGA2950 TA Instruments) at $5^{o}C$ per minute up to $100^{o}C$. Enough polymer was added to completely cover the bottom of the pan in a heterogeneous covering, 3 pans were loaded per sample. Universal Analysis software (version 3.0) was used to analyse the TgA data, i.e. to find the total weight loss at $90^{o}C$ and to find at precisely what temperature this weight loss occurred.

2.1.8 Mechanical Testing

Mechanical testing was performed to investigate the elastic properties of the electrospun scaffolds. Using an Instron 1122 tensile tester to apply 200 g/cm^2 load at 5 mm/min until breakage was detected. Breakage was detected when no resistance to load was measured. Modulus was calculated by dividing maximum stress (Pa) by maximum strain. Maximum stress and strain were taken to be the yield point on the graph i.e. the final point of the linear point of the graph before it curves over to the rubbery plateau.

2.2 Degradation Study

Electrospun PLGA was peeled away from the foil collector and placed into a Petri dish. Spin coated PLGA was not peeled away from the glass slide it was spun onto as this kept the polymer sheet at the bottom of the well, thus totally immersed in the solution. The solution was PBS (PAA) with 0.02% sodium azide (NaN_3) (Sigma-Aldrich) to prevent microbe growth. Samples were placed in a large plastic box with a damp paper towel lining to create humidity and slow evaporation of PBS solution. This plastic box was then placed in an orbitally shaking incubator, shaking at 70 rpm, with the temperature set at 37^{o}C. Samples were taken at intervals throughout the study, after each sample retrieval PBS solution was removed and measured for pH and fresh PBS with NaN_3 solution was added to the remaining samples. Samples to be analysed were rinsed 3 times with distilled water to remove salts deposited by the PBS as this may interfere with the analytical methods employed. Wet weight was measured after blotting each sample on paper towel before weighing; these samples were then left at room temperature overnight to allow any remaining water to evaporate and weighed again for dry weight. SEM samples were

mounted and gold sputter coated as described earlier and visualised using the Topcon SEM or the Zeiss EVO SEM on full SEM mode.

2.3 Cell Studies

2.3.1 Myoblast Cell Culture

C2C12 murine myoblast cell line was purchased from ECACC (The European Collection of Cell Cultures – number 91031101). This cell line was chosen because it is well documented in the literature as an immortal cell line derived from cells from the C3H mouse model obtained 70 hours after crush injury (Yaffe and Saxel, 1977) which adheres readily, differentiates rapidly and produces contracting myotubes expressing characteristic muscle proteins (HPA, 2010). For growth and expansion, cells were kept in 75 cm^2 tissue culture flasks with DMEM (Dulbecco's Modified Eagles Media) (PAA) with 10% FBS (Foetal Bovine Serum) (PAA) 1% antibiotic (penicillin/streptomycin) (PAA). For differentiation induction, FBS serum content was reduced to 5% FBS or 2% horse serum (Sigma-Aldrich) was; all other components remained the same. There was no noticeable difference in cell behaviour between the two serum types for differentiation induction. Cells were not allowed to become >80% confluent and were split using Trypsin-EDTA (Sigma-Aldrich) at 37^oC for 5 minutes or until the cells became rounded, as checked by light microscopy. Cells were passaged at a 1:6 or 1:12 ratio cells to fresh media. Cells were grown in a humidified atmosphere at 37^oC with 5% CO_2.

2.3.2 Macrophage Cell Culture

J774A.1 murine macrophages (ECACC number: 91051511) were cultured in high glucose DMEM (Sigma-Aldrich) supplemented with 1% L-glutamine (PAA), 20% FBS, and 1% penicillin/streptomycin. Because these cells are not fully adherent a cell scraper was utilised to passage them instead of trypsin. Cells were passaged every 2 days at a 1:6 ratio.

All scaffolds/substrates were sterilised using UV light incubation for 10 minutes on either side. Glass coverslips were additionally sterilised in 70% ethanol before cell seeding. Electrospun scaffolds were not sterilised using ethanol as this disrupted the architecture of the fibrous meshes. Sterile well plate inserts (Scaffdex, Finland) were used to secure electrospun scaffolds at the bottom of the wells.

2.3.3 SEM Preparation

Cells were fixed in 4% glutaraldehyde (Sigma-Aldrich) in 0.1 M phosphate buffer for 30 mins then dehydrated using an increasing ethanol concentration series from 50% EtOH to 100% EtOH, finally 200 µl HMDS (hexamethyldisilazane) (Sigma-Aldrich) was added to each sample and left to evaporate overnight in a chemical flow cabinet. Dehydrated samples were then mounted on aluminium stubs via an adhesive carbon sticker, gold sputter coated as described earlier, and visualised on a Topcon scanning electron microscope (SEM).

2.3.4 Alamar Blue assay

Cells were seeded onto scaffolds at 100,000 cells per well with 2 ml growth media and 100 µl/ml alamar blue solution (Resazurin sodium salt (Sigma: R7017) in PBS) and incubated for 2 hours at 37^{o}C. 200µl of Alamar blue/media solution was then fluorescently measured using a FLUOROstar Optima 230V at excitation: 530 nm, emission: 590 nm in a clear 96 well plate.

2.3.5 DNA assay

At specified culture times media was removed from the cells and washed three times with PBS. 200 µl distilled water was then added to each sample and placed in the -20^{o}C freezer until frozen. When frozen, samples were removed from the freezer and allowed to thaw. This freeze-thaw cycle was repeated three times in order to lyse cells and release DNA into the water. The DNA assay uses the Hoechst 33342 (Invitrogen) fluorescent stain to detect DNA presence in a sample. Hoechst integrates with double stranded DNA and can be fluorescently tracked by measuring the excitation at 355 nm and the emission at 460 nm. Hoechst was used at 0.02 mg/ml diluted in TNE buffer. TNE buffer consists of 10 mM Trizma base (Sigma-Aldrich), 2mM NaCl (Sigma-Aldrich), and 1mM EDTA (Sigma-Aldrich) pH to 7.4 using HCl.

2.3.6 F-actin cytoskeleton staining

C2C12 myoblasts were seeded on electrospun scaffolds and glass coverslips at 100,000 cells per well. At the appropriate time points the growth media was removed and samples

were washed three times in PBS. Cells were then fixed in 3% PFA (paraformaldehyde) (Sigma-Aldrich) at room temperature for 15 mins. Samples were then washed a further 3 times with PBS. Cells were blocked and permeabilised with ICC (immunocytochemistry) blocking buffer for 30 minutes at room temperature. ICC blocking buffer consists of 1% goat serum, 1 mg/ml BSA (bovine serum albumen), and 0.1% Triton X-100 (Sigma-Aldrich). Powdered fluorescein-phalloidin (Sigma-Aldrich) was dissolved in 1.5 ml methanol to yield a final stock solution concentration of 200 units/ml (6 µM). To each sample, 5 µl of this stock was added to 200 µl 1% ICC block buffer and incubated at room temperature for 20 mins. Samples were mounted with DAPI (4',6-diamidino-2-phenylindole)-Prolong (Invitrogen) to stain nuclei blue. Samples were viewed on a Leica Confocal microscope (LCS SC5) with optical zoom.

2.3.7 Peroxide Assay for Macrophage Activation

J774A.1 murine macrophages were seeded at 100,000 cells per well on electrospun scaffolds, tissue culture plastic, copper discs were used as a positive control in 2 ml of Dichlorofluorescein-diacetate (DCF-DA) (Sigma-Aldrich). At 2, 4, and 6, hours 100 µl aliquots of each sample was taken in triplicate and measured fluorescently at: excitation: 485nm, and emission: 530, then returned to original samples.

2.3.8 Interleukin 1β (IL-1β) Enzyme-Linked Immunosorbent Assay (ELISA) for Macrophage Activation

J774A.1 murine macrophages were seeded at 100,000 cells per well on various substrates; electrospun PLGA scaffolds, TCP, and spin coated PLGA. The positive control was 10µg/ml lipopolysaccharide (LPS) (Sigma-Aldrich) in media. Media samples were taken at 2 hours and 48 hours and kept at -20^{o}C until needed.

The ELISA was undertaken in maxisorb 96 well plates (Nunc 442404) following the protocol set out by the manufacturers of the ELISA kit (R&D systems ®). All incubations were performed in the dark. Capture antibody (part 840134) rat anti-mouse IL-1β was reconstituted to 720 µg/ml in PBS (without carrier protein) then diluted 1:180 prior to an overnight incubation at room temperature in the 96 well plate. Wells were then washed 3 times with wash buffer (0.05% Tween 20 in PBS) then blocked with blocking buffer (1% BSA in PBS) for one hour at room temperature. Wells were again washed 3 times with wash buffer then 100 µl media sample or standard was added to each well. The standard was recombinant mouse IL-1β (part 840136) in reagent diluent (0.1% BSA, 0.05% Tween 20 in PBS with 20 mM Tris and 150 mM NaCl) at a stock concentration of 360 ng/ml. The standard curve high was 1000 pg/ml, and a 7 fold serial dilution created the points down to 0 pg/ml. Media samples and standards were incubated for 2 hours at room temperature. Samples were then washed 3 times with wash buffer then incubated with detection antibody (part 840135) at a working concentration of 600 ng/ml for 2 hours at room temperature. Detection antibody was biotinylated goat anti-mouse IL-1β reconstituted to a stock solution of 108 µg/ml in reagent diluent. Samples were then washed 3 times in wash buffer. Streptavidin conjugated horseradish-peroxidase (HRP) was used as a catalyst for the colourimetric reaction. The working concentration was a 1:200 dilution in reagent diluent

of the stock provided by the manufacturer and was incubated at room temperature for 20 minutes. Samples were then washed 3 times with wash buffer. A 1:1 mixture of substrate solutions was then made up and 100 µl was added to each sample and incubated for 20 minutes at room temperature. Colour Reagent A was hydrogen peroxide and Colour Reagent B was tetramethylbenzidine (Cat number: DY999 R&D Systems). The reaction was stopped with the addition of 50 µl 1 M sulphuric acid to each sample and the optical density was measured at 450 nm and 540 nm. The 540 nm reading was subtracted from the 450 nm reading in order to correct for imperfections in the plate.

2.3.9 Vinculin staining

C2C12 were seeded on growth media scaffolds at 100,000 cells per well. Cells were fixed, permeabilised, and blocked at specified time points post seeding, as described for f-actin staining. Primary antibody for vinculin was monoclonal anti-vinculin antibody produced in mouse from Sigma Aldrich (V4505), and was used 1:500 in ICC block buffer incubated for 1 hour at room temperature. Secondary antibody was goat anti-mouse Alexa Fluor 546 (A11003). F-actin was also stained for this experiment using the FITC-phalloidin as described in section 1.4.4.

2.3.10 Differentiation Staining

C2C12 murine myoblast cells were seeded at 100,000 cells per well on both types of electrospun fibres and glass coverslips as a control. 24 hours post seeding, growth media was replaced with media with reduced serum (5% FBS or 2% horse serum – as described in

section 2.3.1) content to induce differentiation into myotubes: differentiation media. Cells were fixed at specific time periods (as per section 2.3.6), indicated with the relevant figures, as described above. Cells were also blocked and permeabilised with ICC block buffer as above. Primary antibody mouse monoclonal IgG [MY-32] to fast skeletal myosin (ab7784-250) was used at 1:1000 in ICC block buffer and incubated at room temperature for 1 hour. Secondary antibody was goat anti-mouse Alexa Fluor 488 also used at 1:1000 in ICC block buffer.

2.3.11 Sarcomeric Myosin Staining

C2C12 murine myoblast cells were seeded at 100,000 cells/ml to the substrates – random fibres, aligned fibres, and glass coverslips. Growth media was replaced with differentiation media 24 hours post seeding to induce differentiation into myotubes. Cells were fixed and stained 14 days after seeding as per section 2.3.6. ICC blocking buffer was used to permeabilise and block the cells. Sarcomeric myosin was probed using the primary antibody A1025 at 1:100 concentration in ICC blocking buffer. A1025 antibody was a generous gift from Dr. Michelle Peckham of The University of Leeds. Secondary antibody used was goat anti-mouse Alexa Fluor 546, FITC-phalloidin was also used to stain the F-actin element of the cytoskeleton.

2.3.12 Reverse Transcrtiptase Polymerase Chain Reaction (PCR)

2.3.12.1 Cell Pelletting

2.3.12.1.1 For integrin expression studies

Cells were seeded at 400,000 cells per well in growth media onto electrospun scaffolds or tissue culture plastic. Cells were cultured for 4 hours or 24 hours before they were removed from the substrates for cell pelleting. Total mouse embryo (10-12 days old (Ambion AM7828) RNA was used as a positive control of expression.

To acquire a cell pellet, media was removed from the relevant samples and washed twice with PBS. The samples were then moved to a fresh well plate and washed twice again with PBS before incubating with 2 mls trypsin-EDTA for 10 minutes at 37^{o}C. A fresh well plate was used to ensure only cells on the polymer samples, not the underlying tissue culture plastic were taken. After trypsinising for 10 minutes, 2 mls growth media was added to neutralise the trypsin. This total volume of 4 mls was then transferred into a sterile 15 ml centrifuge tube and centrifuged at 1500 rpm for 5 minutes to make a cell pellet. The supernatant was removed from the centrifuge tube and the pellet was resuspended in 1 ml PBS and transferred into a sterile 1 ml Eppendorf tube to be re-pelleted. Re-pelletting was performed in a microfuge at 6000 rpm. Again the supernatant was removed post spinning and the pellet was stored at -80^{o}C until RNA extraction.

2.3.12.2 RNA Extraction

RNA extraction was done according to the Qiagen Qia-shredder manufacturer's guidelines. Briefly the defrosted cell pellet was resuspended in lysis buffer containing β-mercaptoethanol and applied to the first Qia-shredder column and centrifuged at 15,000 rpm for 2 minutes. Supernatant was then applied to the second Qia-shredder column with

70% RNAse free water and centrifuged at top speed for 30 seconds. DNA was removed using a DNAse enzyme incubation at room temperature for 15 minutes. RW1 buffer (supplied in the Qiagen RNeasy kit) was used to wash the sample by centrifugation at top speed for 30 seconds. Samples were then washed with two separate centrifugation washes using RPE buffer (supplied in the Qiagen RNeasy kit). RNA was collected from the column using 30 µl RNAse free water and centrifuged at top speed for 1 minute. RNA content was quantified immediately after extraction using a nanodrop.

2.3.12.3 cDNA Creation via reverse transcription

Using the quantification of RNA it was possible to calculate how much RNA is needed to generate a 1 µg/ml cDNA solution.

To add to 20 µl RNA and water solution calculated from the RNA quantification, 20 µl of Master Mix was added. Master Mix per sample consisted of 2 µl oligo DT, 8 µl 5X reverse transcriptase buffer, 4 µl dNTP, 5.2 µl water, and finally 0.8 µl AMV transcriptase.

cDNA was created using a reverse transcription enzyme: AMV (avian myeloblastosis virus) reverse transcriptase. Prior to reverse transcription, the RNA was incubated for 3 minutes at 65^{o}C in order to open any auto-pairing within the strands then kept on ice to maintain this feature in order to encourage efficient reverse transcription of the RNA into cDNA

2.3.12.4 PCR Reaction

15 µl was the total volume for each PCR reaction. This 15 µl consisted of 7.5 µl Bioline Biotag, 1 µl forward primer, 1 µl reverse primer, 4.5 µl RNAse/DNAse free water, and 1 µl cDNA.

Cycle conditions were determined by ensuring equal band intensities from the housekeeping gene. To create equal band intensities the amount of cDNA was manipulated, therefore the amount of water in the master mix for samples with more or less than 1 µl cDNA was modified accordingly. GAPDH was used as the housekeeping gene to compare integrin expression against. GAPDH cycle conditions were: 60^{o}C for 22 cycles.

GAPDH Primer Sequence: Forward: 5'-CAT CAC CAT CTT CCA GGA-3'

GAPDH Primer Sequence: Reverse: 5'-ATT GAG AGC AAT GCC AGC C-3'

Alpha integrin subunit cycle conditions:

1 – 6: 60^{o}C for 35 cycles

7: 64^{o}C for 35 cycles with 2% DMSO

8: 60^{o}C for 35 cycles

10: 64^{o}C for 37 cycles with 2% DMSO

11: 64^{o}C for 35 cycles with 2% DMSO

Beta integrin subunit cycle conditions:

1: 60^{o}C for 29 cycles

2 & 3: 60^{o}C for 35 cycles

4: 60^{o}C for 33 cycles

5: 62^{o}C for 36 cycles

8: 64^{o}C for 35 cycles with 2% DMSO

Integrin subunit primer sequences were generated using NCBI PubMed nucleotide and primer Blast software. Sequences with the highest percentage sequence homology to the subunit were selected.

Table 1: *Alpha subunit integrin primer sequences and expected product size*

Subunit		Primer Sequence		Product Size (bp)
Alpha 1	3’	TAGGCCGCAGGGGTGGTCTC	5’	654
	5’	ACCGAGGCTGCCCAGCGATA	3’	
Alpha 2	3’	AGCCGGAAGTGCCCCAGTGA	5’	678
	5’	TCACCACACCAGCGAGCCCT	3’	
Alpha 4	3’	GCCACTACGATCGCTCCGCC	5’	590
	5’	AGGGTGACCCCCAGCCACTG	3’	
Alpha 5	3’	GCGTGCCCAAGGGGAACCTC	5’	673
	5’	TCCAGGCTGCAACTGCGCTC	3’	
Alpha 6	3’	CTCTACCTGTCCGCGGGGCT	5’	219
	5’	GCCCCCTGTTCTGTTCGCCC	3’	
Alpha 7	3’	GCTTGTGGGCTCCCTGGCTG	5’	457
	5’	CTGGCCAGGTGCTTGCCTCC	3’	
Alpha 8	3’	CGTGGGCTGGCCGTTCTCTG	5’	301
	5’	TCCTCCCAGGCGACCCACTG	3’	
Alpha 9	3’	CTCGCTGTAGCCCATCGCCG	5’	472
	5’	AGGTCTTCCCACAGGGCGCA	3’	
Alpha 10	3’	AGGCTGCTGAGGCTGGTTCACA	5’	700
	5’	CGGGGCGGAGGATAACCTTCTT	3’	
Alpha 11	3’	CTGGGTGCCGGCAGTGACAG	5’	488
	5’	GGGCCAGCCTCAGGTTGCAG	3’	
Alpha X	3’	CCGTCTGAGTACCCGGGCCA	5’	495
	5’	CGCTGCCACTGCTGGTCCTC	3’	
Alpha V	3’	CACAGCTCGGCAGTTCGGGG	5’	392
	5’	CCGGCGGCTGGATGAGCATT	3’	

.

Table 2: *Beta subunit integrin primer sequence table with expected product size.*

Subunit		Primer Sequence		Product Size (bp)
Beta 1	3’	TGCAGGTGCAATGAGGGGCG	5’	597
	5’	AGGATCGACCTGCACCGGCT	3’	
Beta 2	3’	TTCGACCAACGGGGGCAACG	5’	596
	5’	TGGCAGCGGCCATCATTGGG	3’	
Beta 3	3’	GCTGGCGGGCGTTGTTGTTG	5’	629
	5’	AGCGGGACACCTGGTCGGTT	3’	
Beta 4 (V2)	3’	TTAAGGCGCGCAATGGGGCA	5’	467
	5’	AGCCCCACGGGAATCTTGGGA	3’	
Beta 5	3’	CGTCAGCACATGCAGGGCCA	5’	522
	5’	ACAGGGGGTTTGAGGCTTTGGA	3’	
Beta 6	3’	TCACGGCTTCCAGCTTTGGTGCT	5’	564
	5’	CTCTTTGGCCAGCCGGGAGC	3’	
Beta 7	3’	TGCTGGTTCTGGGCGGAGGT	5’	603
	5’	GCTTGGAGGGCACGGTGCTT	5’	
Beta 8	3’	CGGGCCATCGGCTGTCCAAG	5’	454
	5’	CAGCTGGAGGCACCTGGCAC	3’	

PCR products were run on a 1% agarose gel containing ethidium bromide to stain DNA to make visualisation under UV light possible. Gels were run for 1 hour at 100 V with a 1 kilobase ladder (Bioline Hyperladder 1).

Kathryn J. Aviss

Chapter 3: Scaffold Characterisation

Investigations into the physical characteristics of electrospun PLGA

The University of Manchester

3.1 Introduction

Electrospinning is a versatile method to produce fibrous meshes with distinct architectures. Depending on the method of collecting the fibres, it is possible to make a mesh consisting of randomly oriented fibres or aligned fibres. PLGA (poly lactide-co-glycolide) is biodegradable polymer that has been electrospun into randomly oriented fibres (Huang et al., 2006; Li et al., 2006) and used for cell culture. Using an aligned fibrous scaffold for cell culture has been shown to influence the directionality of growth of different cell types (Bashur et al., 2006; Choi et al., 2008; Li et al., 2007; Wang et al., 2009; Zong et al., 2005). Cells have been shown to respond to topographical cues by aligning and elongating with the directionality of the surface (Aviss et al., 2010).

The physical and chemical attributes of a polymeric scaffold for tissue engineering are vital to ensure the scaffold is mechanically and physically relevant for the tissue, and that the polymer will not release any toxic elements into the extracellular environment that may prohibit cellular growth and affect behaviour. The characterisation techniques commonly employed to investigate a given polymer are as follows: DSC (differential scanning calorimetry) for investigating thermometric behaviour and crystallinity of a polymer, water contact angle to investigate hydrophobicity of the polymer, FTIR (Fourier transform infrared spectroscopy), TgA (thermogravimetric analysis) for monitoring any residual solvent that may be within the scaffold, SEM (scanning electron microscopy) for visualising the surface topography of the scaffold, and mechanical testing to determine the tensile strength and elasticity of the scaffold.

The hypothesis for this project is that for skeletal muscle tissue engineering, an elastomeric polymer would be optimal. This could avoid cell detachment during myoblast

differentiation: differentiating myoblasts will begin to spontaneously contract which often leads to mass cellular detachment from stiff surfaces (Engler et al., 2004; Levi-Mishali et al., 2009; Ren et al., 2008). This scaffold should also contain the topographical cues necessary to encourage myoblast, and consequently myofibre alignment, which should result in optimal cell behaviour. Electrospinning provides an easy method to create such a scaffold with the relevant polymer. Synthetic polymers that have been electrospun for tissue engineering include; Nylon (Huber et al., 2007), PCL (polycaprolactone) (Choi et al., 2008; Li et al., 2007), PLLA (poly-l-lactide) (Blackwood et al., 2008; Huang et al., 2006; Wang et al., 2009), PLGA (Aviss et al., 2010; Li et al., 2006), and blends of PCL and collagen (Choi et al., 2008). The range of tissues this encompasses includes heart tissue (Zong et al., 2005), skin (Blackwood et al., 2008), skeletal muscle (Choi et al., 2008; Riboldi et al., 2005), nerve regeneration (Wang et al., 2009), bladder tissue engineering (Baker et al., 2009) and stem cell culture (Li et al., 2007). The work in this project used electrospun PL85:GA15 (the DL form of lactide) as the scaffold as it is an elastomeric, biodegradable, FDA approved polymer that is easily electrospun with no requirement for post-spinning cross-linking or processing.

It is widely known that the DL-lactide, used commonly in co-polymer blends of lactide and glycolide, is slower to biodegrade than the glycolic acid even though it is amorphous like glycolide (Ratner et al., 2004). Combining lactide and glycolide in varying ratios can result in differing degradation rates; increasing lactide content lengthens the degradation process. Important aspects of scaffold degradation when it is to be used in tissue engineering is the maintenance of structural integrity, this can be monitored by measuring the mass of the polymer as it degrades and also obtaining a visual of the scaffold over the degradation time using SEM. SEM will provide information about the surface morphology

of the scaffold, which is what any cells cultured on the scaffold will encounter. It is also important to monitor the pH of the media surrounding the degrading scaffold. Because PLGA is made up of acidic components it is important to ensure these acidic monomers do not alter the pH of the environment in a way that will cause detriment the cells.

Electrospinning is an effective method to use for skeletal muscle tissue engineering as the parameters of the process can be altered to control the fibrous mesh product to the specifications needed for the application (as discussed in Chapter 1). For skeletal muscle tissue engineering, the ease at which aligned fibres can be produced is highly advantageous as an oriented scaffold will encourage consequent cellular alignment and fusion via the topographical cues the template provides.

3.2 Results and Discussion

3.2.1 DSC

DSC (differential scanning calorimetry) is a thermoanalytical method to determine crystallinity within a polymer, and the glass transition phase (Tg). Crystalline polymers present traces with a definite peak in heat flow as melting occurs, whereas amorphous polymers, such as PLGA, with the DL form of lactide used here, do not exhibit a melting temperature, but present a Tg instead (Callister, 2007).

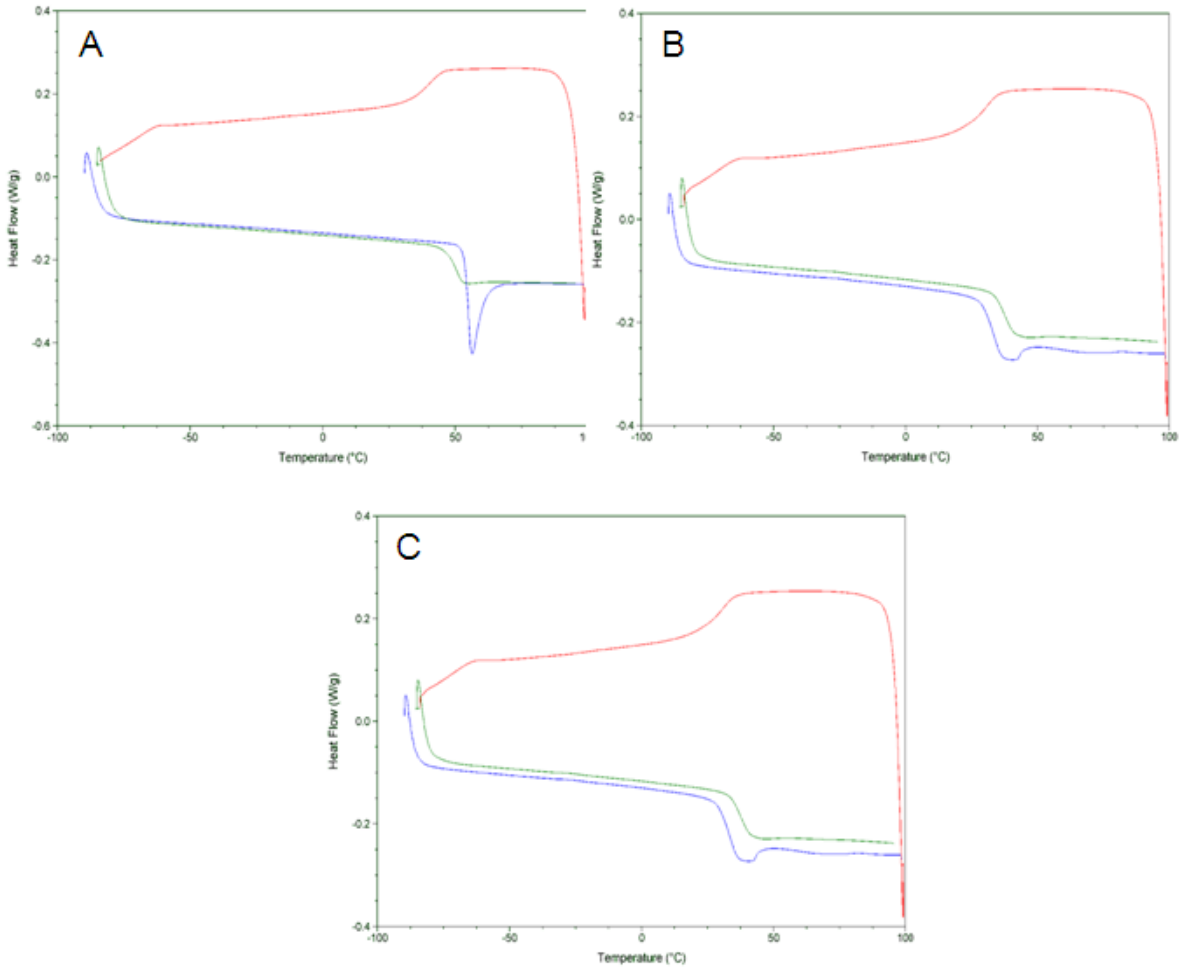

Figure 9: *DSC traces of PLGA; A represents PLGA pellets pre-spinning, B represents aligned electrospun fibres, and C represents randomly oriented electrospun fibres. Blue line indicates initial heat cycle, red line indicates cool cycle, and green line indicates final heat cycle.*

The traces shown in figure 9 compare PLGA pellets with electrospun random and aligned fibres. From the cooling cycle (red line) it is possible to note that this type of PLGA with the DL lactide is indeed amorphous as there is no peak to indicate crystallinity within the polymer. We can also determine the glass transition temperatures (Tg) from both heating cycles: see table below. There is no melting temperature for PLGA as it is an amorphous polymer; upon heating PLGA will degrade rather than melt.

Table 3: *Results from DSC: Average Tg (n=3) for each PLGA type values shown ± standard deviation.*

	Pellet (n=3)	Aligned (n=3)	Random (n=3)
Tg 1st heat	54.2°C ±0.26	35.01°C ±0.9	38.03°C ±5.83
Tg 2nd heat	50.25°C ±0.25	41°C 0.63	41.48°C ±2.94

From the DSC results shown in table 3, it can be concluded that electrospinning lowers the Tg temperature by approximately 3°C, by comparing the first and second heat cycle Tgs from the electrospun samples. It is unlikely that the electrospinning process itself is the cause for this lowered Tg, it is more likely to be due to residual solvent within the mesh as this solvent will plasticize the polymer for the first heat (blue line); the solvent will have evaporated for the second heat cycle (green line) thus yielding a true Tg for electrospun PLGA itself with no solvent. For cellular studies, the electrospun polymer scaffold will be in an environment with a temperature around its Tg: 37°C. This difference between Tg and environmental temperature may have an effect on the malleability of the scaffold, perhaps making it softer. Looking at the DSC trace from the unprocessed PLGA pellet (figure 9 A), there is a large peak in the first heat, which yields a 4°C higher Tg than on the second heat. This could be due to physical ageing of the polymer from the point of production. The second heat cycle Tg, which is lower, shows the Tg of fresh, unprocessed PLGA as the first heat cycle erases all thermal history. Electrospun samples appear to have a generally lower Tg than the unprocessed pellet, this could be due to the PLGA being dissolved in the solvent HFIP which will relax the polymer chains and also erase thermal history.

3.2.2 Residual Solvent

Residual solvent is important to monitor as the solvents used in electrospinning may be toxic in order to dissolve the polymers used. Fourier Transfer Infrared (FTIR) spectroscopy can be used to look for the presence of solvent in the scaffold by looking for the relevant peaks in the spectra. Thermogravimetric analysis is a method that uses controlled increase in temperature to monitor weight loss within the sample. Using TgA it is possible to look for weight loss at a specific point e.g. the boiling point of the solvent. This data will show at what temperature the weight loss occurred and be able to calculate total weight loss. Total weight loss in a properly constructed experiment will give a percentage of weight that is lost through residual solvent. Residual solvent in electrospun scaffolds was investigated by Nam et al (Nam et al., 2008). Nam et al found that up to 250 ppm of HFIP had no significant ($P = >0.05$) detrimental effect on chondrocyte culture in HFIP doped media over 2 days culture. When the concentration was increased to 500 ppm and 1000 ppm the number of proliferative chondrocytes significantly decreased ($P = <0.05$) (Nam et al., 2008).

Residual solvent may be an issue if the solvent used in the processing is highly toxic to cells. HFIP is a by-product of sevofluorane, an anaesthetic routinely used for decades (Holaday and Smith, 1981), and the excretion rate of this compound has been extensively studied (Holaday and Smith, 1981; Kharasch et al., 1995a; Kharasch et al., 1995b). HFIP is glucouronised in the body to be excreted in urine. HFIP has also been used as a sterilising agent (Nam et al., 2008).

3.2.2.1 FTIR

To measure residual solvent being released from the electrospun PLGA scaffolds FTIR (fourier transfer infrared spectroscopy) was used to get an approximate idea of the presence of HFIP by looking for OH band stretching in the spectra that would indicate presence of solvent as it is not present in PLGA.

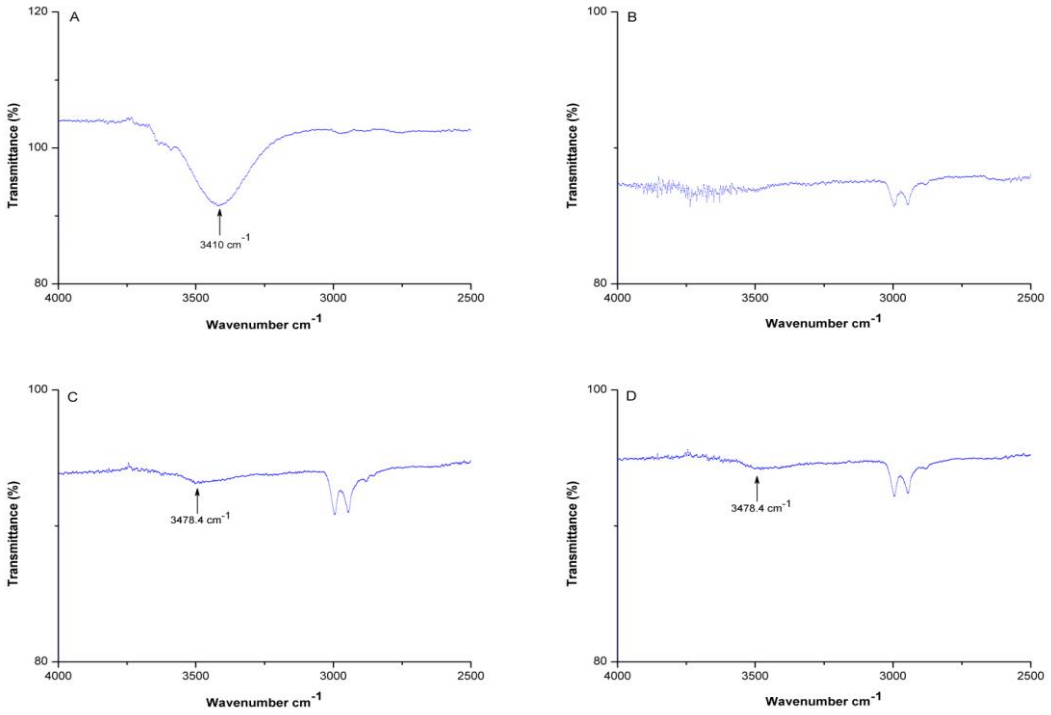

Figure 10: *FTIR spectra illustrating distinct OH banding indicating presence of solvent. Spectra A illustrates HFIP solvent alone, B a PLGA pellet prior to electrospinning, C aligned electrospun PLGA 24 hours after spinning, and D shows random electrospun PLGA 24 hours after spinning.*

From the above FTIR spectra in figure 10 we can see the peak in the region corresponding to the OH banding region is highlighted in each spectrum. In A, as it is solvent alone, the solvent OH peak is definite at wavenumber 3410 cm^{-1}. In B the spectra trace remains flat as there is no solvent present to create a peak in the OH region. In

spectra C and D there is a small peak which would indicate presence of solvent at around wavenumber 3500 cm^{-1}, which correlates with the wavenumber of the OH band in HFIP alone. As this is the electrospun sample, it can be assumed that this peak represents residual solvent. FTIR is not a quantitative method however so TgA was also performed to generate a more accurate account of residual solvent within the electrospun scaffold.

3.2.2.2 TgA

Scaffolds measured for TgA had been fabricated through electrospinning 3 days prior to the analysis, having been stored in a desiccator. From the TgA runs, a very small amount of solvent was measured. This was done by using a slow rate of temperature increase inclement between 0^oC and 100^oC (5^oC / min) as HFIP has a boiling point of 60^oC. The maximum weight loss was recorded for each sample, as shown in table 4 this value was always around 60^oC corresponding to the boiling point of HFIP. Total weight loss was measured at around 90^oC in order to include all weight loss occurring and was calculated using Universal Analysis (TA instruments) software and came to an average (n = 3 per scaffold type) of 3.57% in aligned fibres, 4% in randomly oriented fibres, and 11.16% in spin coated PLGA. The amount of residual solvent present in the electrospun fibres is unlikely to create any significant problems with cell culture, indeed over the 14 day period in which cells were cultured for this project no adverse reactions were observed (see section 5.2.5). There is more solvent present in the spin coated polymer; this is to be expected as spin coating does not allow for much solvent evaporation.

Table 4: *TgA results showing weight loss corresponding to residual solvent evaporation. Weight (%) corresponds to the percentage of material weight present at the temperature recorded in the adjacent column. 3 samples of each PLGA form was used, the average values are presented here.*

Form of PLGA	Max Weight Loss Temperature (^{o}C)	Residual Weight (%)	Weight Loss at 90^{o}C (%)
Aligned Fibres	61.65	96.43	3.57
Random Fibres	56.84	85.96	4.04
Spin Coated	75.94	88.84	11.16
Pellet	N/A	99.93	0.07

A scaffold that releases toxic compounds as it degrades may be detrimental to cell survival. In this project, using electrospinning, the PLGA is dissolved in a solvent (HFIP). In high doses this solvent can be harmful (Nam et al., 2008), but it is a byproduct of anaesthetics used in routine medicine so can be easily excreted from tissues at low concentrations (Kharasch et al., 1995a; Kharasch et al., 1995b). In a metabolic tissue like skeletal muscle low concentrations of HFIP may not be toxic; from the electrospinning process the majority of the solvent has evaporated before the polymer collects on the rotating mandrel, as shown by FTIR and TgA.

3.2.3 Fibre Characterisation

3.2.3.1 SEM Analysis – Fibre alignment

Using images captured via SEM it is possible to analyse the morphological characteristics of the electrospun fibres. Fibre alignment is important, although fibres produced here are visually aligned; it is also possible to quantify this alignment statistically.

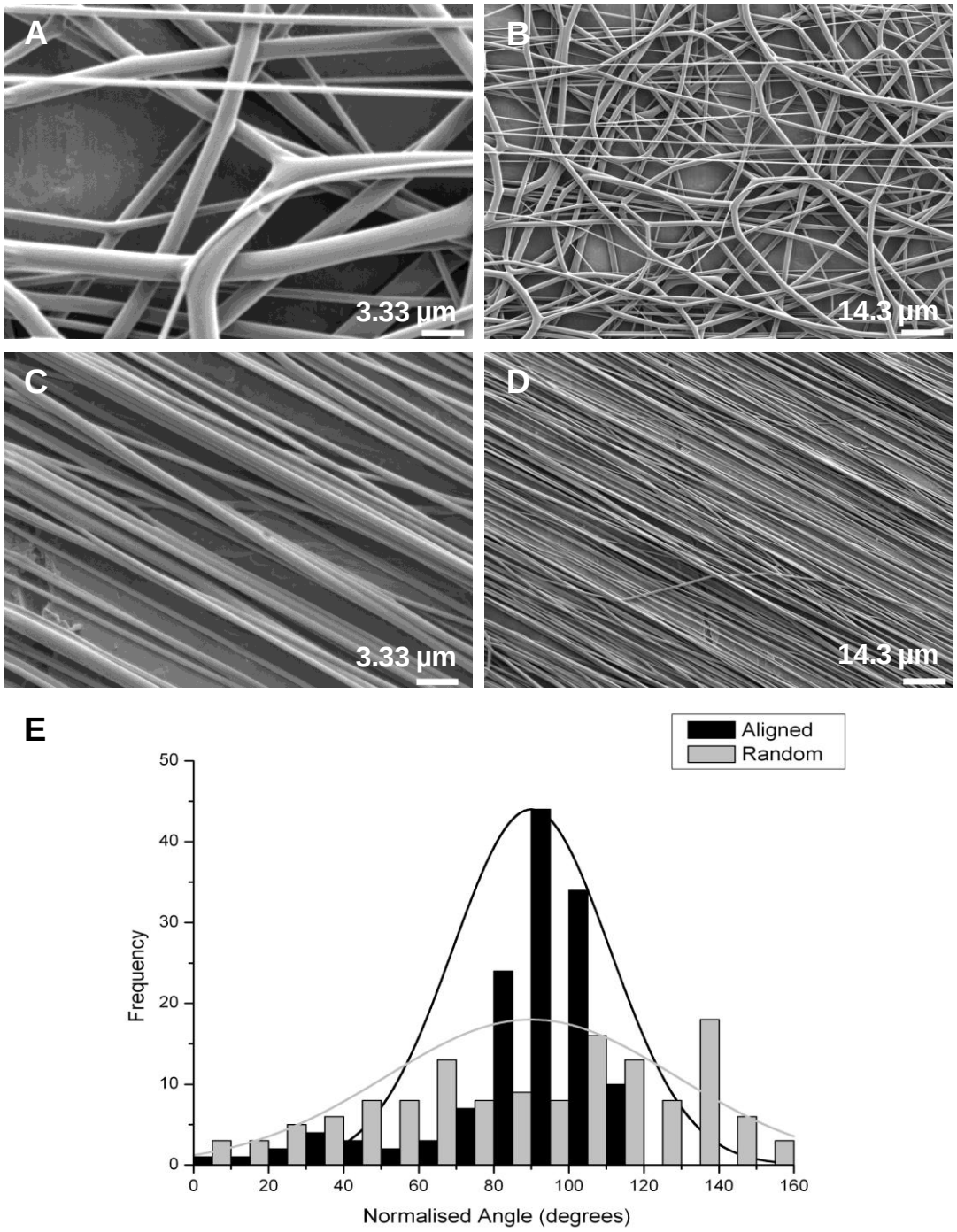

Figure 11: *Scanning electron micrographs of electrospun PLGA aligned and randomly oriented fibres: A (Mag: 3000 x) and B (Mag: 700x) illustrate SEM images of aligned fibres, C (Mag 3000 x) and D (Mag 700x) illustrate SEM images of randomly oriented fibres (Aviss et al., 2010). Graph E shows histogram of average angle distribution in random and aligned fibres. N = 75.*

Images shown here in Figure 11 illustrate the difference in fibre orientation in aligned and random fibres. It is clear to see that the degree of alignment in the aligned fibres, compared to the randomly oriented fibres is high. Graph E in figure 11 shows the distribution of angles in random and aligned fibres normalised to 180^{o} to show the spectrum of angle deviation within the electrospun fibres. These data reinforce that alignment is present in the aligned fibre system compared to random fibres as the majority of aligned fibres lie in the 90.5-100 group and the 100.5-110 degrees groups, this shows most fibres are at or around 90^{o} when all normalised to 180^{o}. A students t-test was applied to the average angle deviation from 90 degrees data, the difference between the fibre types was shown to be significant ($P = <0.05$), with aligned fibres closer to 90 degrees than random.

Table 5: *Standard deviation of mean angle measurements in random and aligned fibres on the left, and average angle measures on the right, measured using Image Tool software (n = 75 per fibre type) (Aviss et al., 2010).*

	Random	Aligned
Standard Deviation	74.7	19.5

Table 5 shows that there is a difference in standard deviation from the mean of angle measurements, a large deviation indicates a large variability in angles in random fibres, whilst a smaller deviation in aligned fibres indicates a smaller variability in the direction of fibres. This table illustrates that the standard deviation, and therefore the variety of angle deviance from 90 degrees, is much greater in random fibres indicating a greater difference in angle measurements. Aligned fibres have a much smaller deviation from the mean as there is greater directionality and parallelism.

3.2.3.2 SEM Analysis – Fibre diameter

Using the same software used to measure fibre alignment, it is also possible to measure fibre diameter. Fibre diameter is an important measure as it determines the range of fibres cells respond to and also may illustrate some interesting differences between aligned and randomly oriented electrospun fibres.

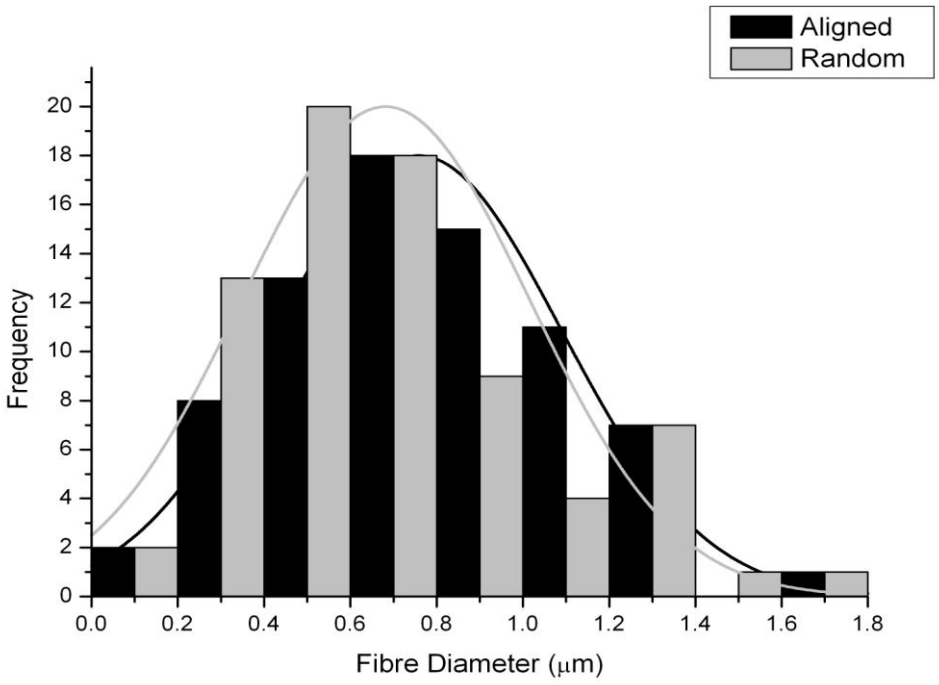

Figure 12: *Histogram illustrating the distribution of fibre diameters in electrospun fibres. Fibre diameters were measured from 10 SEM images per fibre type using ImageJ software.*

From the graph presented in figure 12 it can be seen that there is little difference in diameter distribution between the different scaffold architectures. The majority of random fibre diameters lie between 0.5 μm and 0.8μm. The majority of aligned fibre diameters lie between 0.6μm and 0.9 μm. The moving average trend lines added to the histogram show this shift in fibre diameter. The average fibre diameter in aligned and randomly oriented

electrospun PLGA fibres was not significantly different (P = >0.05, n=75, from 5 different 5 kX magnification SEM images of each fibre type). The actual difference between the average fibre diameters between the two scaffold types is 0.08 µm, with aligned fibres being larger, on average.

3.2.4 Hydrophobicity

3.2.4.1 Water Contact Angle

Hydrophobicity plays a role in the biocompatibility of the scaffold as it influences how proteins will adsorb to the surface. Measuring the contact angle of a water droplet on a surface can give an insight into the hydrophobic nature of the surface; a large contact angle would indicate a more hydrophobic surface. All samples were incubated with the described solution overnight, the solution was then removed and samples were air dried overnight at room temperature before testing for contact angle.

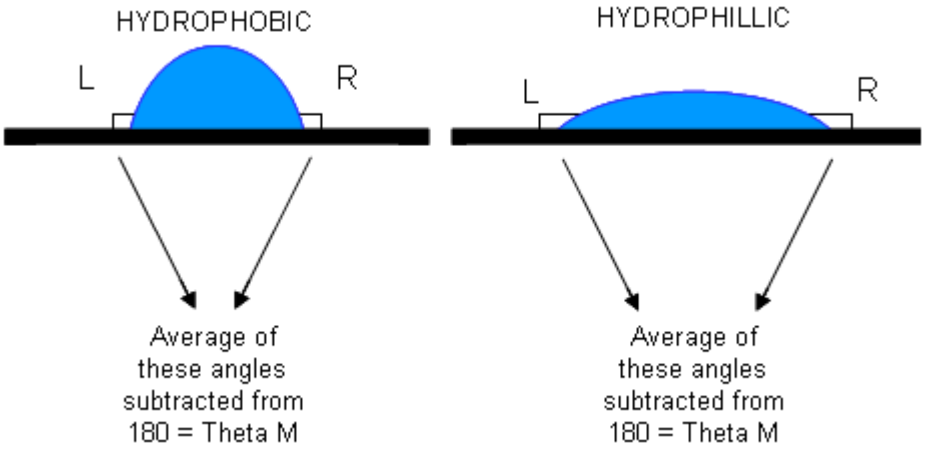

Figure 13: *Schematic to how the theta (M) values are obtained from the drop shape analysis software.*

Figure 13 shows how the measure of contact angle: theta (M) is obtained. Theta (M) is the average of the left and right angles measured in Theta (L) and (R). The angle was measured using a Drop Shaper Analyser (Kruss DSA100) by measuring the angle from the outer edge of the droplet to the surface, and subtracted this number from 180 degrees. PCL was used as a comparison as it is a commonly used polymer for soft tissue engineering. From figure 14 PCL appears more hydrophobic than PLGA, as it has larger Theta (M) values. Water contact angles of the spin coated measured here, are similar to Zhu et al (Zhu et al., 2006) finding a contact angle of 76^{o}, and Wang et al (Wang et al., 2003) finding an angle of 75.5^{o}. Results obtained in the current study are lower than these with the spin coated PLGA being 67^{o}. This could be due to the ratio of lactide to glycolide used; in this study the ratio is 85 lactide:15 glycolide, whereas in both studies it was 75:25. The data shown in figure 12 show that the contact angle of electrospun PLGA scaffolds are double that of the spin coated with random and aligned fibres showing very similar values around 130^{o}. Park et al (Park et al., 2010) electrospun PL50:GA50 and tested hydrophobicity before and after plasma treatment. Before treatment the found that their PLGA scaffolds had a contact angle of 138.8^{o}, and after 180 seconds of plasma treatment this was decreased to 47.4^{o}. Kim et al (Kim et al., 2003) found, with their electrospun PL75:GA25, a contact angle of 105^{o}.

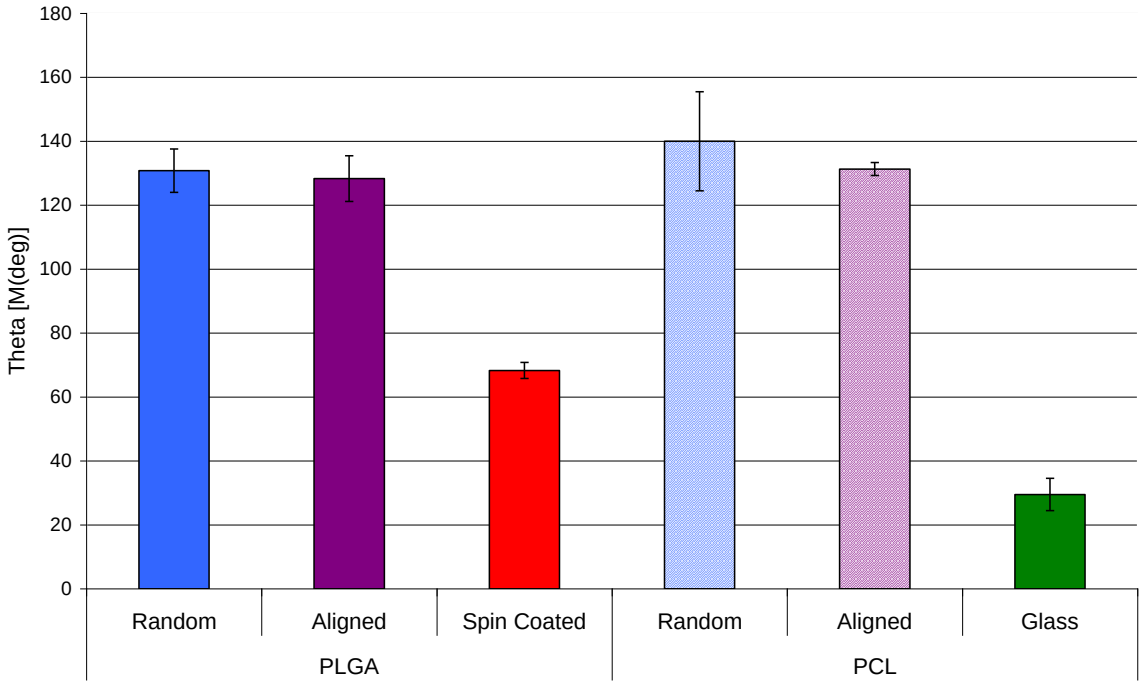

Figure 14: *Average water contact angle measurements for non-conditioned PLGA, PCL and glass mean values shown here, n = 3 +\- standard deviation.*

Adsorption of proteins to a surface influences cellular adhesion to the surface. As proteins adsorb, they will tend to hide their hydrophobic areas, exposing their hydrophilic areas towards the air-liquid interface when contact angle is measured. Because of this we can expect a decrease in hydrophobicity on the surfaces after protein adsorption has taken place. Cell culture media contains serum, which is high in proteins that can adsorb onto the surface of the scaffold. It is common for biodegradable polyester scaffolds to be soaked in growth media prior to cell seeding to enhance cellular adhesion to the hydrophobic surface. Using water contact angle the change in hydrophobicity can be monitored in response to proteins from media containing serum adsorbing to the surface.

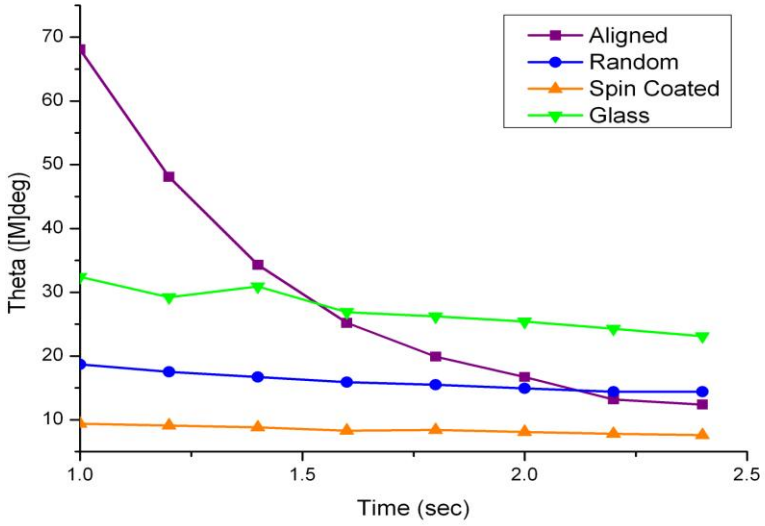

Figure 15: *Water contact angle of growth media conditioned PLGA and glass substrates.*

Figure 15 shows the water contact angle of growth media conditioned substrates. These data indicate that aligned PLGA fibres begin the most hydrophobic surface of the ones tested here, but rapidly (just over 1 second) becomes more hydrophilic than randomly oriented electrospun fibres. The spin coated surface remains the most hydrophilic surface from the beginning of the test to the end (5 seconds long). Glass is the most hydrophobic surface when treated with growth media, apart from the initial data points from the aligned fibres. The difference between the aligned fibres and random fibres throughout the test is interesting, as aligned fibres begin more hydrophobic with a much higher contact angle; the aligned data stops just before the 3 second time point because the droplet became too flat to be measured, i.e. the surface was so hydrophilic the droplet was adsorbed very rapidly. This result is unlikely to be due to the difference in hydrophobicity between fibre types, more over the architecture of the aligned fibres will allow water to wick through thus

giving the appearance of hydrophillicity compared to random fibres which will not allow wicking as freely as aligned fibres.

Kim and Park (2006) tested their electrospun blend of PLGA-*b*-PEG-NH2 diblock copolymer for hydrophobicity and found that addition of RGD sequences to the surface of the scaffold drastically decreased the water contact angle in a similar fashion to the results presented in figure 15 (Kim and Park, 2006). Comparing the non-conditioned data here in figure 14 to the PLGA as in Kim and Park it can be seen that inclusion of the hydrophilic PEGylated polymer decreases the water contact angle by approx. 50 degrees, comparing the random fibres from figure 14 to their fibres, which are all random.

3.2.5 Mechanical Testing

The importance of measuring the elasticity of a scaffold for tissue engineering of skeletal muscle has been discussed at great length in this thesis. Using tensile testing it is possible to measure the Young's modulus and hence the stress and strains the polymer tolerates under controlled loading conditions. Constant load was applied uni-directionally to the scaffolds, along the length of the fibres as spun in the direction of the mandrel rotation, parallel to expected fibre orientation and perpendicular to the mandrel rotation direction. See figure 16 below for visual description.

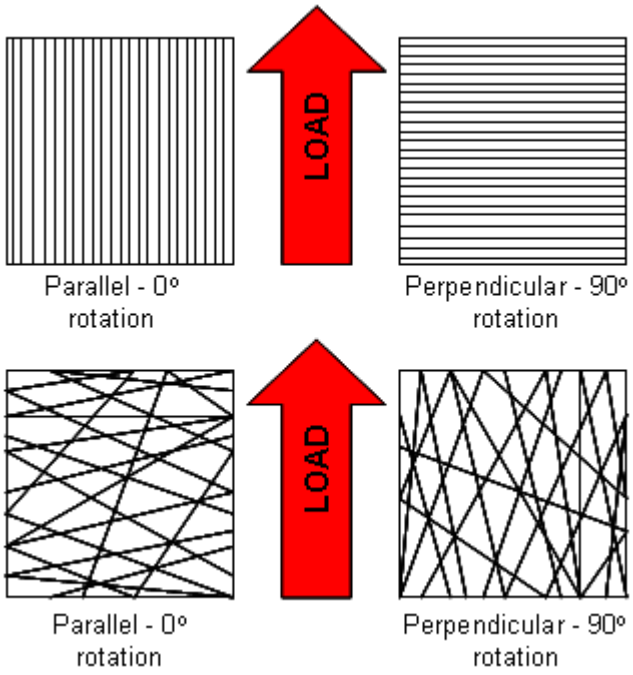

Figure 16: *Diagrammatic illustration of load application to the direction of fibre orientation; top panel illustrates aligned fibres, bottom panel illustrates random fibres, arrow indicates direction of load application.*

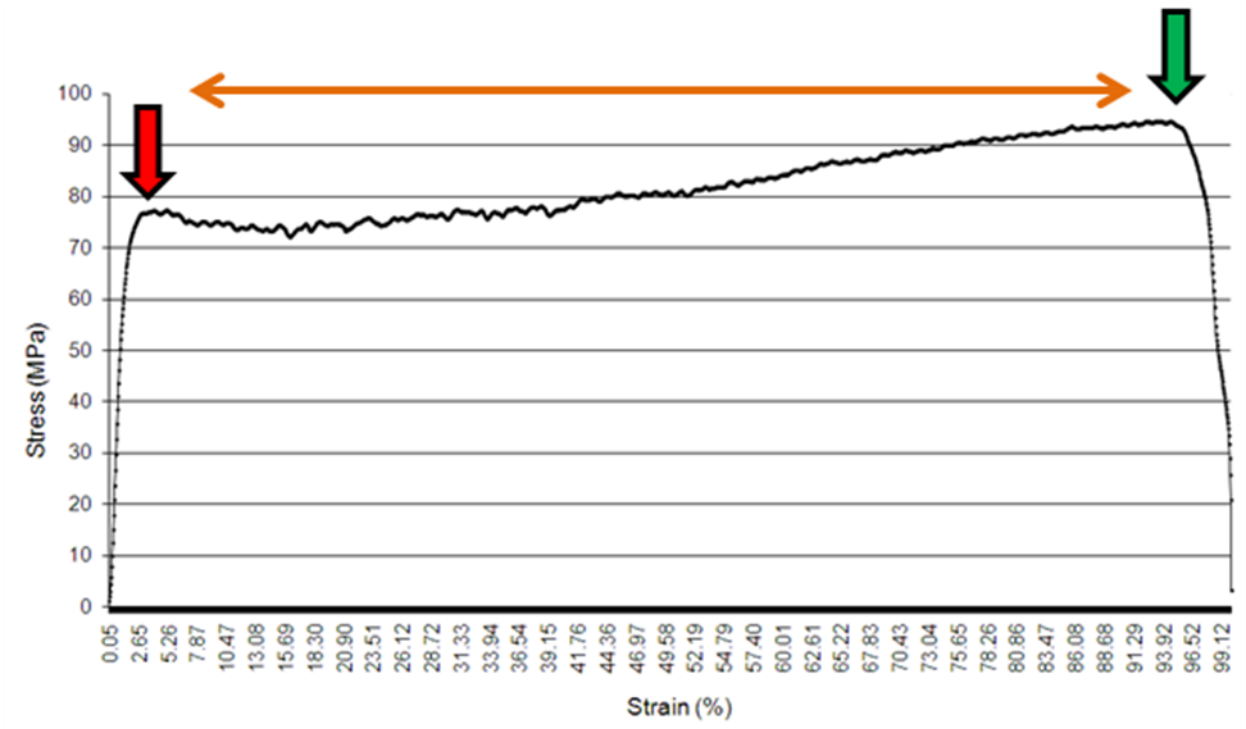

Figure 17: *A typical representative stress-strain curve. From an aligned mesh with load applied perpendicularly.*

Figure 17 illustrates the shape of a typical stress-strain curve which is representative for all samples tested, random and aligned, parallel and perpendicular. The red arrow indicates the yield point of the mesh, the orange arrow indicates the rubbery plateau, and the green arrow indicates the ultimate tensile stress (UTS) point. Young's Modulus is calculated by dividing stress by strain at the yield point. The straight area of the curve, from the origin to the yield point, is where the material could elastically retract back to its original length after loading up to the yield point.

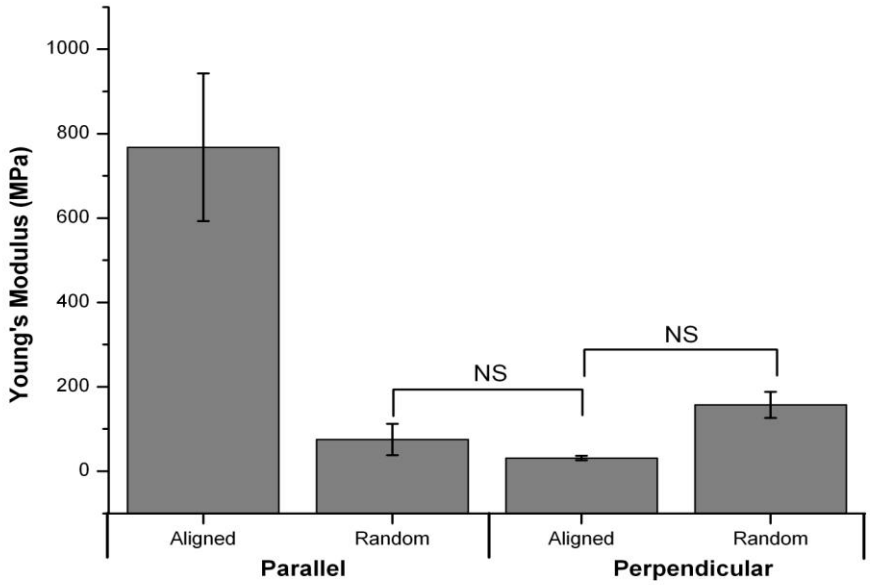

Figure 18: *This graph illustrates the average Young's Modulus calculated from stress-strain curves of random and aligned PLGA fibres, both parallel and perpendicularly tested (n = 7 for parallel, n = 4 for perpendicular), bars indicate standard deviation, brackets indicate values that were not significantly different by student's t-test P = >0.05), all other values are significantly different from each other (P = <0.05) (Aviss et al., 2010).*

Figure 18 illustrates the average Young's Modulus of electrospun PLGA tested by loading samples parallel to direction of rotation of mandrel and perpendicularly from this. These data show that aligned fibres, tested with the load applied parallel to the direction of the fibres as collected from the mandrel, are much stiffer than random fibres tested in the same way and also both types of fibre with load applied perpendicular to the direction of mandrel rotation. All average Young's Modulus values were significantly different (P = <0.05 student's t-test) from each other apart from those labelled with brackets and NS (not significant) on the graph in figure 18. The augmented difference between the methods of

load bearing in aligned fibres, compared to random fibres reinforces the indication of alignment within the aligned fibres as it would be expected that pulling aligned fibres perpendicularly; i.e. pulling them apart from one another, would yield such a difference in tensile strength. There would be very little resistance to the load application in perpendicular aligned fibres compared to parallel as in parallel fibres the load is transmitted along the length of the fibres, applying stress equally. In random fibres it is interesting to note that there is a significant difference between fibres pulled in either direction; fibres perpendicularly tested were stiffer than those tested parallel to the mandrel rotation direction. It is expected that random fibres appear much more elastic than aligned fibres when load is applied along the length of the fibres as the load will initially straighten out the fibres in the random mesh before any real load is absorbed by the polymer fibres. In aligned fibres the load is applied directly along the length of the fibres, increasing true strain instantly as all fibres can contribute to load bearing.

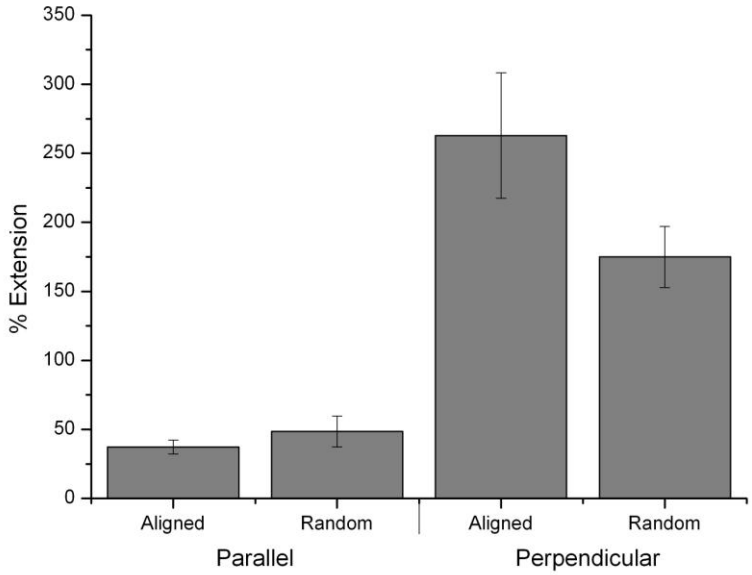

Figure 19: *Graph showing percentage extension from tensile testing of electrospun random and aligned scaffolds tested parallel and perpendicular to direction of mandrel rotation.*

The percentage extension of the scaffolds is shown in the graph in figure 19. Percentage extension increases dramatically when fibres are tested perpendicularly. This could be due to the effect described before with the fibres becoming aligned in response to the load thus yielding an artificially low modulus. The difference in extension in random fibres tested parallel and perpendicular is quite interesting, especially when one takes into account the Young's modulus data simultaneously, figures 18 and 19. There is not a great difference in elasticity in random fibres tested either way, but there is a difference between random fibres' percentage extension when comparing parallel and perpendicular.

Table 6: *Mechanical properties of electrospun PLGA tested parallel and perpendicularly. Values shown are ± standard deviation.*

	Parallel (n = 7)	**Perpendicular (n = 4)**
Average Young's Modulus (MPa)		
Aligned	767.28 ± 175	31.38 ± 5.2
Random	75.235 ± 37.01	157 ± 30.7
Average Yield Point (MPa)		
Aligned	1614.835 ± 266.06	115.55 ± 35.92
Random	227.341 ± 61.01	294.32 ± 35.7
Average Ultimate Tensile Strength (MPa)		
Aligned	1342.330 ± 232.05	132.85 ± 36.76
Random	195.703 ± 50.66	277.3 ± 9.06

As discussed the polymer used for this application requires a degree of elasticity in order for functional, contractile myofibres to develop. Using the stress-strain curves obtained

from mechanical testing, the average Young's Modulus of each type of fibre was determined. Young's Modulus is a measure of stiffness and therefore elasticity. The lower the Young's Modulus value the more elastic a material is, conversely a larger Young's Modulus indicates a stiffer material. The yield point of a material, found using this method of tensile testing, indicates at what point a material ceases to be elastic; i.e. will not retract to original length past a certain point. After the yield point this material enters a rubbery plateau where polymer chains slide past each other, no elastic retraction is possible past the yield point. The ultimate tensile strength (UTS) is the final point in the rubbery plateau, after this point the polymer has ruptured and/or broken losing all tensile strength. Results presented in table 6 indicate that parallel aligned fibres are less elastic, with a modulus of 767.28 MPa, than parallel random fibres with a modulus of 72 MPa. This may be expected as the random fibres will be forced to align as the load is applied then the fibres will start to bear the load and produce a strain; also aligned fibres could be expected to be less elastic than random due to the collection method in the electrospinning process. The difference in Young's Modulus between parallel aligned and random fibres is statistically significant ($P = <0.01$), whereas the difference in Young's Modulus between perpendicular aligned and random fibres is not statistically significant ($P = >0.01$). In both types of fibre architecture, the amorphous PLGA chains will be kinked and coiled, when load is applied the chains will elongate and straighten (Callister, 2007). Before the yield point, in a true elastomeric polymer, any deformation that has been incurred in the polymer builds entropy so if load is removed before the yield point the chains can return to their original coiled and kinked positions. Because of the totally amorphous nature of PDLGA, as shown by the DSC traces in figure 9, elastic retraction after the yield point is unlikely to occur as there are no crystalline regions to anchor the polymer chains together. Because of this, PDLGA is

better described as a plastic polymer; however this should not affect the applicability of this scaffold for skeletal muscle cell culture as the cells will not exert enough global force throughout the scaffold to stretch the polymer enough to cause deformation. Cell culture is more likely to result in localised areas of cell contraction, which should not deform the scaffold.

This tensile testing was undertaken while the scaffolds were dry and at room temperature. This is not wholly relevant for the application of the scaffold as the application will require the scaffold to be incubated at 37^{o}C, immersed in media and encountering the stresses and strains of differentiating myoblasts as they contract upon the scaffold. With regards to myoblast growth and differentiation, a 3D construct of myoblasts, described earlier by Huang et al (Huang et al., 2005), is capable of producing a specific force of 40 kN/m^2. 40 kN/m^2 is equivalent to 0.04 MPa, which is much lower than the yield point of the scaffolds.

3.2.6 Degradation study

Samples were measured for pH, wet weight, dry weight, and surface morphology. For a comparison, a flat spin coated PL85:GA15 surface made from a solution the same concentration as used for electrospinning was also monitored, in the same conditions, for degradation.

3.2.6.1 Mass loss

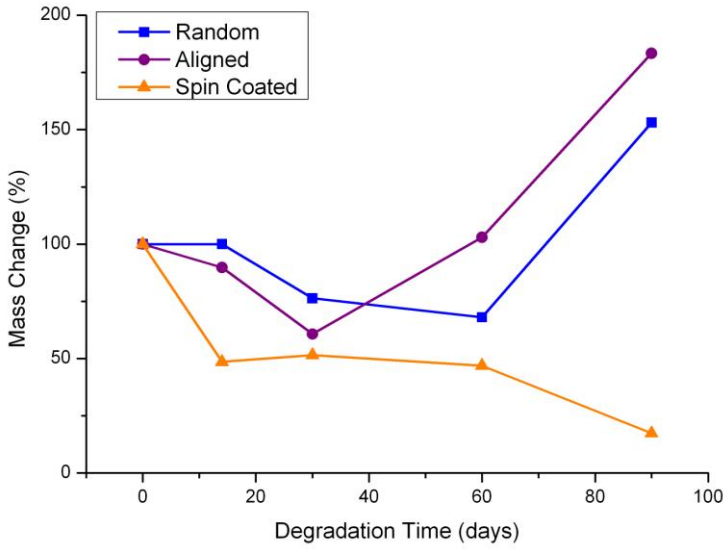

Figure 20: *Graph illustrating the changes in mass of the PLGA scaffolds over 90 days' degradation.*

Mass loss from degradation in PBS of electrospun PLGA is illustrated in figure 20. From these data mass loss appears to be variable and unpredictable. This could be due to the polymer not being fully dried out before dry weight was measured in some samples. Degradation of PGA fibres and pellets was undertaken by Ginde and Gupta in 1987 over 6 weeks in varying conditions. They found that over 6 weeks the PGA pellet lost more mass (~80%) quicker compared to the fibres which lost only around 95%, with the loss occurring after 5 weeks degradation (Ginde and Gupta, 1987). More recently Dong et al compared the degradation of electrospun fibres and pellets of PGA, PLGA, and Poly(L-lactide-co-caprolactone) P(LLA-CL) over 100 days with and without smooth muscle cell culture (Dong et al., 2010). They also found that pellets of the polymers generally degraded faster

i.e. lost more mass faster, and attained morphological defects compared to the electrospun counterparts.

Mass loss over 4 months degradation in PBS occurred quicker in spin coated PLGA than in electrospun scaffolds. This could be due to the structure of the scaffold. Spin coated PLGA may allow for stereotypical bulk degradation to occur – which includes autocatalysis from acidic monomer release (Vey et al., 2008). Because electrospun PLGA has a much greater surface area to volume ratio and is fibrous and porous, its degradation may not adhere to the bulk degradation rules. Results shown in figure 20 indicate that the electrospun fibres increase in mass as degradation time advances. Before day 80, random fibres appear to decrease in mass steadily as could be expected, but at day 90 there is a mass gain up to around 150%. With aligned fibres, this increase in mass occurs after day 30 ending with a mass gain up to around 170% at day 90. This increase in mass could be due to more water retention within the fibres.

3.2.6.2 Change in pH

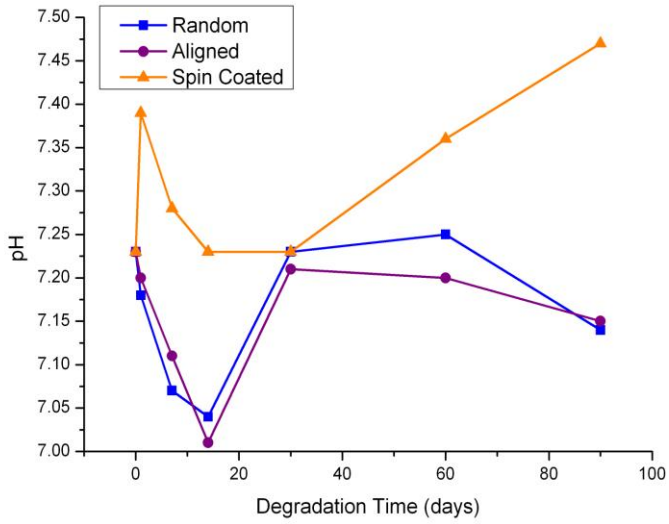

Figure 21: *Graph illustrating the changes in pH of the media surrounding the degrading PLGA scaffolds over 90 days' degradation.*

Change in pH during degradation of PLGA has mixed reviews in the literature. In this study, as shown in figure 21, there is a drop of 0.2 from the electrospun samples and an increase of 0.2 from the spin coated samples during the first 20 days of degradation. Lu et al (1999) looked at the *in vitro* degradation of thin PLGA films and found that the pH of PL75GA25 films dropped by about 0.15 over the first 10 days of degradation (Lu et al., 1999), but Vey et al (2008) show that their films dropped the pH of their surrounding media by a drastic 4 points on the pH scale from 7.5 to 3 (Vey et al., 2008). The solution used as the media for the degradation will have an effect on the changes in pH measured. PBS (phosphate buffered saline) was used for all studies described here. PBS is a buffer so is designed to not allow for great changes in pH, especially if changed for fresh solution at regular intervals which it was in all studies. Results obtained from this current study concur with this as there was not a great change in pH in the samples over the degradation

time. According to the Sigma-Aldrich Cell Culture Manual (3rd edition) (Sigma-Aldrich, 2010) fibroblasts can withstand pH ranging from 7.2 to 7.4, and transformed cells, like the C2C12 immortal cell line used in this study can withstand changes from 7.0-7.4. Results shown here in figure 21 illustrate that the electrospun PLGA is well within the range compatible for cell culture.

3.2.6.3 Architectural Changes

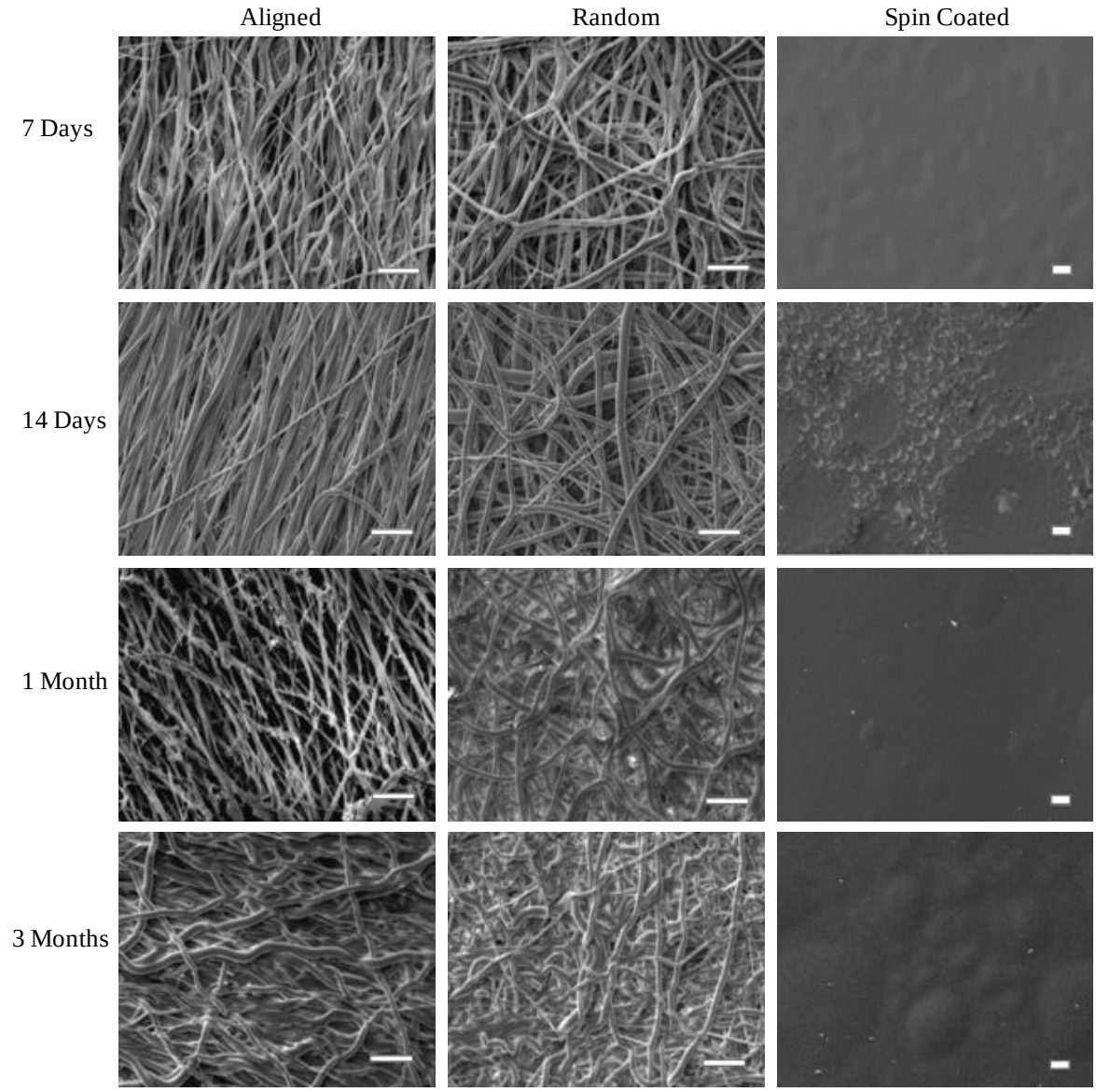

Figure 22: *SEM micrographs of degrading electrospun and spin coated PLGA over 3 months in PBS. Scale bars: on electrospun fibre images = 10µm, on spin coated images = 20µm.*

From the SEM micrographs obtained from degraded scaffolds, shown in figure 22, it can be noted that the architecture of the electrospun scaffolds is maintained over the 3 month

degradation period. It can also be noted that at one month degradation the fibres appear brittle and fractured. At three months however the fibres appear less well defined with an almost squashed appearance but not brittle or fractured. These characteristics were also noted by Meade and Merry (2010 unpublished data) at the same time points.

3.3 Conclusions

Results shown in this chapter illustrate how the physical characteristics of PLGA are applicable for skeletal muscle tissue engineering. The DSC traces shown in figure 9 show that the Tg of electrospun PLGA is between 35 and 38^{o}C, which is near physiological temperature. This may aid malleability of the scaffold which could positively influence the differentiation of myoblasts into myotubes. The DSC also shows that the electrospinning process does not physically change the polymer in any way as the PLGA is still amorphous and does not exhibit a Tm or a crystalline peak.

Investigations into residual solvent within the electrospun scaffolds reveals very little (~4%) HFIP remains within the scaffold. This is unlikely to cause toxicity when introduced to cells as it will be leached out gradually over time and, as discussed, a highly metabolic tissue like skeletal muscle will be able to excrete any it encounters. Also, as mentioned before, HFIP is a byproduct of commonly used anaesthetics so especially at this low concentration it is unlikely to incur any significant toxicity to the cells.

Section 3.2.6.3 describes the architectural characteristics of the electrospun scaffolds, showing that highly aligned fibres can be created, that are not only visually more aligned, as seen in the SEM images, but also statistically more aligned than random fibres, as shown in figure 11. The diameter of the scaffold was also investigated and was shown to be in the

same range as other electrospun scaffolds tested in the literature that encourage directional cellular growth.

Mechanical testing tested the elasticity and strength of the electrospun scaffolds. These data show that electrospun PLGA is strong enough to withstand the stresses and strains differentiating myotubes will exert onto the scaffold. Although these data were generated with dry scaffolds at room temperature it provides fundamental information about the physical capabilities of the scaffold. The mechanical testing also illustrated a significant difference between aligned fibres tested along the length of the fibres (parallel) and pulling the fibres apart from each other (perpendicular) which reinforces the amount of alignment present in the aligned fibre scaffold.

A brief degradation study undertaken here complements the literature with what was found, and shows that as electrospun PLGA degrades over 90 days the pH does not change enough to affect cellular activity, nor does the mass of the scaffold change suddenly so cellular survival will not be impaired by a sudden disappearance of the scaffold. The morphological data obtained from SEM show that the scaffold maintains morphological integrity throughout the 3 month degradation period.

3.4 Future Work

A more relevant mechanical testing technique could be utilised in order to elucidate any differences in the mechanical properties of the polymer when immersed in media at 37^{o}C, and also with active cell culture occurring on the scaffold to test any effect the cellular activity may have on the mechanical properties. Using different ratios of PLGA may alter the mechanical properties of the scaffold too; this could be investigated and optimised for skeletal muscle tissue engineering.

The degradation study could be improved by lengthening the degradation time and investigating molecular weight changes using gel permeation chromatography. Investigations into degradation of the scaffolds after cell culture would provide insights into how cells affect the degradation characteristics of the scaffolds. As Dong et al found with their PLGA scaffold, the smooth muscle cells did survive for 40 days but cells on the P(LL-CL) scaffold survived better.

Kathryn J. Aviss

Chapter 4: Biocompatibility of polymer scaffold

Investigating the initial cellular responses to the scaffold

The University of Manchester

4.1 Introduction

As discussed in chapter 1 it is essential that a material chosen for tissue engineering be biocompatible. Biocompatibility implies that a scaffold will provide a suitable base for cellular growth without releasing toxic compounds into the surrounding environment either by residual solvent from processing techniques, or as the scaffold degrades and is bioresorbed.

How proteins adsorb to a scaffold can affect its biocompatibility. As proteins adsorb to the surface they unfold and bond to the surface using Van der Waals interactions (Ratner et al., 2004), these interactions are quite stable with a urea solution required to desorb them. When the proteins have unfolded on the surface they are likely to exhibit cell adhesion recognition signals such as the ubiquitous RGD (Arg-Gly-Asp) amino acid sequence present in most extracellular matrix proteins. Previous work has shown that if a single protein e.g. fibronectin is used to adsorb onto a substrate, the likelihood of the attachment sequences being 'hidden' during unfolding increases, but introducing another protein in the mix e.g. vitronectin or albumin can provide spatial competition increasing likelihood that the recognition sequences will be displayed on the surface for cells to recognise and attach to (Ratner et al., 2004).

In order to monitor cellular activity on the scaffold two assays can be used in conjunction with each other to monitor cellular proliferation and cellular metabolism. Staining nuclei with DAPI, imaging using a fluorescent microscope then using ImageJ software to count the areas of dense pixels (nuclei) can give quantification of cell number. The advantage of using this method compared to assays such as the DNA assay is that it is more reliably replicable and there is less scope for contamination. The Alamar Blue assay is a

colorimetric assay to measure metabolic activity of cells. This assay is commonly used to measure proliferation – cell number although; because it is an enzymatic assay slight changes in environment could change cellular behaviour thus skewing results.

Measuring the immunogenic and inflammatory effects of the scaffold can be useful. A significant inflammatory response to a scaffold would seriously impede its efficacy as an implantable biomaterial. Seeding macrophage cells onto the scaffold and monitoring their response by measuring release of cytokines such as interleukin 1-β, and hydrogen peroxide which is involved in destruction of engulfed pathogens, along with morphological changes can provide an insight into how immunogenic a biomaterial is. The work described within this chapter will focus on the biocompatibility issues in the electrospun PL85:GA15 scaffolds.

4.2 Results and Discussion

4.2.1 Pre-seed conditioning of scaffold

It is common practice to condition polyester scaffolds in media prior to cell seeding (Choi et al., 2008; Li et al., 2007; Srouji et al., 2008; Wang et al., 2002) in order to deposit proteins to aid cellular adhesion. For the application of tissue engineering, minimising serum interactions with the scaffold where unnecessary is important. This is to minimise the chance of any immune or inflammatory response.

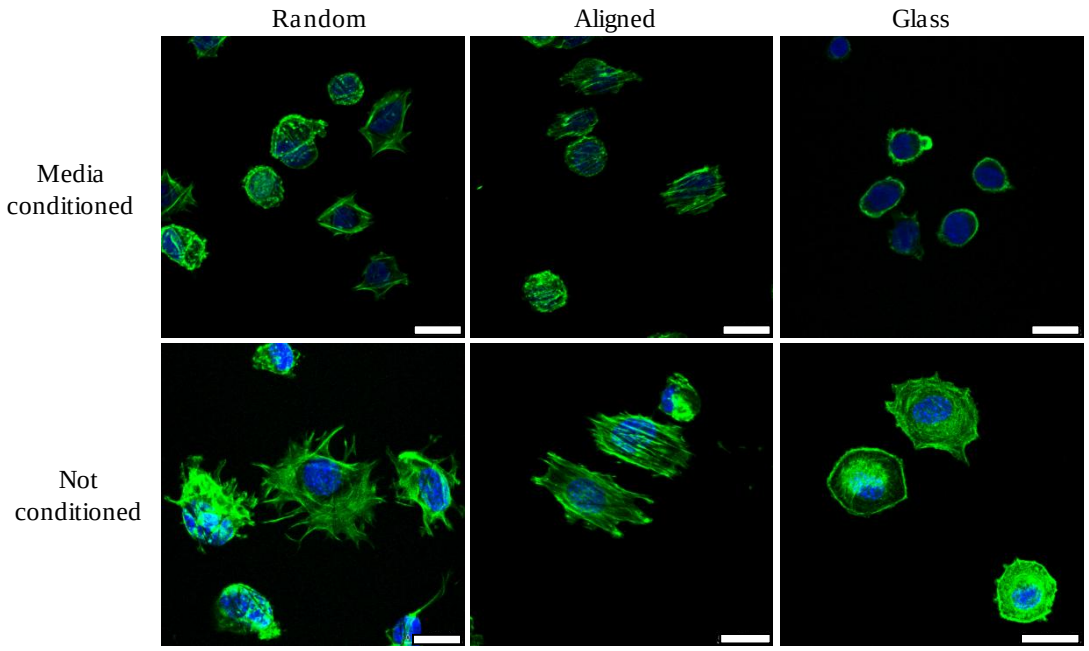

Figure 23: *C2C12 seeded on substrates with and without an overnight pre-seed incubation in growth media. Cells fixed after 30 minutes culture. Scale bars indicate 25 µm.*

The figure above (figure 23) depicts C2C12 fixed and stained for f-actin after 30 minutes culture on the substrates, with or without pre-seed media conditioning. From these images it is clear to see that conditioning the scaffolds before cell seeding is unnecessary as these cells adhere and begin to spread at similar rates whether the scaffold has been conditioned or not. Thus from here on, no scaffolds were conditioned before cell seeding. Ren et al

(2010) also found that pre-conditioning of their polyelectrolyte surfaces was not necessary for adherence and growth of C2C12 myoblasts. Ren et al's hypothesis matches the author of the current work, that the adhesion at short culture periods is due to non-specific interactions such as Van der Waals, electrostatic, and hydrophobic interactions (Ren et al., 2010).

4.2.2 Cell Survival

4.2.2.1 Proliferation Assay

Measuring the cellular response to a scaffold begins with monitoring how they grow over time. This can quickly provide information on if cells attach and proliferate, and if so how rapidly. Results shown in graph A, figure 24, illustrate the metabolic behaviour pattern of myoblasts seeded on electrospun scaffolds compared to tissue culture plastic (TCP). As is to be expected as culture time increases as does metabolism, but as shown in graph B the cell number is also increasing over culture time. Myoblasts appear to be metabolising at a higher rate on random fibres throughout, although there appears to be a large error margin.

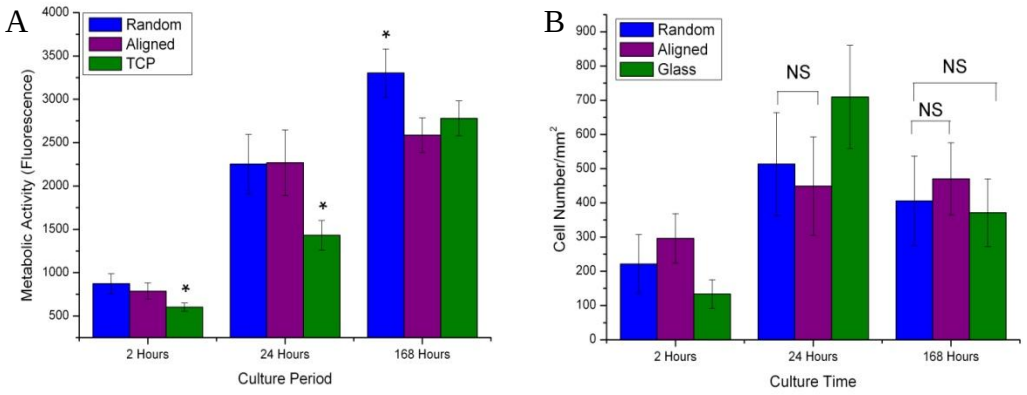

Figure 24: *Graph A shows the metabolic activity of cells over 7 days culture on the substrates determined by the Alamar Blue assay. Graph B shows how cell number changes over 7 days on the electrospun scaffolds compared to TCP determined by DAPI stained nuclei counting using ImageJ. Initial cell density was 100,000 cells per well. Bars indicate standard deviation. Brackets indicate no significant difference (P = >0.05). Stars indicate significant difference (P = <0.05).*

The results shown graph B, figure 24, illustrate that C2C12 attach and proliferate upon the electrospun scaffolds over 1-7 days. This graph may also indicate that cells seeded on the electrospun scaffolds adhere more readily than on glass. This can be concluded because after 2 hours, the cell number/mm^2 is much higher on the scaffolds than on the glass. The cell number decreases after 7 days as cells begin to differentiate. As myoblasts differentiate, only cells capable of fusing will fuse and survive, others will apoptose. After 3 days there appears to be more cells on glass, this could be due to cells maintaining their proliferative state longer than on the electrospun surfaces. Myoblasts exit the cell cycle and cease proliferation as they begin to differentiate, explaining the decrease in cell number to similar levels on all substrates after 7 days culture.

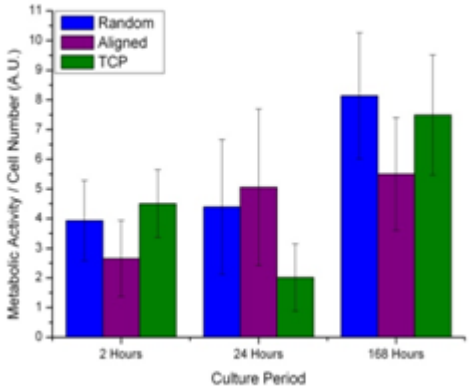

Figure 25: *Cellular metabolism as measured using the Alamar Blue assay divided by cell number to illustrate metabolism related to cell number. Bars indicate standard deviation.*

Figure 25 combines the graphs shown in figure 24 to show the relationship between cell number and metabolic activity. There are large error bars, which is due to the combined error from both the cell counting experiment and the Alamar Blue assay data. Because of the large error margin it is difficult to comment on a trend between substrates. The graph does illustrate that as culture time increases, as does cellular metabolism.

4.2.3 Immunogenicity and Inflammatory response

Macrophages are the first line of defence in the immune system. They are responsible for detecting the pathogen or toxic compound and recruiting other immune cells to the area, increasing the blood flow to the area, and also engulfing and destroying the foreign object. When a macrophage reacts to a foreign object, changes occur to the cell's morphology and also to the local environment around the cell. In response to a foreign object the morphology of the cells becomes more spread and less rounded. The macrophages secrete

an array of cytokines and chemokines in order to attract other immune cells and to increase blood flow to the area. The amount of cytokines secreted can also be measured by sampling the media surrounding the cells. Interleukin – 1β (IL-1β) is a cytokine involved in activating lymphocytes and activate local vascular endothelial cells to increase adhesive capabilities of circulating lymphocytes and also to increase blood flow to the affected area. LPS (lipopolysaccharide) is a bacterial polysaccharide which binds to the CD41 receptor present on macrophage cells. Binding of this LPS ligand to the receptor on the macrophage stimulates activation of the macrophage and therefore increased H_2O_2 release, cytokine release – including Il-1β, and a shift in cellular morphology from round to more spread.

4.2.3.1 Peroxide Assay

The peroxide assay measures the amount of hydrogen peroxide released from macrophages. Hydrogen peroxide is released by macrophages along with nitric oxide, and the superoxide anion (O_2^-) to help destroy the engulfed pathogen. Superoxide is made in what is known as the respiratory burst, where NADPH oxidase (nicotinamide adenine dinucleotide phosphate-oxidase) is utilised in a reaction where it is converted to hydrogen peroxide by the enzyme superoxide dismutase, with an increase in oxygen consumption. Without this respiratory burst, pathogens cannot be eradicated effectively and leads to severe illnesses such as chronic granulomatuous disesase.

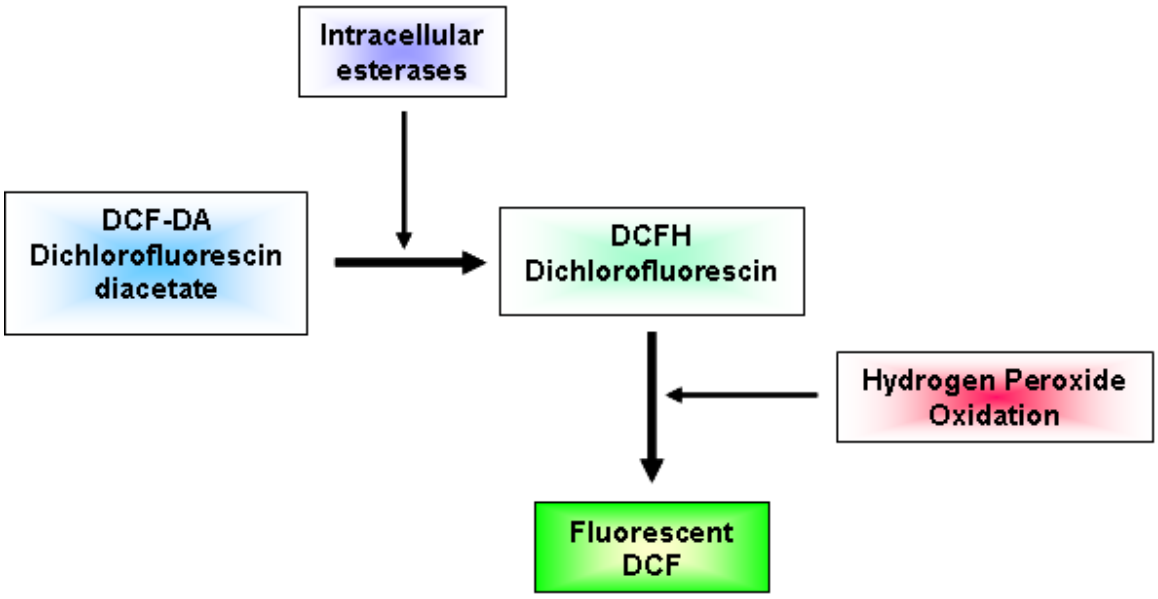

Figure 26: *Flow diagram illustrating how dicholorofluorescin-diacetate becomes fluorescent in response to intracellular esterases and hydrogen peroxide.*

The emitted fluorescence from this assay is directly proportional to the amount of peroxide release (Wang and Joseph, 1999). Hydrogen peroxide is a highly reactive species which oxidises the DCFH (dicholorofluorescein) into the fluorescent DCF. Intracellular esterases hydrolyze the DCF-DA (dicholorofluorescein diacetate) to non-fluorescent DCFH. DCFH is then oxidised by hydrogen peroxide to fluorescent DCF (Hockberger et al., 1996). The process of fluorescence acquisition is illustrated in figure 26.

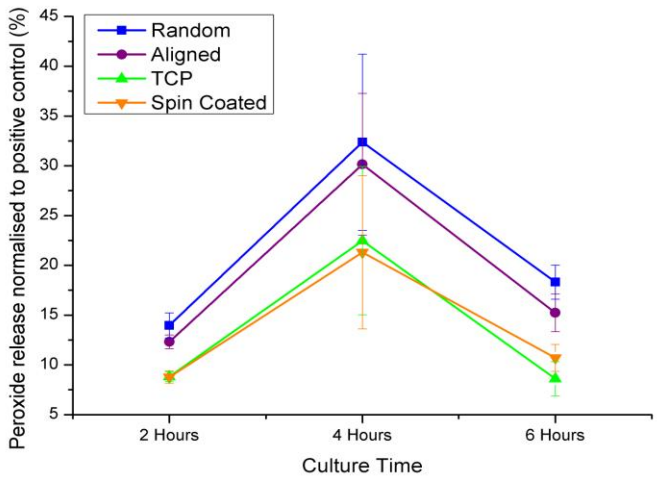

Figure 27: *This graph shows the results from the peroxide assay done on electrospun random and aligned fibres, spin coated PLGA, tissue culture plastic (TCP). Values were normalised to a percentage of the positive control – copper dics. Values shown are mean +/- standard deviation (n = 9).*

The graph in figure 27 shows the results from the peroxide assay, undertaken in triplicate. This assay uses the release of hydrogen peroxide as an indicator of macrophage activation. Hydrogen peroxide is used as a second messenger in the immune response released by activated macrophages. Copper discs are used as a positive control as they induce peroxide release by the macrophages. Graph in figure 27 shows that the electrospun PLGA, either randomly oriented or aligned, elicits a small immune response by the macrophages which is similar to that created by tissue culture plastic (TCP). This would indicate that the scaffold is immunogenic and biocompatible.

4.2.3.2 Interleukin 1-β ELISA

An ELISA is an Enzyme-Linked ImmunoSorbent Assay. It uses antibodies to capture and detect a specific molecule. A colourimetric, enzyme-dependent reaction then takes place. Typically the detection antibody (analogous to a secondary antibody used in ICC) is biotinylated which then can bind streptavidin. This streptavidin can be conjugated with the enzyme hydrogen peroxidase (HRP) which catalyses the colourimetric change. An acid solution is used to stop the reaction so reaction time, and therefore colour development, can be controlled. The positive control in this assay is LPS, as discussed earlier this activates macrophages via the CD41 receptor.

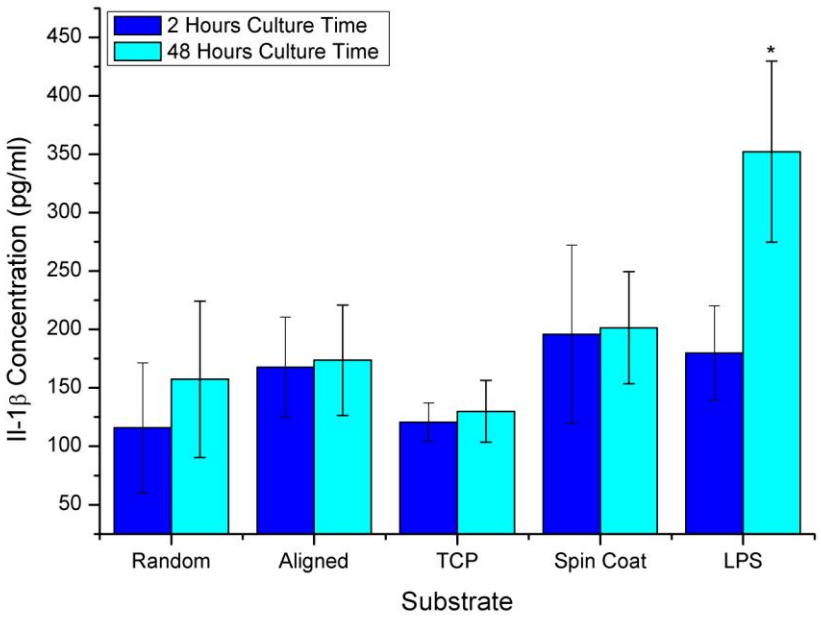

Figure 28: *Graph illustrating the amount of IL-1β secreted by murine macrophages on various substrates after 2 hours (dark blue bars) and 48 hours (light blue bars). LPS (lipopolysaccharide) is the positive control. Bars indicate confidence (95%).*

The graph shown in figure 28 illustrates how much of the cytokine interleukin 1β (IL-1β) is released by murine macrophages after 2 hours and 48 hours culture on electrospun scaffolds, spin coated, and tissue culture plastic (TCP), with lipopolysaccharide (LPS) as the positive control. From this graph it can be seen that there is little difference between the electrospun scaffolds and TCP in the concentration of IL-1β secreted after both 2 hours and 48 hours. The graph shown here is representative of 4 experiments, each with the same trend in cytokine release.

4.2.3.3 Macrophage Morphology

As discussed, macrophages become less rounded and more spread in morphology when activated by foreign objects. This could be due to them forming stronger adhesions to the surface in order to secrete the cytokines and chemokines, and also to create a larger surface area with which to engulf foreign objects.

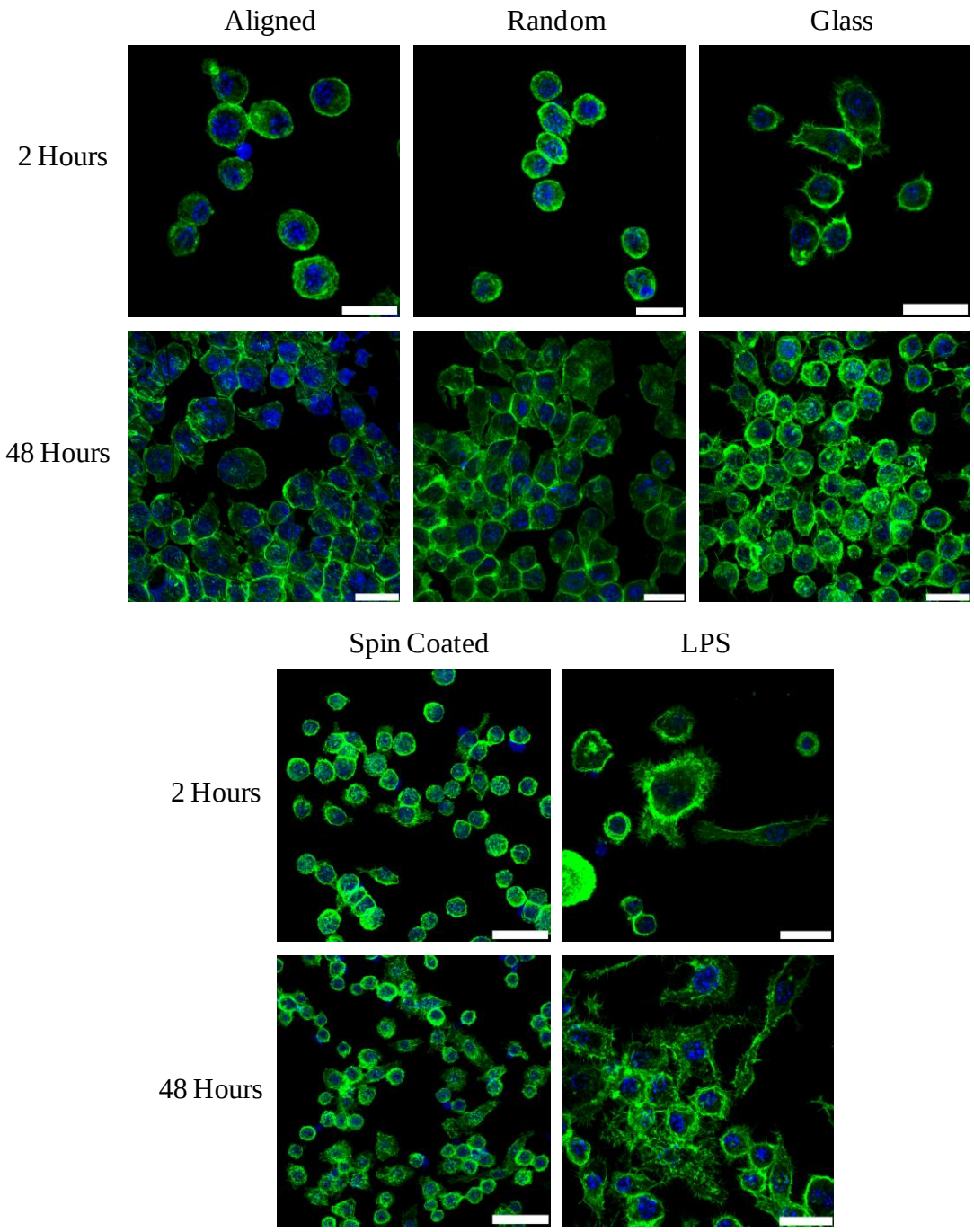

Figure 29: *Cytoskeletal staining of murine macrophages. F-actin stained green with FITC-conjugated phalloidin, nuclei stained blue with DAPI. Cells were fixed at 2 hours and 48 hours to investigate cell spreading. Scale bar indicates 25 µm in all except Spin Coated samples where the scale bar indicates 50 µm.*

The images shown in figure 29 depict cytoskeletal arrangement of macrophages after 2 hours culture and 48 hours culture to coincide with the ELISA. At 2 hours culture, the cells appear smaller and on the glass control compared to on the electrospun fibres. Thus, the roundness seen on the glass control at 2 hours may be due to less cellular adhesion to the glass compared to on the electrospun fibres. At 48 hours, although the cells on the electrospun substrates are fairly confluent, it is clear that they are not as spread and maintain a rounded morphology compared to the glass control where many of the cells have started to spread and extend lamellipodia.

4.3 Conclusions

The data in this chapter indicates further that electrospun PLGA is suitable for cell culture, as the cells adhere without the need for pre-conditioning, proliferate, and any residual solvent present in the scaffold does not elicit a significant immunogenic response from macrophages.

Using a synthetic scaffold that allows cellular attachment and proliferation with no pre-conditioning or incorporation of biologic cues is advantageous as it decreases the chance for immunogenic responses if implanted *in vivo*.

4.4 Future Work

Here it is shown that C2C12 myoblasts adhere and proliferate upon an un-conditioned electrospun PLGA scaffold. While this is advantageous in many ways, the flexibility of the electrospinning technique and the choice of post-spinning modifications introduces a wide array of options to modify the scaffold to possibly control cell responses to the scaffold

with regards their attachment, morphology and differentiation. For example it is possible to include biologic material, e.g. collagen or laminin, into the electrospinning solution. This could take the form of the whole protein, active areas of the protein, or the incorporation of short, synthetic peptide sequences, or glycosaminoglycans (GAGs). It is also possible to use more sophisticated methods to introduce biologic materials to the electrospun scaffolds. Some examples of this include plasma polymerisation of allylamine onto the surface to encourage negatively charged GAGs to bind (Meade and Merry 2010, unpublished data), also peptide sequences can be attached to the surface using novel technologies e.g. Orla Technologies. Peptide sequences can also be co-spun with the polymer to ensure maximum coverage of the peptide – although ensuring the peptide is in a recognisable arrangement may be difficult. Incorporating specific peptide sequences or GAGs could influence and ultimately control cellular behaviour upon the scaffold. This combined with the ECM mimicking architecture of the electrospun scaffold could provide a novel method of dictating cellular fate.

Kathryn J. Aviss

Chapter 5: Cell Proliferation, Alignment and Differentiation

Investigating the response of murine myoblasts to the scaffold with regards morphology, attachment and differentiation

The University of Manchester

5.1 Introduction

The functionality of a biomaterials scaffold must be analysed *in vitro* to ensure correct cellular responses. Using various molecular techniques; e.g. looking at gene expression using PCR, and cellular techniques; e.g. staining specific proteins within the cell at different time periods, it is possible to monitor cellular responses to the scaffold. The topography of a surface has been shown to effect the orientation and morphology of cells growing on the surface (Aviss et al., 2010; Dalby et al., 2003; Dalby et al., 2004). The topographical cues that have been investigated include pillars of varying heights (nm) and distances apart (Dalby et al., 2003), nanogrooves (Altomare et al., 2010; Huang et al., 2006; Lehnert et al., 2004; Yamoto et al., 2008), and fibrous networks with either randomly oriented fibres (Blackwood et al., 2008; Choi et al., 2008; Li et al., 2006; Riboldi et al., 2005; Srouji et al., 2008) or with a degree of organised alignment within the scaffold (Choi et al., 2008; Li et al., 2007; Wang et al., 2009). Choi et al (2008) created aligned and randomly oriented PCL/collagen nanofibre meshes for the application of skeletal muscle regeneration. In this paper Choi et al use collagen as a co-polymer in the spinning solution as it provides greater biocompatibility than PCL alone (Choi et al., 2008). Aviss et al 2010 showed that electrospun PLGA was suitable for the proliferation and differentiation of C2C12 myoblasts with no surface modifications, incorporation of biologic components or serum conditioning of the scaffold prior to cell seeding (Aviss et al., 2010). The alignment of the fibres illustrated in the paper by Choi et al (2008) is shown excellently in the SEM images, although the meshes appear very thin with few fibres present. In the SEM image of the fibres with cells, it is difficult to determine which is randomly oriented and which is aligned. If the same method for collecting the fibres is used in both applications, there

should not be this discrepancy. A rotation speed exceeding 2000 rpm should be sufficient to create highly aligned fibres, as shown by Aviss et al (Aviss et al., 2010).

Another method to control the alignment of myoblasts on non oriented substrates, e.g. glass coverslips or tissue culture plastic, is to use static magnetic fields (SMFs) to manipulate the arrangement of the myofilaments (Coletti et al., 2007). SMFs are used routinely as a therapy for musculoskeletal pain relief, although the background science behind this therapy is unclear. Coletti et al claim SMFs of 80 mT stimulate myogenic differentiation without any topographical cues (Coletti et al., 2007), however when comparing the differentiation noted in Coletti et al's paper it could be noted that the myotubes formed are much wider in diameter than those found in other papers investigating myoblast differentiation, also they measure the percentage of differentiated myotubes by measuring the amount of shared cytoplasm. This is not a well known test for determining the percentage of differentiated myotubes present. The more common method is to calculate the fusion index by dividing the total number of nuclei by those found in cells with more than 2 nuclei present (often confirmed by simultaneously staining for a differentiation marker e.g. myosin heavy chain) and that these nuclei are peripheral to the cell – not in the centre. Looking at the data presented by Coletti et al, the cells that share cytoplasm appear to have clusters of centrally located nuclei therefore may not technically be defined as differentiated myotubes.

This project uses electrospinning to produce sheets of randomly oriented and aligned synthetic elastomeric polymer nanofibres for myoblast growth and differentiation. No feeder layer or surface modifications were needed in order for myoblast adherence, proliferation, alignment and differentiation. The characteristics of these scaffolds have

been discussed in chapters 3 and 4, along with their relevance to the application of skeletal muscle tissue engineering.

5.2 Results and Discussion

5.2.2 Cellular Morphology

Previous work on the morphology and motility of myoblasts has focussed upon the ECM proteins present controlling the adhesion and consequent signalling systems utilised to dictate cell morphology (Siegel et al., 2009). It has been shown that fibronectin is involved in maintaining focal contacts and assembling actin stress fibres, whereas laminin promotes myoblast motility (Goodman et al., 1989). Here it is shown that myoblast cells adhere and elongate in response to surface topology alone with no inclusion of biologic cues.

5.2.2.1 Immunocytochemistry

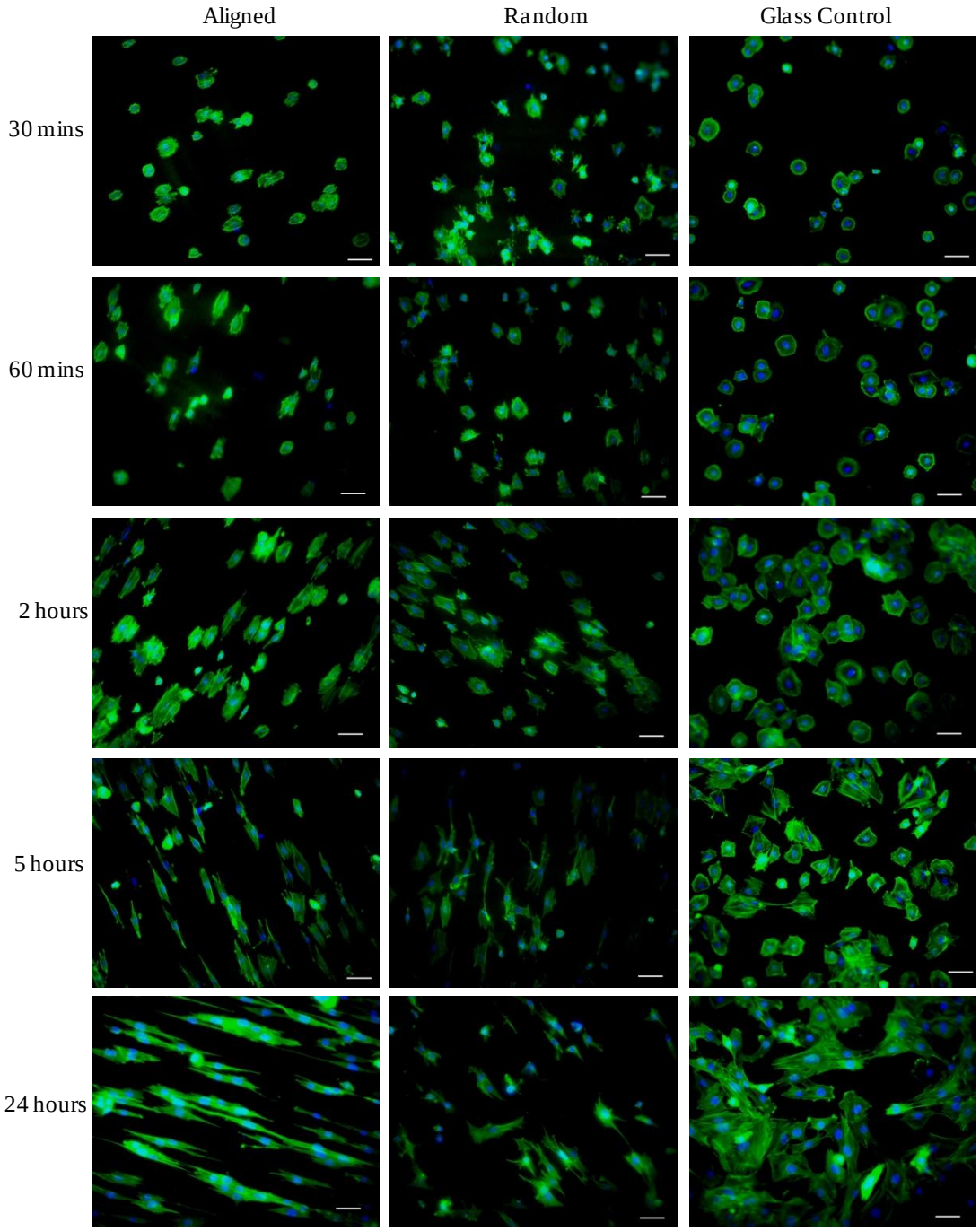

Figure 30: *C2C12 seeded on randomly oriented and aligned electrospun fibres and glass coverslips stained for f-actin with FITC phalloidin (green) and DAPI for nuclear staining (blue). Scale bars indicate 50 µm.*

Images in figure 30 show the gross morphology of the myoblast cells at time points up to 24 hours post seeding. These images suggest that cells seeded on the aligned fibres have a more aligned and elongated morphology which may be consistent with the underlying aligned fibrous scaffold. However because the scaffold is not visible in these images this can only be an assumption. Using scanning electron microscopy (SEM) it is possible to visualise the cellular morphology and the fibrous scaffold together thus how the cells interact with and respond to the scaffold with regards their morphology.

5.2.2.2 SEM Analysis

Using SEM it is possible to look closer at how the cells interact with the scaffold therefore a better understanding of the cellular morphology in response to the scaffold topography is possible.

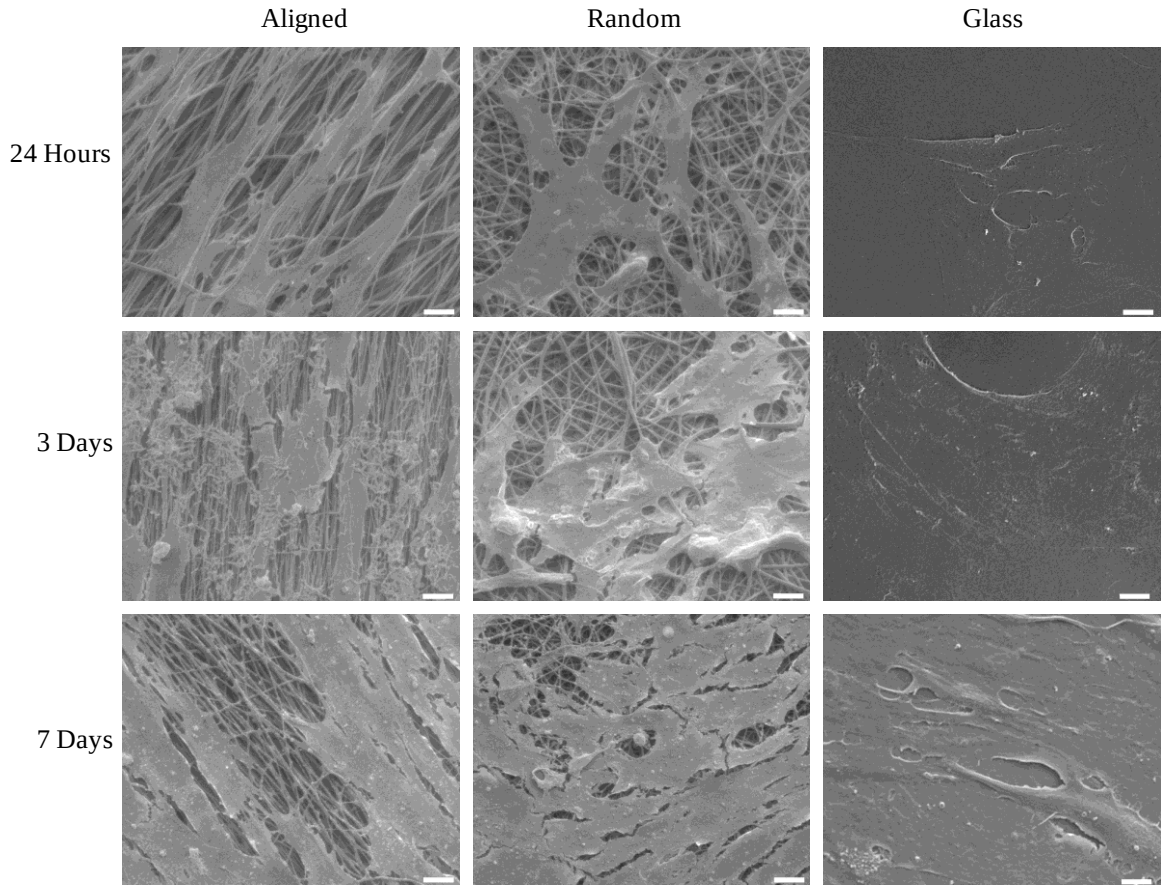

Figure 31: *SEM images of C2C12 seeded on electrospun PLGA scaffolds. Cells were fixed at 24 hours, 3 days and 7 days after seeding. Scale bar indicates 10 µm.*

Figure 31 illustrates how the cells interact with the different orientation of fibres. It can be seen that after only 24 hours the cells appear to have aligned along the topography of the aligned fibres, compared to a less organised morphology on the randomly oriented scaffold. Results after 3 days on the scaffold show similar morphology to that after 24 hours, the

difference being more cells present. After 7 days it would appear that the cells on the randomly oriented fibres have begun to possess a more aligned morphology, but a closer inspection of that image shows that cells are starting to align together locally but in different directions, compared to the aligned fibres where they all align globally following the directionality of the fibres. Myoblast cells will begin to locally align as they start to fuse and differentiate into myotubes, but without any topographical guidance will form swirling patterns (see figure 34 for myotube alignment after 14 days). From this image and later images of differentiation markers (as shown by immunocytochemistry see figure 39) they tend not to align in the same direction which is imperative for functional contraction to take place.

Looking at figures 30 and 31 myoblast morphology is dramatically influenced by the surface topography on which the cells encounter. The aligned fibres cause cells to adopt an elongated morphology, as seen in figure 31, and that this elongation is in accordance with the alignment conveyed by the aligned electrospun PLGA scaffold.

5.2.3 Cytoskeletal Visualisation

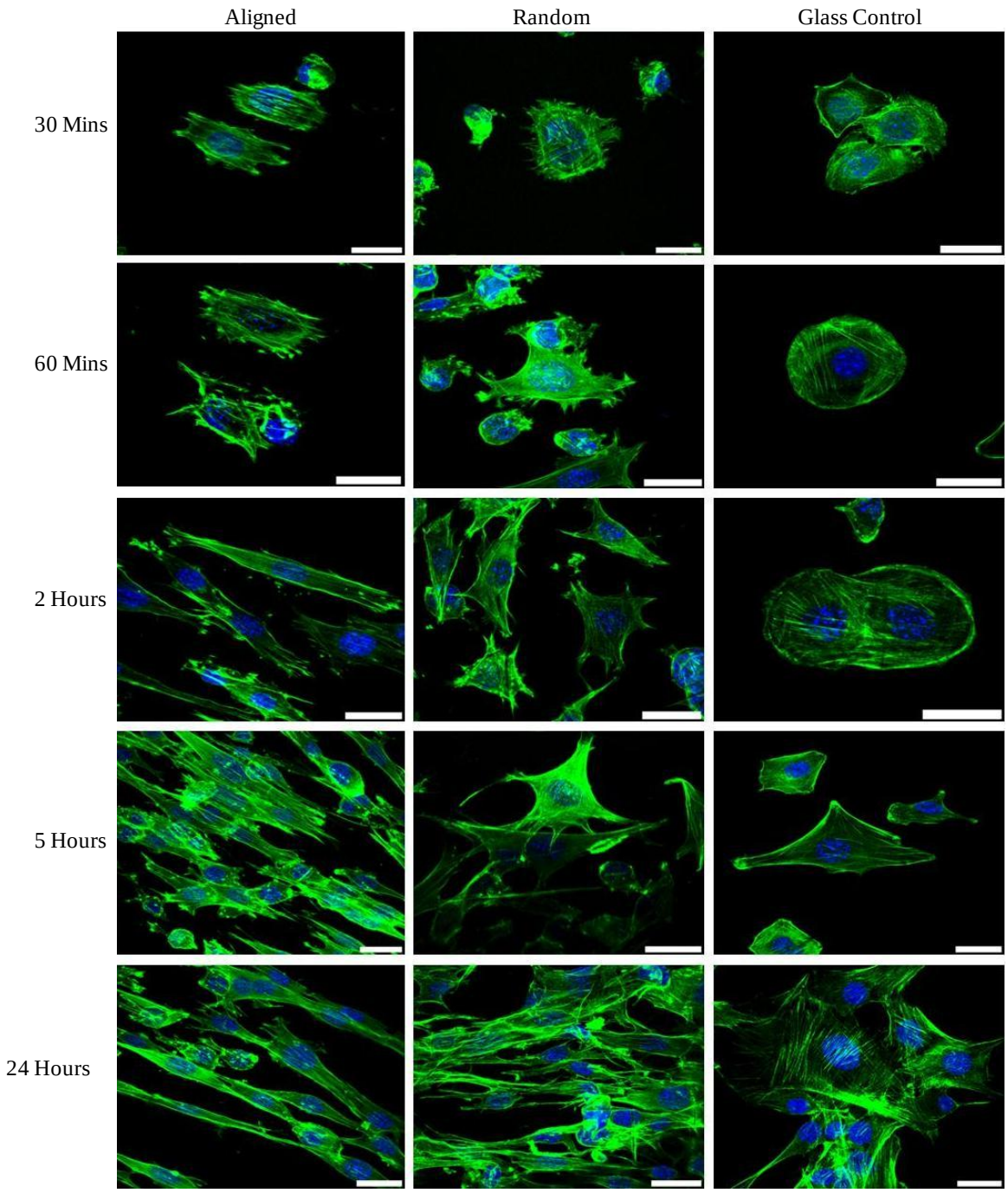

Figure 32: *C2C12 seeded on randomly oriented and aligned electrospun fibres and glass coverslips stained for f-actin with FITC phalloidin (green) and DAPI for nuclear staining (blue). Scale bars indicate 25 µm (Aviss et al., 2010).*

Images shown in figure 32 are higher magnification pictures of those shown in figure 30. A higher magnification allows a closer inspection of the cytoskeleton and how the arrangement of the cytoskeleton varies in cells seeded on the different surfaces. The cytoskeletal f-actin filaments of the cells on aligned fibres appear to be more parallel to each other after just 30 minutes, qualitatively following the overall cellular elongation direction. On random fibres the cellular cytoskeleton shows some form of local order, with multiple actin filaments originating at the leading edges of the extending lamellapodia creating the polygonal morphology of the cells. No bulk alignment of the filaments is observed on the macro scale, however, reflecting the multi-directional spreading of the cells compared to the bi-directionality of those on aligned electrospun fibres. This trend of elongation on the aligned fibres and polygonal spreading on the random fibres and the glass control is continued as time in culture on the scaffold increases. At 24 hours, cells on the glass control appear typically polygonal with actin stress fibres criss-crossing the cell body as the cell spreads. On the aligned fibres however the degree of elongation seen in the gross cellular morphology shown in figure 30 is echoed by the bi-directional parallel cytoskeletal f-actin filaments.

5.2.4 Degree of Elongation

Quantification of cellular elongation was undertaken by measuring the aspect ratio of the cells so as to statistically illustrate the difference in elongation on the different substrates over time. Aspect ratio is the length of the cell divided by its width.

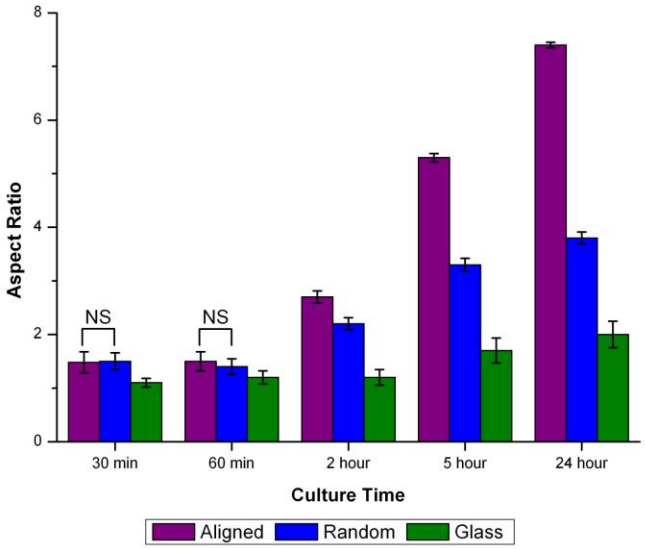

Figure 33: *Graph quantifying cellular elongation, as measured by aspect ratio of cells upon the scaffold and statistical difference determined via a student's t-test – NS over brackets indicates no significant difference was found, all other results were significantly different from each other (Aviss et al., 2010).*

Images in figures 30, 31 and 32 illustrate the morphology of C2C12 seeded on electrospun fibres of both random and aligned orientation, compared with glass coverslips. Figure 33 shows the quantification of this alignment by measuring the aspect ratio of the cells. Cells were fixed after 30 minutes, 60 minutes, 2 hours and 5 hours and 24 hours after seeding and stained with FITC-phalloidin to visualise the actin cytoskeleton. After 30 minutes cells have shown attachment as they are on the scaffold and stained positively for both f-actin (green) and nuclei (blue). From the 20x magnification images in figure 30 show the number of cells attached and provides an insight into cellular morphology and elongation, the individual stress fibres are not discernable at this relatively low magnification. From the 20x magnification the number of cells attached increase up to the 2 hour time point. To have a closer look at the actin cytoskeleton responsible for cellular

morphology, the magnification was increased to 60x, as shown in figure 32. With these 60x images the elongation of the cell morphology becomes clearer. After just 30 minutes on the aligned electrospun fibres, the actin cytoskeleton appears to be arranging to create bipolar cells with elongation properties rather than the rounded properties found in cells seeded on glass coverslips at the same time. Cells seeded on random fibres appear to have a spiky morphology with lamellipodia extending all around the cells; again this can be compared to the smooth roundness on cells seeded on coverslips after 30 minutes and 60 minutes. As culture time on the scaffold increases, the elongation of the cells on the aligned fibres increases, with them all aligning in the same direction on each sample – indicating a close interaction with the scaffold. This statement cannot be conclusive from these images and graph alone, however; when looked at in conjunction with the SEM images in figure 31 it becomes clear that the cells do indeed align along the aligned fibres, and maintain a less regular morphology on randomly oriented fibres. To quantify cellular elongation from these immunofluorescent images, the aspect ratio of the cells was measured. Aspect ratio is the length of the cell divided by the width. Figure 33 illustrates the results from this measurement, and provides further evidence towards the cellular elongation upon the aligned fibres. A students' t-test was undertaken on the data collected (n = 20 per substrate type and time point) and this is illustrated by the NS brackets on the graph shown in figure 33. All other values were statistically significant from each other.

5.2.5 Longer Term Maintenance of Cellular Morphology

It has been shown that C2C12 myoblast cells adhere and align on aligned electrospun fibres after just 30 minutes culture, figures 30 and 32. For tissue engineering of skeletal

muscle it is important that this elongated, parallel morphology be carried on throughout cellular fusion and differentiation. Extending the f-actin staining to after 14 days reveals how the morphology of the cells is maintained throughout fusion and differentiation (figure 34).

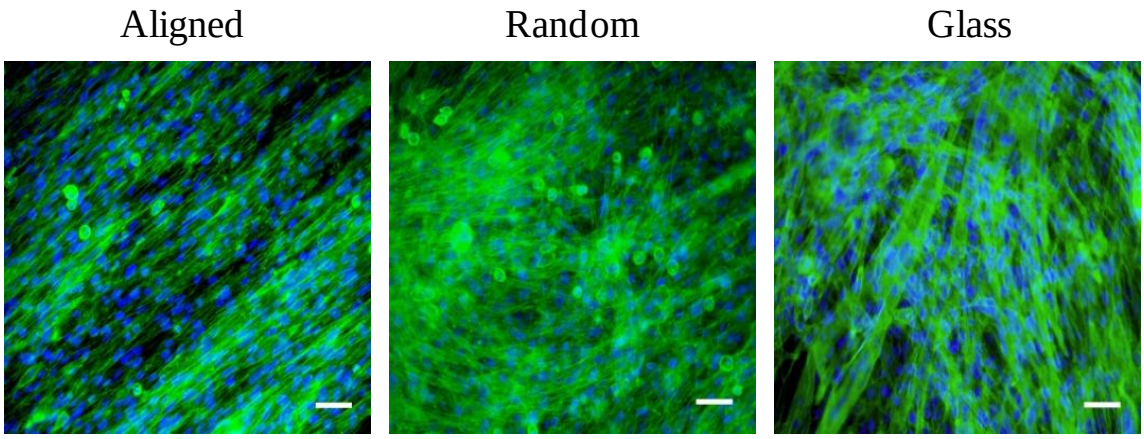

Figure 34: *F-actin (green) and nucleic (blue) staining of C2C12 after 14 days proliferation on the scaffolds. Scale bar indicates 200 µm (Aviss et al., 2010).*

Cells seeded on the random fibres appear to grow in the typical swirling patterns, seen at earlier time points on glass coverslips. After 14 days seeded on glass, the fibres have no directionality, and appear slightly wider and more spaced out from each other; this would hinder fusion as myoblasts require close proximity to one another to fuse efficiently. This result is important as it shows that the initial alignment and elongation of the myoblasts is maintained as the cells differentiate, over 14 days, into multinucleated myotubes. Maintaining global alignment and elongation is important for proper contractility as a syncitium to occur within the construct.

5.2.6 Cellular Adhesion

5.2.6.1 Vinculin Staining

Cellular adhesion is chiefly mediated by integrins forming the focal adhesion complex (FAC) between ECM proteins such as fibronectin and vitronectin. Integrins are composed of two subunits, an alpha subunit and a beta subunit. Different combinations of alpha and beta subunits can lead to different cellular responses. The focal adhesion complex is made up of a characterised faction of proteins e.g. focal adhesion kinase (phosphorylated), α-actinin, catenins, talin, and vinculin (Beckerle, 2001). Vinculin is often used as a marker for the focal adhesion complex and was discovered by Benjamin Geiger in 1979 when he successfully isolated it from chicken gizzard (Geiger, 1979). Using immunostaining against vinculin it is possible to find out whether myoblasts utilise the focal adhesion complex when adhering to the electrospun scaffold.

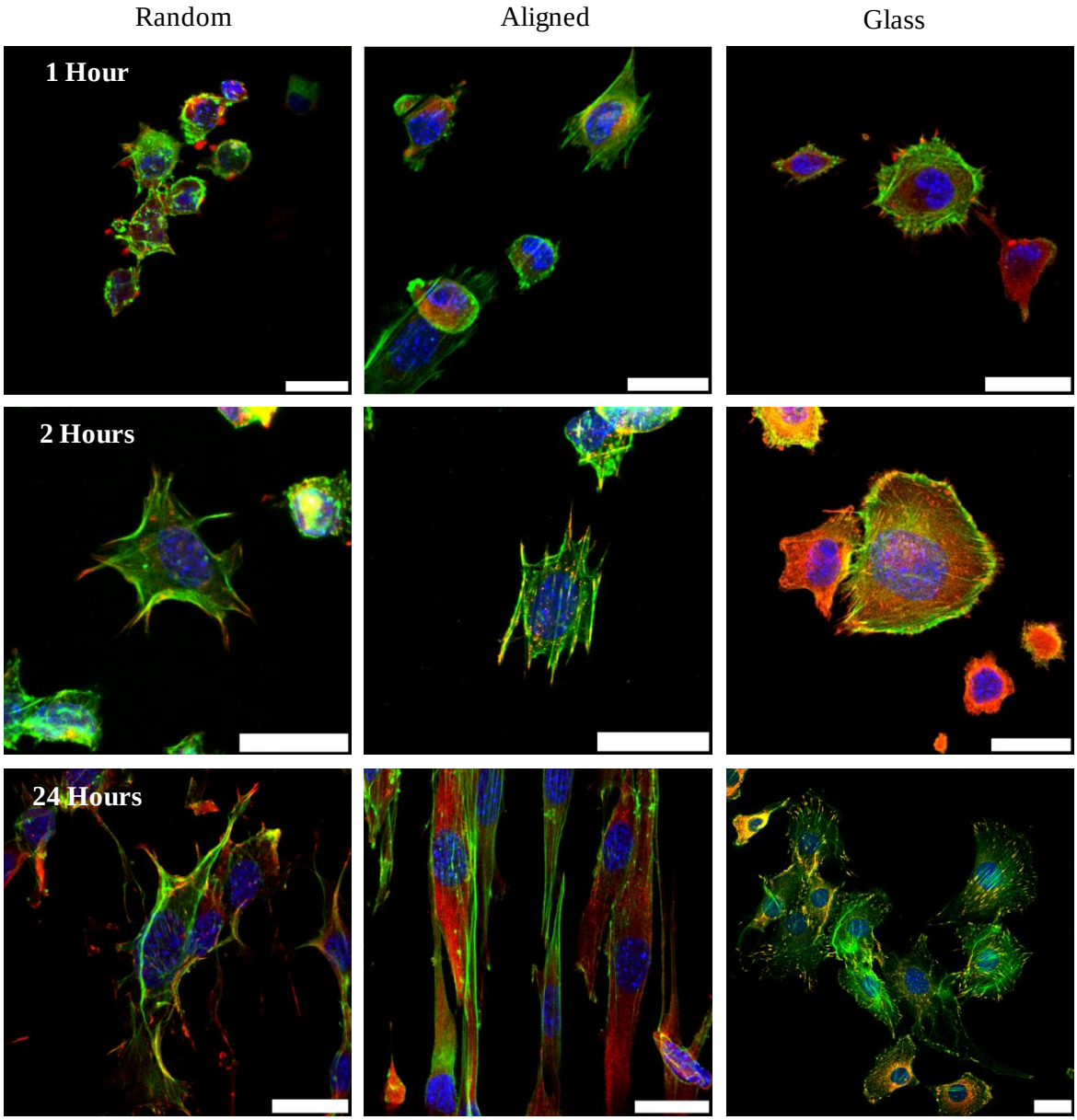

Figure 35: *Confocal micrographs showing vinculin staining (red) of focal adhesions, f-actin stained with FITC-phalloidin (green), and nuclei stained blue with DAPI. Scale bars indicate 25 µm.*

Figure 35 shows vinculin staining of myoblasts seeded on random and aligned electrospun scaffolds compared to a glass control. These images illustrate the typical vinculin pattern staining in punctuate areas around the periphery of the cell. This is

especially clear in the glass control panel for all time points; any area of yellow shows co-localisation between the green f-actin and the red vinculin. These cells were cultured in serum containing media which will contain ECM proteins such as fibronectin and vitronectin, so FACs can be expected to form (cells grown in serum free media do attach to the scaffold but not as rapidly – cells would have to secrete their own ECM proteins in order to form FACs. For attachment to occur before protein synthesis and excretion cell membrane proteins may form weak hydrostatic bonds with the polymer). After 24 hours on aligned fibres, punctate FAC areas are difficult to find compared to those on random fibres and the glass control – red streaked areas at sites of lamellipodia are clear on cells seeded on both random fibres and glass control after 24 hours. Cells on aligned fibres after 24 hours appear to have red staining which is not membrane associated but mainly non-distinct internal staining.

5.2.7 Integrin Expression

To date, the literature investigations into integrin expression in myoblasts have focussed on how the expression changes between proliferation and differentiation and which ECM molecules are involved in these changes. This may be the first time investigations into myoblast mRNA expression of integrin subunits has been undertaken at very early adhesion (4 hours) and after 24 hours culture in growth media on substrates with different topologies.

The main integrins shown to be important for myoblast adhesion are alpha 7 beta 1 and alpha 5 beta 1. It is known that alpha 7 beta 1, splice form A, is involved in the attachment and motility of myoblasts in response to laminin (Yao et al., 1996). Alpha 5 beta 1 is also an abundant integrin which mediates adhesion by primarily binding to fibronectin (Glenn et al., 2009).

Subunits tested were chosen purely on the accuracy of the online primer design tool provided by NCBI, i.e. the ones chosen and presented here had over 80% accuracy to the specific integrin subunit sequence, and ones with less than 80% were not selected for the study. Figures 36 and 37 compare the mRNA expression of the alpha and beta subunits on the different substrates, figure 38 compares the difference in mRNA integrin expression between 4 hours and 24 hours culture in growth media.

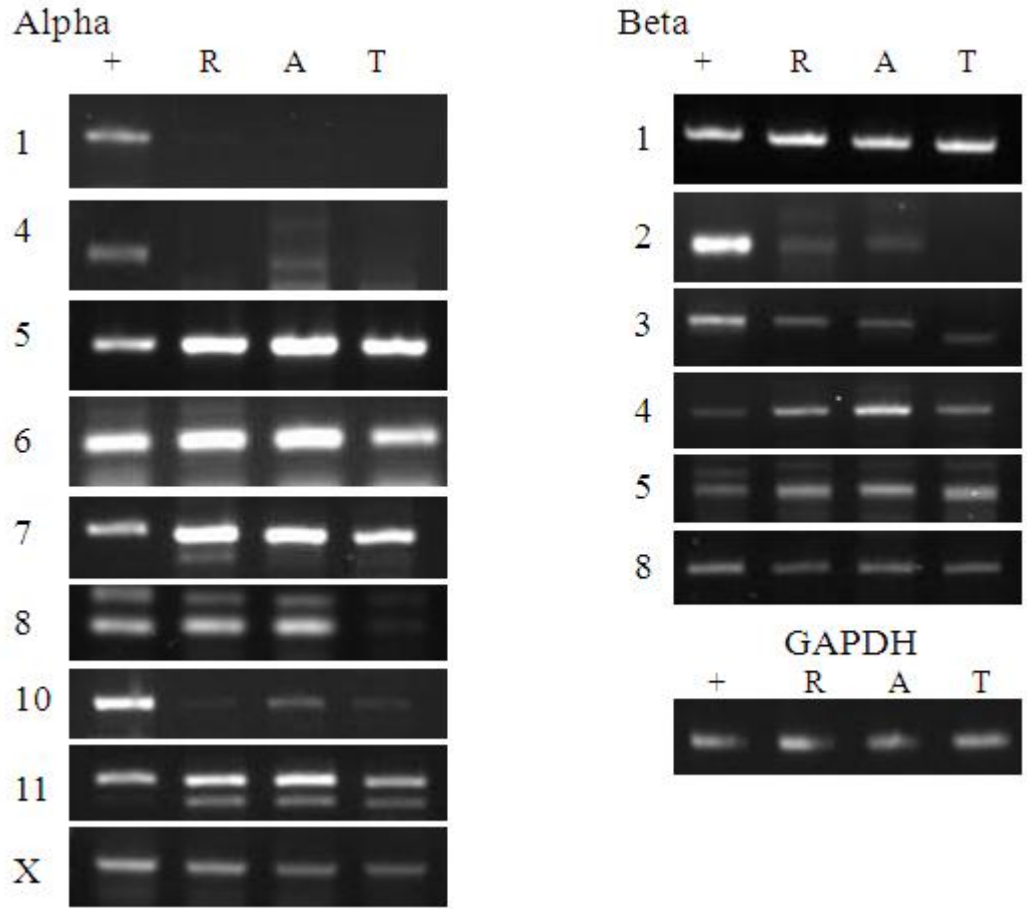

Figure 36: *Integrin mRNA expression PCR agarose gels from cells cultured for 4 hours on the different substrates before pelletting. + is the positive control of total mouse embryo RNA, R = random fibres, A = aligned fibres, T = tissue culture plastic. GAPDH was the housekeeping gene.*

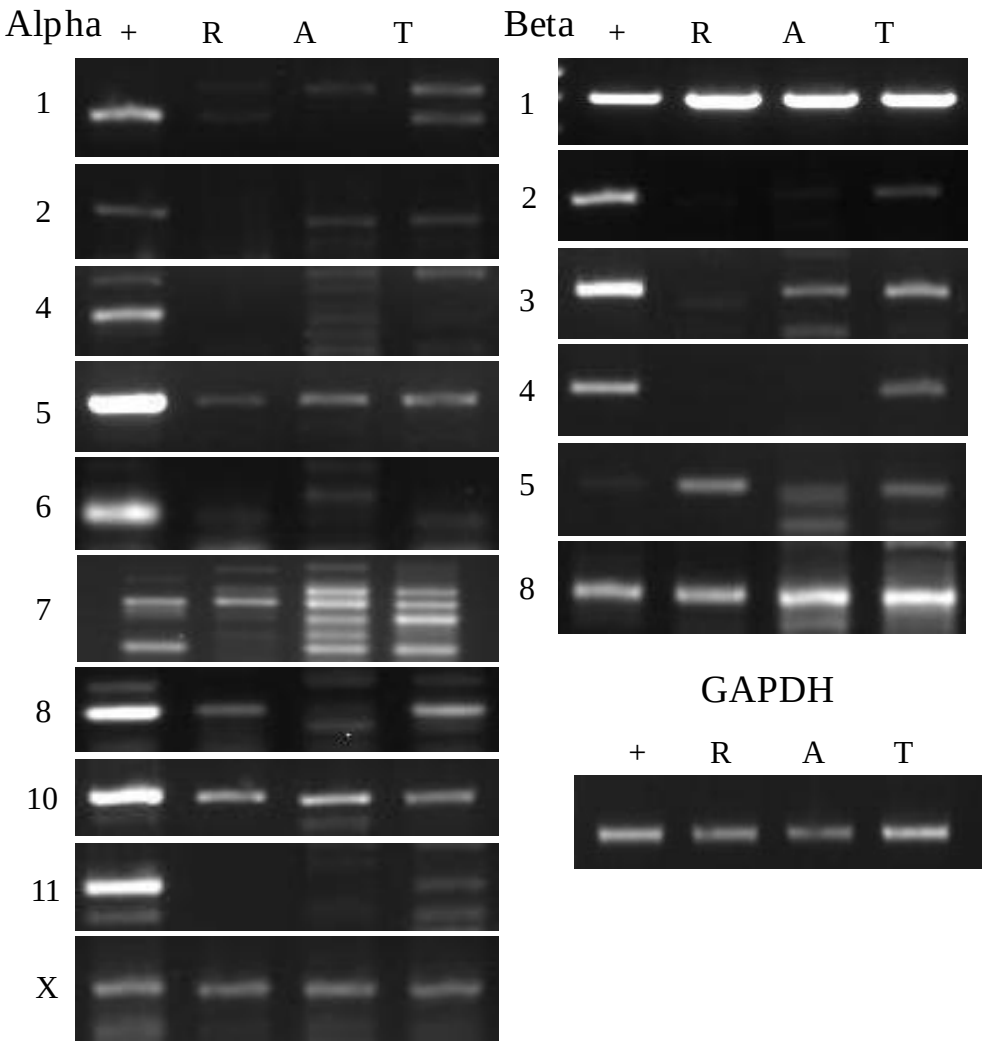

Figure 37: *Integrin mRNA expression PCR agarose gels from cells cultured for 24 hours on the different substrates before pelletting. + is the positive control of total mouse embryo RNA, R = random fibres, A = aligned fibres, T = tissue culture plastic. GAPDH was the housekeeping gene*

Figures 36 and 37 present agarose gels of PCR products of integrin subunits of C2C12 myoblasts pelletted after 4 hours and 24 hours respectively culture in growth media on random fibres, aligned fibres, and tissue culture plastic with total mouse embryo as the positive control. As far as can be found from the literature, investigations into integrin expression at such an early time in adhesion have not been undertaken, especially not on scaffolds with different topographies. Table 7 summarises the expression profile of the subunits found from figures 36 and 37 and also the major functions of each integrin subunit, each discussed in more detail in the text.

Table 7: *Summary of integrin subunit functions and expression. ++ means highly expressed, + means expressed, and – means not expressed.*

Subunit	Common cell type/location	Function in Myoblasts	C2C12 expression 4 hours			C2C12 expression 24 hours		
			R	A	T	R	A	T
Alpha 1	Somites, smooth muscle, cardiomyocytes	None Found	-	-	-	-	-	-
Alpha 5	Ubiquitous RGD receptor	Maintenance of proliferation	++	++	++	+	+	+
Alpha 6	Epithelial tissue	Laminin receptor during differentiation	++	++	++	-	-	-
Alpha 7	Skeletal and cardiac tissue	Splice variants associated with differentiation	++	++	+	+	++	++
Alpha 8	Nervous system of embryo. Smooth muscle	None Found	+	+	-	+	-	+
Alpha 10	Chondrocytes and sarcolemma of skeletal muscle	Adhesion of sarcolemma	-	+	-	+	+	+
Alpha 11	Uterus, heart, skeletal muscle	Collagen receptor and migration	+	+	+	-	-	-
Alpha X	Immune cells e.g. T cells	None Found	+	+	+	+	+	+
Beta 1	Ubiquitous, promiscuous	Adhesion to RGD containing proteins	++	++	++	++	++	++
Beta 2	Inflammatory cells e.g. neutrophils	Hypertrophy in response to injury	-	-	-	-	-	+
Beta 3	Vascular and smooth muscle cells	Receptor to laminin, fibronectin and collagens 1 and 4	+	+	-	-	+	+
Beta 4	Keratinocytes	None Found	+	+	+	-	-	-
Beta 5	Apical surface of eye	Adenovirus entry route	+	+	+	+	-	+
Beta 8	Brain Development	None Found	+	+	+	+	+	+

In figures 36 and 37 alpha 1 is only found in the positive control after 4 hours and 24 hours' culture; this is due to it only being expressed in stage 20 of the somites as it extends towards the ventral regions of the embryo *in vivo*. *In vitro*, alpha 1 has been shown to be expressed on a wide variety of cell types including smooth muscle, cardiomyocytes, and neurons, but not in skeletal muscle (Dubard et al., 1992).

From figure 36 alpha 5 appears to be expressed highly in cells seeded on all substrates after 4 hours, with perhaps a slightly stronger band present from cells seeded on aligned fibres. As shown in figure 37, after 24 hours culture, alpha 5 is weakly expressed on all substrates, with the weakest banding from cells seeded on random fibres. Sastry et al (1996) investigated the roles of alphas 5 and 6 with regards their joint relationship with maintaining proliferation of myoblasts or their role in differentiation into myotubes. They found that when genetically modified cells that cannot endogenously produce alpha 5 were introduced to ectopically express alpha 5, the cells were maintained in the proliferative state with differentiation inhibited. They also found that using antisense suppression of alpha 6 also inhibited differentiation, but using genetically modified cells that cannot express alpha 6 and introducing them to ectopically expressed alpha 6 had the opposite effect: inhibition of proliferation but not differentiation (Sastry et al., 1996). Work from Sastry et al show that alpha 5 may have a negative effect on differentiation. Strong expression of alpha 5 after 4 hours culture, figure 36, shows that these cells are not differentiated and are thus in a proliferative state. Combining Sastry et al's work with the results shown in figure 36 could yield alpha 5 as an indicator for undifferentiated myoblasts.

In figure 36, alpha 6 is strongly expressed on all substrates with the strongest bands appearing on the electrospun scaffold. However, there appears to be no expression of alpha

6 on any substrate after 24 hours culture. Ulrike Mayer reviewed in 2003 that the alpha 6 subunit in myoblasts is often joined with the beta 1 subunit and together they form a receptor for laminin and is involved in differentiation of myoblasts (Mayer, 2003). Results shown in figure 36 indicate that alpha 6 is expressed at only 4 hours in culture indicating that it may have another function than solely differentiation as these cells will not be differentiating, even at the high density they were seeded at after just 4 hours. Figure 32 shows that C2C12 myoblasts will adhere and begin elongating on aligned fibres after just 30 minutes in culture; but in figures 39 and 40 it was shown that these cells show no signs of differentiating even after 3 days in culture with differentiation media, thus it is highly unlikely that expression of alpha 6 shown here is linked with fusion or differentiation. Sastry et al (1996) concluded that the relationship between alphas 5 and 6 and the ratio at which they are both expressed not only determines whether a myoblast will continue proliferating or whether it will differentiate, but the relationship between these two integrin subunits has an effect on the functionality of the sarcomeric arrangement (Sastry et al., 1996).

Alpha 7 expression, after 4 hours culture, yields a single strong band from all samples, with slightly stronger bands appearing from cells cultured on the electrospun scaffolds. Generally it is thought that alpha 7 is involved in differentiation when paired up with beta 1. However this is normally when its various splice variants are being expressed which would yield multiple bands on the gel. In figure 36 it is shown that just one isoform of alpha 7 is expressed after 4 hours culture. However, after 24 hours culture, presented in figure 38, alpha 7 shows multiple banding which is indicative of splice variant expression since measures were taken to abolish any non-specific amplification during the PCR. There appears to be more splice variants from cells cultured on aligned fibres and tissue culture

plastic. As discussed this could be due to cells beginning to fuse and differentiate. Yao et al showed that alpha 7 was also integral to myoblast motility. They found that blocking the alpha 7 integrin on cells cultured on laminin substrates halted migratory behaviour (Yao et al., 1996).

Alpha 8 was initially discussed by Bossy et al in 1991. They found it mainly in the nervous system of an embryo. But its expression was also noted to vary throughout embryonic development, appearing in the smooth muscle and epithelia of the gut, to the epidermis and capillaries of the skin by E11 of embryonic development (Bossy et al., 1991). Here alpha 8 shows weak expression on all samples at both time points with the strongest expression on the electrospun scaffold, and apparently no expression from cells seeded on tissue culture plastic. Since Bossy et al's study in 1991, other groups have investigated the location of alpha 8 and its expression patterns in different cell/tissue types. Schnapp et al found that in human smooth muscle cells alpha 8 co-localised with vinculin containing focal adhesions when plated on fibronectin and vitronectin, but not on collagen (Schnapp et al., 1995). More recently Hartner et al in 2008 found alpha 8 to be involved in fibrotic re-modelling of myocardial tissue (Hartner et al., 2009).

Camper et al (2001) showed that alpha 10 is involved in chondrocyte adhesion to collagen 2. They also found mRNA expression of alpha 10 in other tissues including heart, brain, spleen, liver and lung, but not skeletal muscle (Camper et al., 2001). Having carried out immunohistochemistry of alpha 10 on the tissues, they found that the protein was expressed in all tissues positive for mRNA expression, but they also found the protein expressed in the sarcolemma of skeletal muscle (Camper et al., 2001). In the current study alpha 10 has weak expression, but there is a stronger band from cells seeded on aligned fibres compared

to random fibres and tissue culture plastic after both 4 hours and 24 hours culture. Siegel et al (2009) also found that alpha 10 mRNA was expressed by C2C12 myoblasts; however they tested expression after 4 days' culture (Siegel et al., 2009). Because alpha 10 integrin protein has been shown to be expressed in fully mature skeletal muscle tissue, as opposed to a monolayer of myoblasts, it is unclear why there is a difference in expression between the substrates tested here.

Alpha 11 is expressed in all samples after 4 hours culture, with the strongest bands occurring from cells seeded on the electrospun scaffolds. Alpha 11 was discovered in skeletal muscle by Gullberg et al (Gullberg et al., 1995) and was noted to be a collagen binding I domain integrin by Velling et al (Velling et al., 1999). Velling et al also showed that alpha 11 integrin was expressed in a wide variety of tissues including uterus, heart, and skeletal muscle but the cellular origin of this expression remained unknown (Velling et al., 1999). Tiger et al (2001) found that alpha 11 expression in human embryos was restricted to nonmuscle cells in areas dense in collagen. *In vitro,* Tiger et al showed that alpha 11 partnered with beta 1 is involved in collagen mediated cellular adhesion and migration, along with collagen synthesis and organisation (Tiger et al., 2001). Because it was shown that alpha 11 is involved in adhesion to collagen, it could be concluded that the increase in expression on the electrospun substrates, compared to the tissue culture plastic, after 4 hours culture, is because the architecture is more favourable to ECM deposition and so more collagen is expressed and alpha 11 is utilised to adhere. After 24 hours, as shown in figure 37, the expression of alpha 11 has diminished. This could be due to the cells having formed mature adhesions to the substrate so it is not necessary to continue producing new protein for this function. This reduction in expression after 24 hours could also be due to a reduction in migration (Tiger et al., 2001).

To date, alpha X, (more commonly known as CD11c, or ITGAX) expression in myoblasts has not been publically reported. Alpha X, is commonly associated with the complement branch of the immune system and is found on cells, such as T cells, where it is co-expressed with CD8 (Vinay and Kwon, 2010). Alpha X is also associated with dendritic cells (Vorup-Jensen et al., 2003). Here it is shown that alpha X is expressed in C2C12 myoblasts at low levels in all samples at both time points.

Alpha V is a receptor for vitronectin (Sinanan et al., 2008), and is thought to be the most promiscuous alpha subunit with 5 known beta subunit partners which are all RGD receptors (Hynes, 2002). Unfortunately the primers sourced for this experiment did not yield product at the expected size and time did not allow for investigations into why this occurred nor how to solve the problem.

Beta 1 integrin is the most promiscuous beta subunit with at least 12 different alpha subunit binding partners ranging from collagen receptors to laminin and RGD receptors (Hynes, 2002). This would explain why at both time points and on all substrates beta 1 has very strong banding. This could be due to an increase in beta 1 subunits pairing with alpha subunits as cells begin to differentiate.

Beta 2 is not strongly expressed after 4 hours culture but there are very faint bands present from cells seeded on the electrospun scaffolds. After 24 hours there is very weak expression of beta 2 with the strongest band occurring on tissue culture plastic. Beta 2 integrins (CD11/CD18) are mainly expressed on cells derived from the haematopoetic lineage that are involved in the inflammatory response such as neutrophils and macrophages. Beta 2 is also known as CD11b and is involved with the immune system, notably it is expressed and used widely by eosinophils to adhere to the cell wall of fungi.

The eosinophils use that adherence to inject toxic cytokines into the fungal cell (Yoon et al., 2008). Marino et al (2008) investigated a possible relationship between the inflammatory response and the beta 2 integrins in skeletal muscle undergoing hypertrophy or in response to injury. They found that a decrease in beta 2 expression slowed down hypertrophy and repair; they also concluded that beta 2 integrin is not expressed in proliferating C2C12 myoblasts (Marino et al., 2008).

Beta 3 has similar banding to beta 2 although from the data shown in figure 36 it appears that there is no product at the correct size from cells cultured on tissue culture plastic – the band present is slightly lower than the others which are at the correct size for the predicted product length. Blaschuk et al (1997) investigated the beta 3 subunit, with regards to myoblast differentiation, due to its association with alpha V. αVβ3 interacts with various ECM molecules, including laminin, fibronectin, and collagens 1 and 4. It is also upregulated by the myogenesis inhibiting TGF-β1 and phorbol esters. Blaschuk et al showed that the expression of beta 3 decreased 4 fold from cultures at subconfluence to when the myoblasts had differentiated into mature myotubes. Expression of beta 3 after 24 hours appears to be exclusively on aligned fibres and tissue culture plastic. Ren et al 2010 found that blocking integrin subunits beta 1 and beta 3 had effects on cell spreading. They found that blocking beta 1 alone did not have any effect on spreading, but blocking beta 3 and both beta 3 and beta 1 together yielded a noticeable decrease in cellular spreading (Ren et al., 2010).

Beta 4 is weakly expressed in all samples after 4 hours culture, but has the strongest expression from cells seeded on aligned fibres. Beta 4 appears to only be expressed by cells seeded on tissue culture plastic after 24 hours.

After 4 hours culture beta 5 expression is weak. Beta 5, when paired with alpha V, is the sole integrin present in the retinal pigment epithelium-photoreceptor interface at the apical surface, and is involved in maintaining retinal adhesion and phagocytosis of dead photoreceptor cells (Nondrot et al., 2006). Beta 5 has also been implicated in angiogenesis promotion in human mammary carcinoma by promoting epithelial cell migration (Beauvais et al., 2009). Due to these, and other systems unrelated to skeletal muscle, it is expected that expression in C2C12 myoblasts is low. After 24 hours culture beta 5 has very weak banding from the positive control but there appears to be expression from the myoblasts seeded on random fibres and tissue culture plastic. There is a band present on aligned fibres but this may be slightly too small to be considered to be correct. Beta 5 has been shown to be an adenovirus entry point, only in myoblasts not myotubes (Cao et al., 2001).

After 4 hours culture beta 8 expression is weak. It has been shown that beta 8, when paired with alpha V is involved in neurovascular development in the brain (Lakhe-Reddy et al., 2006; Mobley et al., 2009). Mobely et al (2009) show that mice null for alpha 8 develop deficiencies in neurovascular physiology and neurogenesis. Therefore alpha 8 has a function in the neurovascular development and maintenance in the brain (Mobley et al., 2009). Lakhe-Reddy et al (2006) report that alpha 8 is a unique integrin as it has no reported inside-out or outside-in signalling, nor is it involved with cellular adhesion. Instead, Lakhe-Reddy et al found that it is mainly involved with cellular migration and signals through the Rac or cdc42 pathways (Lakhe-Reddy et al., 2006). Expression of beta 8 seems quite strong after 24 hours culture on all samples, but is strongest on aligned and tissue culture plastic.

5.2.7.1 Culture time expression differences

Subunits chosen to investigate differences in expression in response to culture time were those which showed a significant difference in the separate gels shown in figures 36 and 37. Observational differences found from the vinculin staining data shown in figure 35 prompted the comparison of integrin expression between the two time points – 4 hours and 24 hours.

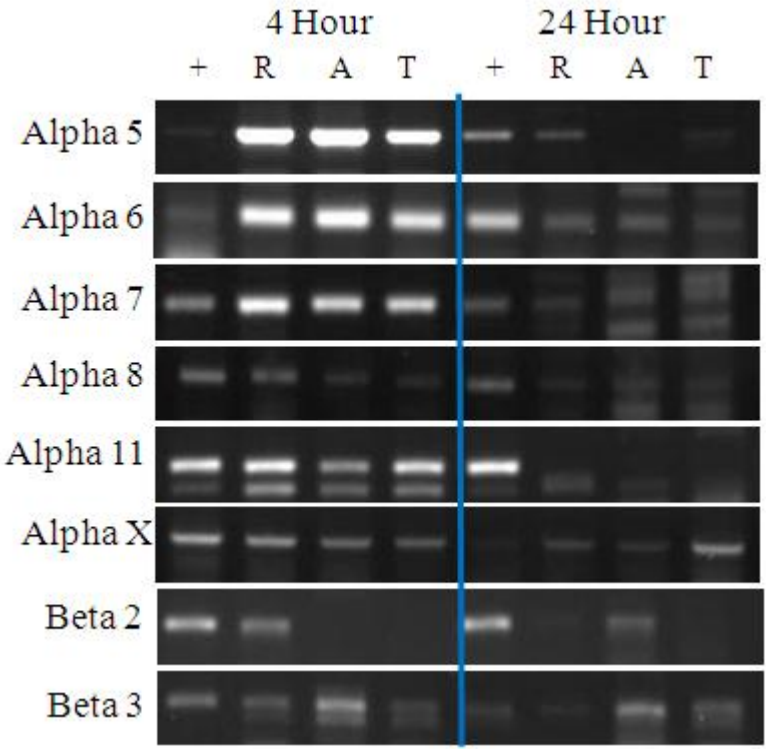

Figure 38: *Comparing integrin mRNA expression in cells cultured for 4 hours and 24 hours.*

There are few definitive theories about integrin expression and signalling as there are many different combinations of subunits and some of these also have splice variants to introduce another level of complexity. It is known that in myoblasts α5β1 is chiefly responsible for binding the ECM protein fibronectin, and α7β1 is involved in binding to

laminin. It is thought that signalling from α5β1 binding to fibronectin maintains myoblasts in a proliferative state whereas signalling from α7β1 binding to laminin enhances differentiation (Glenn et al., 2009; Mayer, 2003; Yao et al., 1996).

From the data presented here, in figure 38, it can be seen that alpha 5 is only expressed in C2C12 myoblasts during early adhesion as it is expressed strongly after 4 hours culture and decreases drastically after 24 hours culture in growth media on all substrates tested here. This could be due to the very high density the cells were seeded accelerating fusion due to the close proximity of the cells.

The expression of alpha 6 differs greatly between 4 hours and 24 hours culture; it is much stronger after 4 hours culture compared to 24 hours. Nath et al 2000 review briefly that integrin α6β1 is a laminin receptor expressed on various cell types during embryogenesis including the myocardium, lens, and gonads. Also in the adult mouse in fibroblasts and Schwann cells among others (Nath et al., 2000). Their main conclusion was that ADAM-9 (A Disintegrin And Metalloprotease domain) can bind to integrin α6β1 and influence fibroblast morphology and enhance migration on a laminin substrate. They also demonstrated that blocking alpha 6 in two cell types (fibroblasts and fibrosarcoma cell lines) greatly reduced adhesion (Nath et al., 2000).

The expression of alpha 7 between the two culture time periods may also indicate that cells are beginning to differentiate as it is very clearly expressed as one clear band after 4 hours culture (figure 38) but this changes to a multi-banded product after 24 hours culture (figure 38) which would suggest splice variants present. A new isoform of alpha 7 (alpha 7A) was identified in 1993 by Collo et al. They found this new isoform was only present in skeletal muscle and C2C12 myoblasts and not heart muscle or brain tissue. Also this

isoform was found to be just over 100bp larger than the original alpha 7B isoform. This correlates with data presented in figure 38, as primers used in this study have an expected product size of 457bp, and the extra band appearing after 24 hours of culture is about 100bp larger than this (see appendix 1 for full gels with ladder). This extra band is indeed alpha 7A, which is only expressed in myoblasts and skeletal muscle tissue. Collo et al also report that the new isoform alpha 7A is only expressed in C2C12 after 2 days in differentiation media. Glenn et al suggest that as myoblasts differentiate they express both isoforms of alpha 7 integrin (Glenn et al., 2009). Primers used in this experiment (figures 36, 37, and 38) were designed to be able to amplify these splice variants along with the original sequence. Measures were taken to make sure the extra bands shown were indeed specifically picked up by the primers and not non-specific banding. From Glenn et al and Collo et al, it could be concluded that the expression of the isoforms 7A and 7B in C2C12 myoblasts is consistent with differentiation.

Figures 36, 37, and 38 all show that there is a decrease in expression of mRNA for the alpha 11 subunit. As touched upon, this could be due to it being a collagen receptor, and after 4 hours culture collagen is still utilised for adhesion. Tiger et al also hinted that alpha 11 beta 1 may be involved in the migratory behaviour of myoblasts (Tiger et al., 2001). Results in figure 38 could indicate that this is the case as cells may be more motile at the earlier time point. Comparing this to other subunit expression, e.g. alpha 5 expression diminishing after 24 hours culture, and the splice variant expression of alpha 7 after 24 hours, could indicate myoblasts entering the differentiation route, thus halting proliferation and migration, which could account for the lack of alpha 11 expression after 24 hours.

These data presenting the differences in integrin expression between myoblasts cultured on different topographical substrates and from different times in culture show a vast range of integrin subunit expression. Although this is interesting, it must be understood that these results show only RNA expression and not functional protein expression or relations between the integrin pairings. In order to investigate this further protein expression profiling must be undertaken, e.g. western blotting or immunocytochemistry.

5.2.8 Differentiation

Myoblasts fuse and differentiate into fully functional myotubes in response to mitogen withdrawal. It is important to elucidate whether myoblasts cultured on the electrospun scaffolds will differentiate into myotubes. It is also of interest to elucidate whether the topography of the aligned electrospun scaffold will enhance fusion and differentiation. It is expected that the alignment of the scaffold will encourage fusion of myoblasts thus enhance differentiation into myotubes. Fast myosin heavy chain (fast MyHC) is used as a marker to illustrate differentiated cells as they will only express this protein when they have differentiated.

5.2.8.1 Fast Myosin Heavy Chain Staining

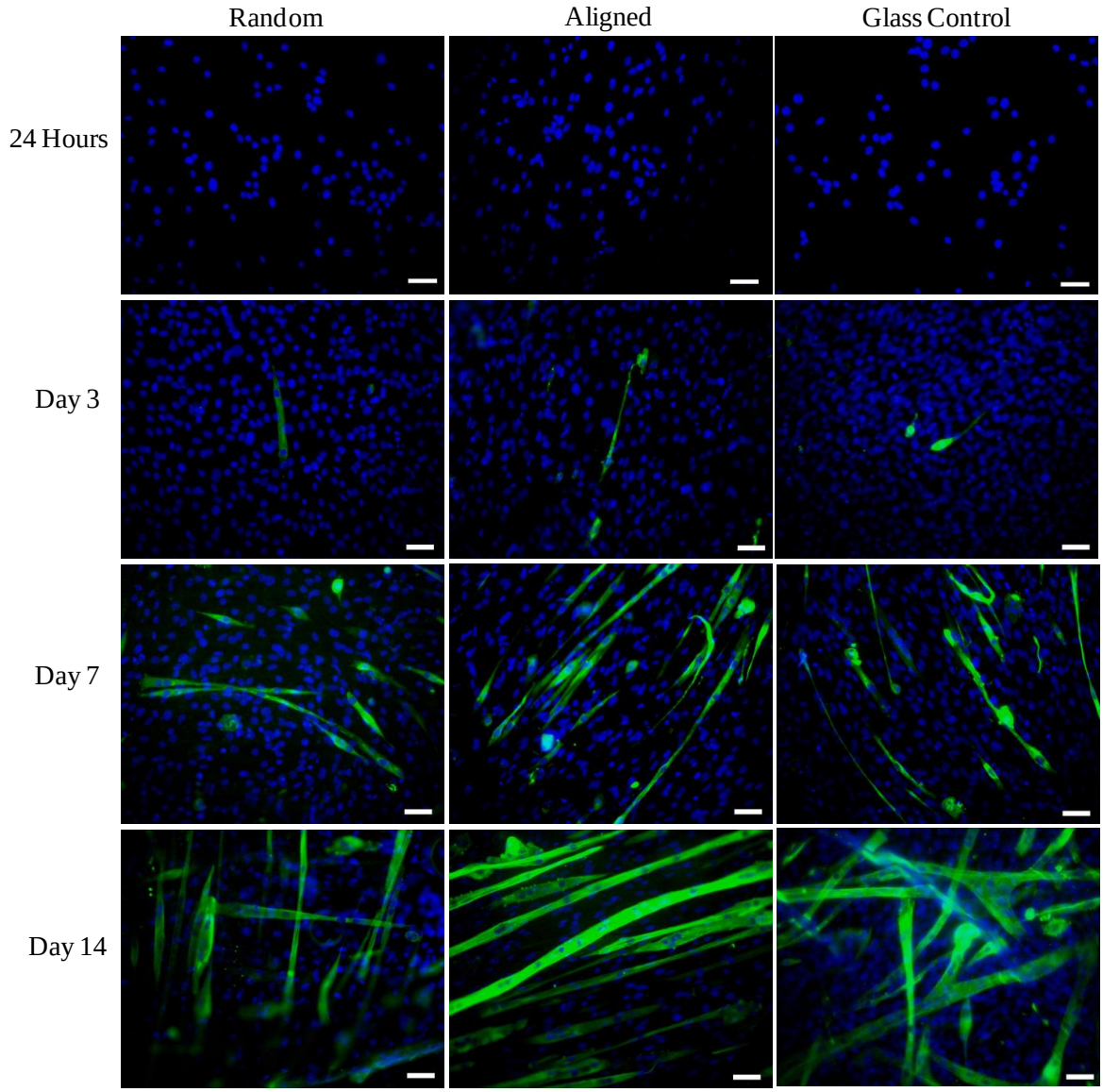

Figure 39: *Fluorescence micrographs showing C2C12 immunostained with the differentiation marker fast myosin heavy chain, seeded on randomly oriented and aligned electrospun PLGA fibres and glass coverslips. Scale bars indicate 50 µm.*

Figure 39 illustrates C2C12 myoblasts expressing the differentiation marker fast myosin heavy chain (fast MyHC) as shown by immunocytochemistry. Cells were seeded then fixed and stained after 24 hours, 3 days, 7 days and 13 days. C2C12 have previously been

shown to express this marker from 7 days when seeded on glass coverslips (Cooper et al., 2004). No differentiation is seen after 24 hours (figures 40 and 41). Images in figure 40 illustrate that C2C12 myoblasts start expressing fast MyHC after just 3 days on electrospun PLGA, earlier than what has previously been reported. After 7 days more fast MyHC positive myotubes are found, and the morphology of the myotubes is again visible with the cells being more aligned together on aligned fibres. By day 14 myotubes that are too long to fit in a 20x magnification image are found mainly on aligned fibres. This could be due to the alignment of the myoblasts prior to differentiation aiding fusion into myotubes as the cells are able to fuse laterally and longitudinally. Myoblasts seeded on grooved substrates have been shown to have impaired fusion due to lack of lateral fusion as the groove prohibits cell-cell contact, thus these cells rely on longitudinal fusion (Clark et al., 2002). Here cells are able to be influenced by the topography of the electrospun fibres, but are still able to form cell-cell contacts from every direction – thus aiding fusion into multinucleated myotubes. Efficient contraction requires long, parallel myofibres as found on aligned fibres. Looking at the day 14 image on glass (figure 39) there are numerous unparallel fast MyHC positive multinucleated myotubes, with irregular morphologies. This is not conducive to efficient contraction as a syncitium.

5.2.8.2 Quantification of Differentiation

Graph shown in figure 40 illustrates the quantification of differentiation obtained using the ICC staining of fast myosin heavy chain (fast MyHC). Percentage of fast MyHC multinucleated myotubes was calculated by dividing number of nuclei in fast MyHC positive multinucleated myotubes by the total number of nuclei in the images (n = 5 per surface type).

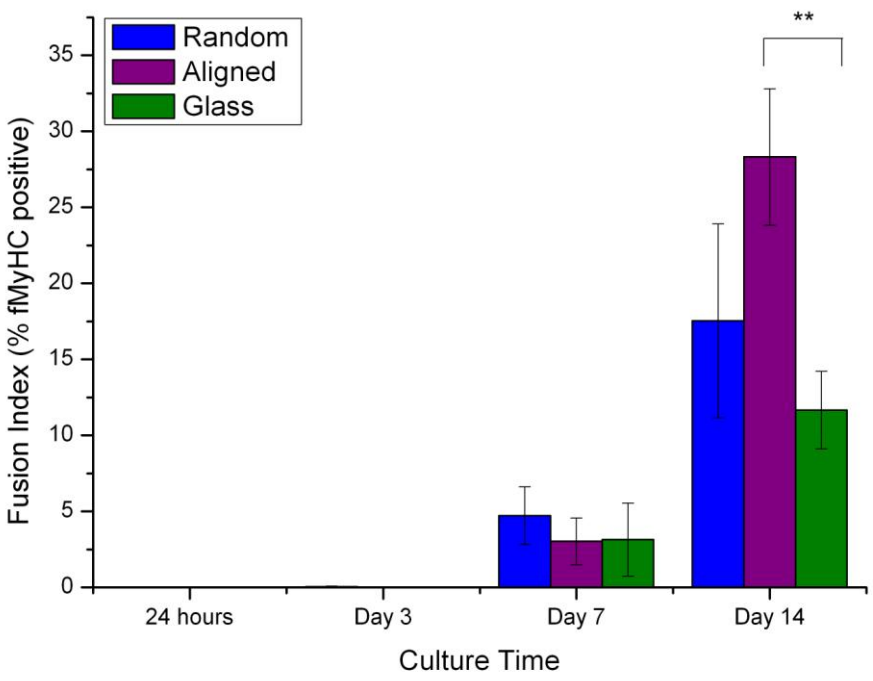

Figure 40: *Quantification of differentiation – percentage of fast myosin heavy chain positive multinucleated myotubes. Bars indicate standard deviation, n = 5 per group, stars over brackets indicate significant difference (P = < 0.05) as shown by the student's t-test.*

After 24 hours there is no differentiation, this is to be expected as the cells adhere and proliferate upon the surface. After 3 days in differentiation culture media, less than 5% cells have begun to differentiate – it must be stressed that at this point any fast MyHC positive myotubes only had multinucleation of 2 nuclei. At 3 days differentiation, cells upon the electrospun scaffolds have expressed fast MyHC significantly more than on glass, and aligned fibres have significantly more than random fibres (P = < 0.05). This could be expected as the alignment of the fibres encourages cellular alignment but does not hinder cell-cell contacts like some grooved surfaces (Clark et al., 2002), leading to greater fusion affinity compared to less organised cells on random fibres and the flat glass control.

Aligned fibres have around 30% fast myosin heavy chain positive cells compared to around 20% on random, and only 10% glass control. This result indicates that the alignment of the cells in response to the topography on aligned fibres enhances fusion and differentiation.

5.2.8.3 Sarcomeric myosin expression

Differentiated myotubes on the scaffold must have the ability to contract. As discussed, contractility in skeletal muscle arises from the contractile sarcomeric myofilaments actin and myosin. In order to test the ability of contraction, the use of immunocytochemistry to mark the sarcomeric proteins is common. In figures 41 and 42, sarcomeric myosin has been stained red in order to visualise the fully differentiated myotubes. Using a confocal microscope also allows the visualisation of the striated appearance of myotubes.

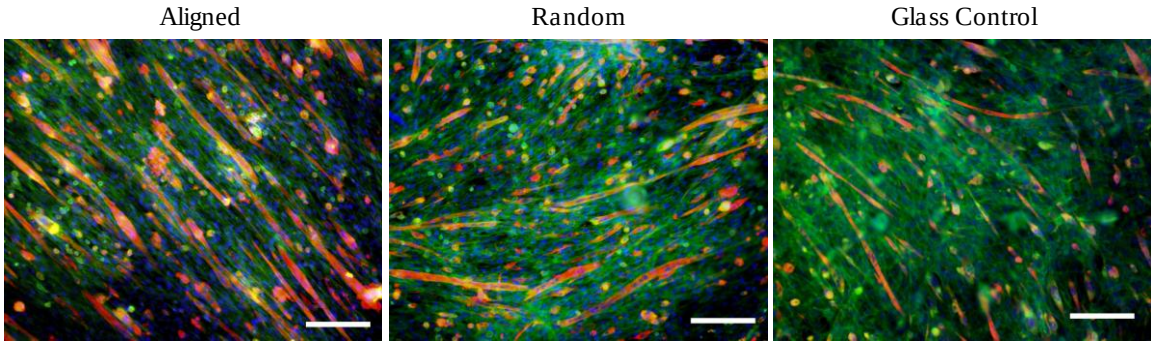

Figure 41: *Low magnification (10x) images of myoblasts stained red with sarcomeric actin, green with FITC-phalloidin, and nuclei are blue. Scale bar indicates 200 µm.*

Figure 41 shows representative images taken from the sarcomeric staining with primary antibody A1025, which was a generous gift from Dr. Michelle Peckham of the University of Leeds, against sarcomeric myosin (red). From these images it is possible to note two findings: the orientation of the myotubes on the different substrates, and the amount of sarcomeric myosin positive myotubes. As shown previously in figures 34 and 40, the

elongated morphology of the myotubes is maintained throughout differentiation. This staining illustrates how the myotubes also maintain an elongated morphology; the red myotubes are parallel with the direction of the not fully differentiated (red negative) myotubes.

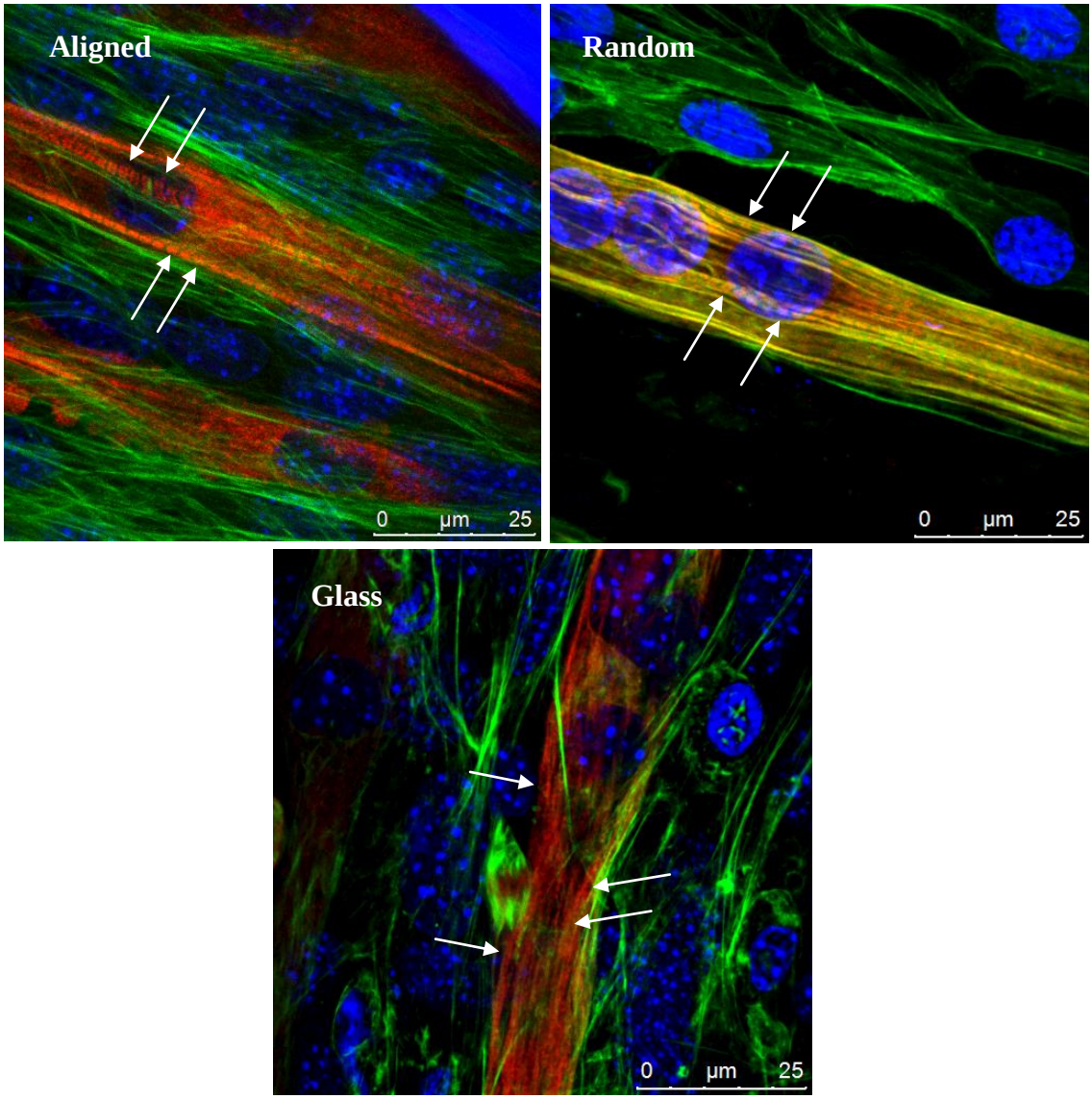

Figure 42: *Confocal microscope images showing sarcomeric myosin (red), f-actin (green), nuclei (blue). Arrows indicate myosin dense area – the A band. Scale indicates 25 µm (Aviss et al., 2010).*

Images shown in figure 42 illustrate positive sarcomeric myosin staining in the expected orientation to form contractile myofibres. From these images it appears that clearer striations occur in cells seeded on the PLGA scaffold. This could suggest C2C12 myoblasts differentiate more efficiently on the scaffold compared to on glass coverslips. This result would concur with Engler et al (Engler et al., 2004) as they discuss how myoblasts differentiate optimally upon less stiff substrates. There appears to be no difference between the types of substrate in these images (figure 42). This is due to the high magnification and zoom used to visualize the all important sarcomeric banding.

5.3 Conclusions

The data in this chapter has shown that myoblasts will elongate and align in response to the topographical cues inferred by the aligned fibrous scaffold. This alignment was then shown to increase during differentiation over 14 days on the aligned scaffold compared to randomly oriented fibres and the glass control. This increase in differentiation on aligned scaffolds may be due to the proximity of similarly oriented myoblasts so fusion can occur more efficiently. Alternatively the alignment of the actin stress fibres in the myoblasts can aid myofibrillogenesis (Lloyd et al., 2004). Myofibrillogenesis is the process that leads to the formation of the sarcomere. This chapter has also shown that the differentiated myotubes express the sarcomeric protein sarcomeric myosin in the correct organization to allow for contraction to take place given the stimulus to do so. This striated appearance is definitive of skeletal muscle. Therefore its appearance shows that these cells, when on the scaffold, do express the structure.

Along with differentiation, this chapter has also looked at myoblast adhesion to the scaffold. Vinculin staining indicated that the cells utilized focal adhesion complexes.

However, on closer inspection of this staining, there appeared to be fewer focal adhesions present on the elongated cells on the aligned scaffold after 24 hours culture. To investigate this further mRNA expression of integrin subunits was measured with cells cultured for 4 hours and 24 hours on the 3 substrates: aligned fibres, random fibres and tissue culture plastic as a control. From this study it was shown that an unexpectedly vast array of integrin subunits are expressed at the mRNA level in proliferating C2C12 murine myoblasts. Most of these will not make it through protein processing and to the surface of the cell to be paired with the opposing subunit. From this experiment it is unclear which of these will be expressed and functionalized at the protein level. More work is needed to clarify precisely how myoblasts attach via integrins to different topographies, and how this adhesion mechanism changes over culture time.

5.4 Future Work

To take this work further it would be interesting to do a number of experiments. Live cell imaging on the different fibre orientation scaffolds could be used to investigate the motility of the cells on the different scaffolds, i.e. to see if the cells moved along the length of the aligned fibres and how this is different to the motility on random fibres and the glass control.

Electrical stimulation of the cells could elucidate the contractile ability of the cells and see whether the organization of the cells on the different substrates plays a role in contractile efficiency. It could be expected that cells seeded on the aligned fibres would be able to produce greater force due to their parallel arrangement leading to a more efficient propagation of stimulus and ability to act as a greater syncitia. Cells seeded on random fibres and glass could also produce force as they also express the sarcomeric machinery

necessary for contraction, but this may not be as efficient as that produced from cells on the aligned fibres.

As has been hinted at previously it could be possible to incorporate short peptide sequences into the scaffold in order to control cellular fate. This could be done to maintain cells in a proliferative state or to encourage differentiation. It is known that, via integrins, laminin and fibronectin have opposing effects on skeletal muscle differentiation; fibronectin sequences could be used to maintain cells in a proliferative state whereas laminin sequences could be used to stimulate differentiation. Due to the flexibility of electrospinning, it could be possible to create a scaffold that displays proliferation signals for a certain amount of time, e.g. using a core-shell arrangement with differentiation signals, which will stimulate differentiation globally throughout the scaffold at the same time to control cellular differentiation. This idea could be translated into other cell types – namely stem cells as this could be used to determine differentiation lineage.

Using this scaffold could be the basis for a three-dimensional construct if combined with a gel e.g. fibrin gel. As discussed in chapter 1 fibrin gel has been used by Huang et al (Huang et al., 2005) and Lam et al (Lam et al., 2009) used fibrin gel in conjunction with a microgrooved PDMS scaffold to create a 3D scaffold with the aligned architecture of the myoblasts from the microgrooved substrate transferred into the gel. Using this as inspiration the electrospun scaffold could be incorporated into the gel as it could maintain the alignment and also contribute to the mechanical stabilization of the construct until the cells can support it themselves. An advantage of incorporating the electrospun scaffold into the gel, as opposed to removing the cells from the PDMS substrate is that layering could take place to get more cells into the construct by layering cell seeded aligned electrospun

scaffolds with gel. The natural diffusion limits of 3D constructs will be an issue that will need addressing.

Finally, the tentative results obtained here displaying the changes in integrin expression could be more fully investigated by looking into changes in expression during differentiation. Also looking at the full heterodimeric structure of the integrin instead of just the subunits would give a more specific insight into the mechanisms of integrin expression and signaling. Also knocking out subunits that have different expression profiles from 4 hours and 24 hours culture and monitoring how these affect adhesion at different time points could show which subunits are involved in adhesion, be that cell-matrix adhesion or cell-cell adhesion.

The University of Manchester

Chapter 6: Final Conclusions

Concluding and summarising the major findings of this work

Kathryn Aviss

6 *Final discussion*

The aim of this thesis was to introduce a novel, synthetic, biodegradable scaffold that would infer topographical signals for efficient skeletal muscle tissue engineering. The clinical need is that no satisfactory skeletal muscle repair system is in place for patients with severe 4th degree burns; skin can be engineered and replaced as a graft, but no such material is available for skeletal muscle. Without external aid, skeletal muscle cannot repair such a large defect naturally which means the patient will not regain full power of the effected limb. Natural skeletal muscle regeneration occurs via fibrosis thus naturally regenerated tissue will never be as functional as pre-injury tissue (Chan et al., 2003; Gurtner et al., 2008; Jejurikar et al., 2006). Creating a tissue engineered skeletal muscle graft could help patients regain power after significant trauma to skeletal muscle, and also provide a true-to-life experimental system for studies into diseases affecting skeletal muscle e.g. muscular dystrophies.

Electrospinning has been shown to be a flexible and efficient method to produce fibrous meshes with controllable architectures. In order to dissolve polymers to create scaffolds suitable for cell culture, harsh solvents, which would not be applicable for cell culture, have to be used. The advantage of electrospinning is that the majority of the solvent is evaporated before the fibres are deposited. The amount of residual solvent in the electrospun PLGA fibres was measured here using FTIR and TgA (thermogravimetric analysis). TgA results indicated that a maximum of 4% total weight of the electrospun meshes consist of solvent. This 4% is unlikely to cause any adverse reaction to any cells cultured on the scaffold.

The creation of aligned fibres for the application of skeletal muscle regeneration originates from the precise parallel hierarchy of skeletal muscle tissue. In order to create a

scaffold for tissue engineering it is essential to consider the architecture of the natural tissue one wishes to recreate/support during regeneration. It was previously shown that aligned electrospun fibres do convey the correct topography for contact guidance to allow for cellular elongation along the fibre length (Aviss et al., 2010; Bashur et al., 2006; Choi et al., 2008; Huang et al., 2006; Huber et al., 2007). A topographical scaffold is necessary for skeletal muscle regeneration as, although myoblast cells will align locally with neighbouring cells, they will form swirling patterns on flat surfaces which are not conducive to an efficiently contractile tissue. Using highly aligned fibres as a template for alignment guarantees global alignment over the whole construct thus creating a tissue with greater contractile prospect (Aviss et al., 2010).

PLGA was used for this study because it is a biodegradable polymer, and has mechanical properties that will enhance myoblast attachment and differentiation. Polyesters such as PLGA can also be modified easily to provide biologic cues to the cells if desired. An example of when this might be interesting in the context of skeletal muscle tissue engineering could be incorporation of matrix metalloproteinases such as MMP-1, which Bedair et al showed to be able to remove scar tissue formed by naturally regenerating skeletal muscle (Bedair et al., 2007). By including this, perhaps incorporating the protein into the electrospinning solution to be expressed both on the surface of the fibres and also released as the polymer degrades, could aid in scar tissue formation reduction if inserted into a damaged tissue.

It was shown that pre-conditioning of the electrospun PLGA scaffolds with serum containing media prior to cell seeding is unnecessary as myoblasts will adhere and proliferate upon scaffolds that have not been conditioned with serum containing media. This increases its clinical applicability as cells can be cultured in totally defined medium,

thus reducing the risk of any adverse immunogenic response from the foreign proteins that are present in serum. Investigations into a possible inflammatory response were undertaken using macrophage culture upon the scaffolds. Cytokine release from the macrophages was monitored using assays such as ELISA and showed that the reaction of the macrophages was not dissimilar to that from tissue culture plastic. Indicating no inflammatory response was elucidated from the macrophages on the electrospun scaffolds. Wang et al created a novel biodegradable polyester which, if electrospun, may be a better alternative for skeletal muscle tissue engineering. The polymer they created was poly(glycerol-sebacate). They compared the inflammatory response of flat films of PGS with PLGA and found that PGS had an even smaller inflammatory response than PLGA. However they do suggest that a small inflammatory response during tissue repair may be beneficial as this will encourage the necessary growth factors and cytokines to the site, positively influencing the repair process (Wang et al., 2002). However, PGS would be difficult to electrospin as it needs to be cured at high temperatures. In the electrospinning process this would need to occur 'on-the-fly', which means as the polymer exits the needle. This poses problems as specific heaters would need to be employed which may contravene health and safety when combined with the high voltage required for the process. PLGA and it's components lactic acid and glycolic acid also have the advantage of already being in clinical use as biodegradable sutures since the 1960's (Gilding and Reed, 1979).

Investigations into cellular adhesion mechanisms have been undertaken, but these studies often concentrate on cells that have been on the scaffold for days, if not weeks. Here early adhesion via focal complexes and integrin expression was investigated. Using immunostaining it was possible to visualize focal adhesions by staining for a component of the adhesion – vinculin. From these images it was shown that clear punctuate areas, rich in

vinculin, were visible around the periphery of all cells cultured on the scaffolds except those seeded on aligned fibres and stained after 24 hours culture. In these cells, focal contacts were not clearly visible. To investigate this further, PCR of integrin-coding mRNA was undertaken to elucidate which integrins the cells were expressing in response to the scaffolds. Data from the integrin PCR showed that there was a wide array of integrin subunit mRNA expression, perhaps more than could be expected, and that further investigations are necessary. These investigations should include immunostaining of the integrins illustrated in figure 39 to show distinct differences between 4 hours and 24 hours culture. The expression of alpha X in all samples at all time points is interesting as this has not been shown before in myoblasts. Future work to take these data further could include: Western Blotting in order to find out if the protein is expressed and how much. Also some quantitative PCR could be performed in order to elucidate finer detail of the integrin expression profile. In order to progress this research further, looking into signalling pathways thought to be associated with the integrins expressed, e.g. rho pathway, to elucidate any definitive roles for the subunits, and the effect they have on cellular behaviour.

Finally, an investigation into the differentiation and contractile potential of myoblasts seeded onto the scaffolds was undertaken. Quantification of differentiation via the fusion index illustrated that after 14 days around 30% of myoblasts seeded on aligned fibres had differentiated compared to 25% on random and 10% on glass. This shows that the electrospun fibres, especially the aligned fibres are conducive to effective fusion and differentiation of myoblasts. This could be due to two mechanisms: 1) the cells are already parallel to each other so fusion signalling via cell-cell contact is more efficient, or 2) alignment of actin stress fibres in the myoblasts aids myofibrillogenesis (the formation of

myofibres) (Lloyd et al., 2004). Immunostaining for a protein present in the sarcomere showed that all myoblasts seeded on the electrospun fibres expressed sarcomeric proteins and arranged them in the stereotypical array creating the striated appearance so characteristic of skeletal muscle.

6.1 Future Work

Further work necessary before this study could progress towards clinical application includes a more detailed degradation study. This degradation study would include investigations into molecular weight changes by using GPC. It would also include studies using cell culture medium as the degradation media, in cell culture conditions, i.e. at 37^{o}C in a humidified atmosphere with 5% carbon dioxide. Another aspect of degradation would involve monitoring degradation with active cell culture. Two types of cell degradation studies could take place: one with a monoculture of muscle cells, another with a dual culture of myoblasts and macrophages as per Pan et al (Pan et al., 2008). A final study would bring the whole degradation profile together: a degradation study that could be undertaken would be an *in vivo* study using a mouse model. These studies should provide an extensive insight into the degradation profile of electrospun PLGA thus total control can be had of the scaffold when implanted providing reliable predictability.

A histological study of the scaffold could also provide essential insights necessary before progression further towards clinical application. This would be especially beneficial if a tri-culture of cells was used with and without a more 3D substrate e.g. a gel as it would portray fully the organisation of myofibres, but also if HUVECs/pericytes were included in the culture system, formation of small blood vessels could also be monitored. In order to form a fully functional 3D muscle, blood vessels are essential.

Other future work investigates further the cellular behaviour on the scaffolds. This would include cell motility studies which could lead to a detailed study upon fusion mechanisms on the different topographical surfaces. It could be predicted that the initiation of fusion occurs sooner on the aligned fibres compared to random and glass, for reasons previously discussed. Also, as mentioned, a more detailed investigation into early adhesion behaviour by monitoring integrin protein expression and also quantitative real-time PCR could be undertaken to provide a more holistic view of these mechanisms.

Incorporation of synthetic biologic cues such as small protein fragments or peptide sequences could be utilised to convey further control and predictability of cellular behaviour. As mentioned, incorporation of MMPs could provide another dimension of application *in situ* as a skeletal muscle graft by slowing the formation of collagenous scar tissue in the defected area.

In order to progress the clinical application of this study, incorporating the electrospun fibres into a degradable gel, e.g. fibrin, could be undertaken to investigate the possibility of a 3D construct. Contractility studies involving stimulating contraction of the myotubes using electrophysiological techniques could be performed. This would determine if both the monolayer of differentiated cells on the electrospun scaffold, and any 3D constructs, are capable of producing force, and if so how much. As briefly mentioned, a tri-culture of myoblast cells, with a fibroblast cell type (e.g. MEFs) and a cell line such as pericytes or HUVECs could encourage vascularisation of the construct (Levenberg et al., 2005). By combining the aligned electrospun scaffold with a gel, the cellular alignment conveyed by the scaffold is not lost when introduced into a 3D environment (Huang et al., 2005).

6.2 Final Conclusions

The data in this thesis aimed to show that a biodegradable electrospun mesh with topographical cues could promote myoblast elongation and alignment. From the data presented it can be concluded that electrospinning of highly aligned PLGA fibres does produce a scaffold suitable for skeletal muscle tissue engineering. Further work based on this thesis could provide insights into both the fundamental aspects of myoblast adhesion on topographical substrates, and differentiation in response to topographical cues, and progress the development of a 3D construct that could potentially have valuable clinical applications.

Kathryn Aviss

Appendix 1

Data not shown in main document

The University of Manchester

7.1 Appendix 1

7.1.1 Complete FTIR Spectra

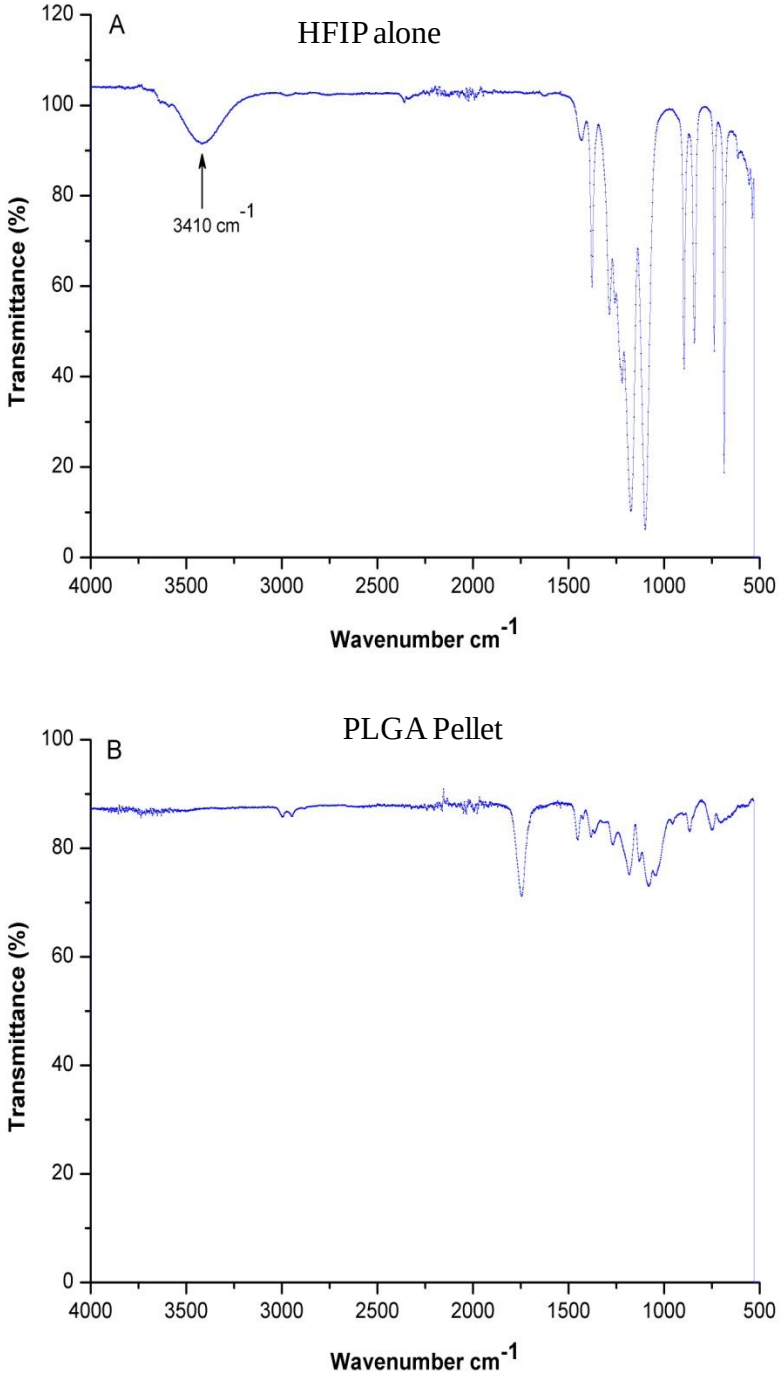

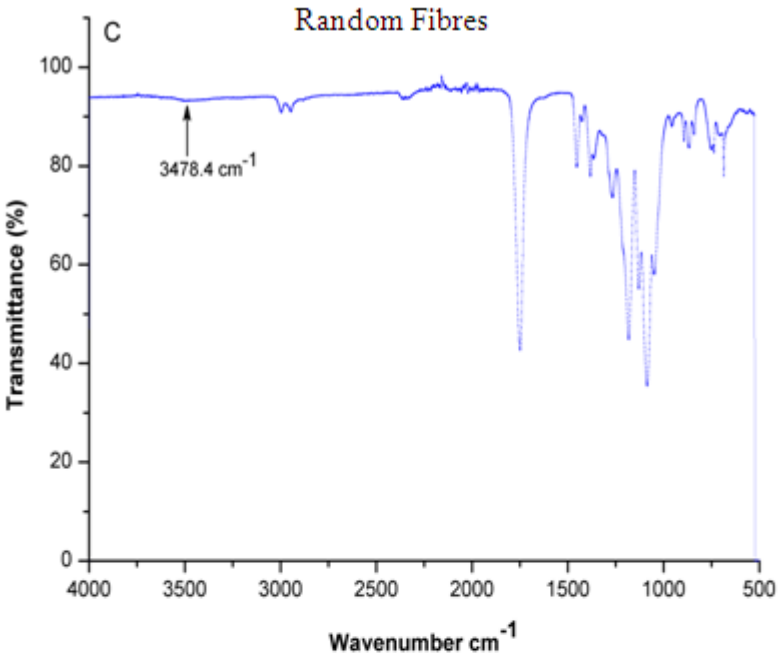
C
Random Fibres
100
80
60
40
20
0
3478.4 cm-1
Transmittance (%)
4000
3500
3000
2500
2000
1500
1000
500
Wavenumber cm-1

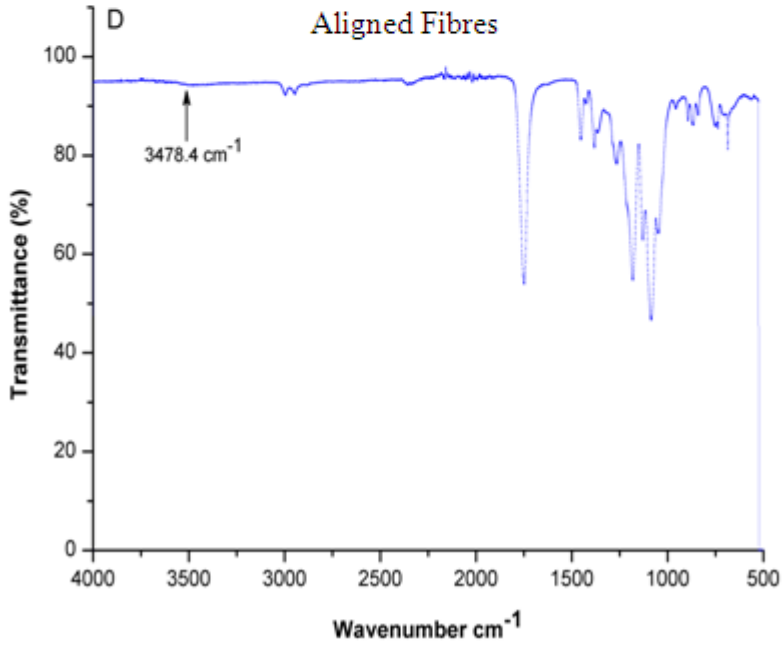
D
Aligned Fibres
100
80
60
40
20
0
3478.4 cm-1
Transmittance (%)
4000
3500
3000
2500
2000
1500
1000
500
Wavenumber cm-1

7.1.2 Full Integrin PCR gels

7.1.2.1 4 Hours Culture

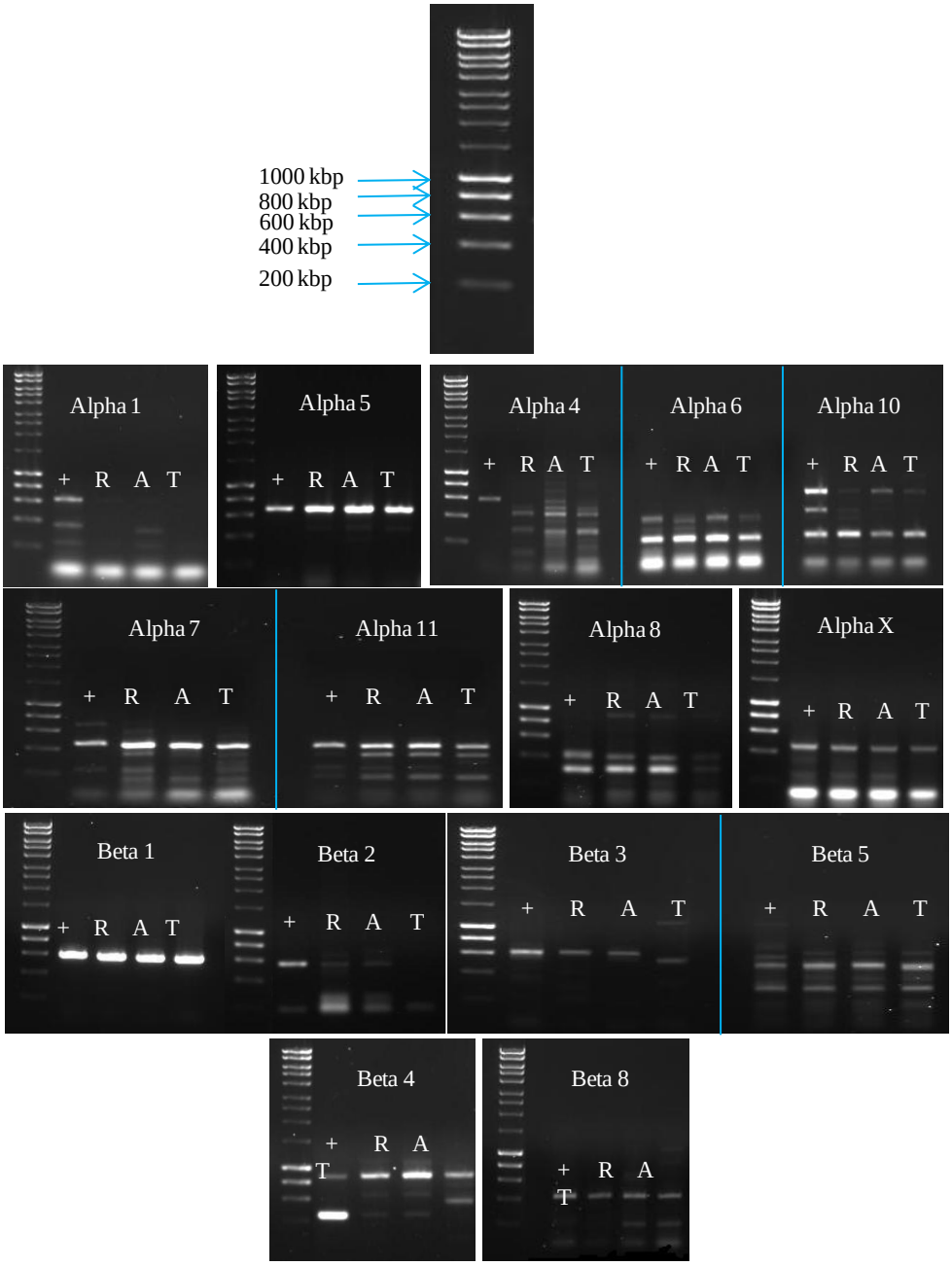

7.1.1.2 24 Hours Culture

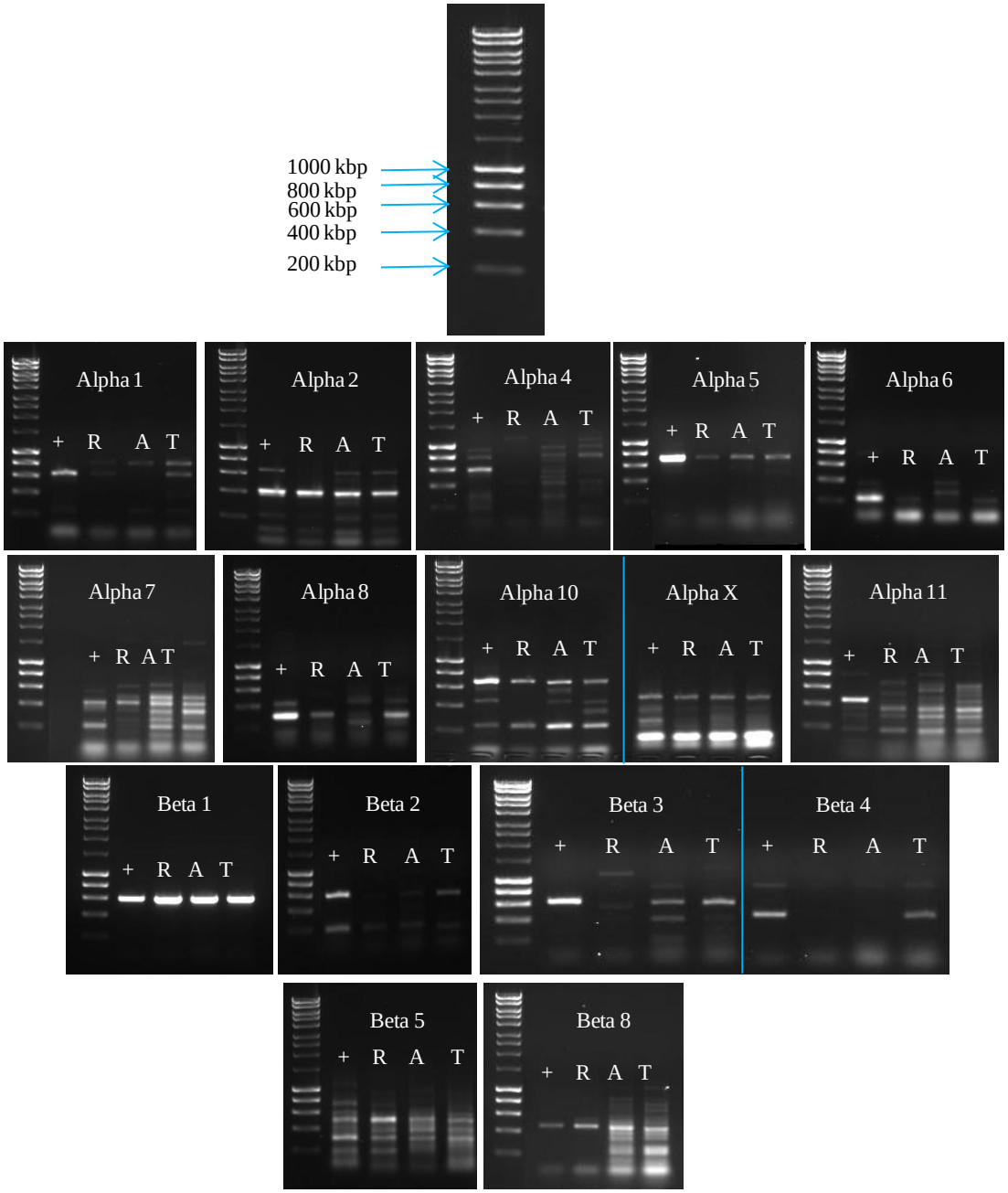

Kathryn Aviss

Appendix 2: Publications

Publications from presented work

The University of Manchester

8.1 Appendix 2

8.1.1 Conference Presentations and Publications

ESB 2007, Brighton UK, Poster Presentation; Regeneration of Skeletal Muscle Using Polymer Nanofibres

UKSB Liverpool UK, Aural presentation; Aligned Nanofibre Constructs for Skeletal Muscle Tissue Engineering

Alternative Muscle Club, Manchester UK, Poster Presentation; Aligned Electrospun Polymer Fibres for Skeletal Muscle Regeneration

TCES 2010, Manchester UK; Electrospinning Highly Oriented Elastomeric Fibres for Skeletal Muscle Regeneration

European Cells and Materials Vol. 19 2010 (pages 193-204) ISSN 1473-2262

ALIGNED ELECTROSPUN POLYMER FIBRES FOR SKELETAL MUSCLE REGENERATION

K.J. Aviss, J.E. Gough, and S. Downes*

School of Materials, Biomaterials Group, The University of Manchester, Manchester, M1 7HS, UK

Abstract

Skeletal muscle repair is often overlooked in surgical procedures and in serious burn victims. Creating a tissue-engineered skeletal muscle would not only provide a grafting material for these clinical situations, but could also be used as a valuable true-to-life research tool into diseases affecting muscle tissue. Electrospinning of the elastomer PLGA produced aligned fibres that had the correct topology to provide contact guidance for myoblast elongation and alignment. In addition, the electrospun scaffold required no surface modifications or incorporation of biologic material for adhesion, elongation, and differentiation of C2C12 murine myoblasts.

Keywords: Electrospinning, myoblasts, alignment, PLGA, surface topography.

*Address for correspondence:
Sandra Downes
School of Materials, Biomaterials Group
The University of Manchester
Manchester, M1 7HS, UK
E-mail: sandra.downes@manchester.ac.uk

Introduction

Skeletal muscle is a highly organised and hierarchical tissue. Creating and maintaining myoblast to myotube morphology has been a challenge in tissue engineering of skeletal muscle (Huang *et al*., 2006; Riboldi *et al*., 2005). Grown on surfaces with no contact guidance, myoblasts grow in random swirling patterns; which is not conducive to the formation of efficient contraction. In order to contract as a syncytium, muscle fibres must grow parallel to one another with identical anisotropy. This can be done by using a scaffold with the relevant topography to induce this behaviour via contact guidance (Bashur *et al*., 2006; Dalby *et al*., 2003). It is known that the structural components of the extracellular matrix (ECM) and their interaction with transmembrane proteins, such as integrins play a role in the organisation of tissues, including the organisation of myoblasts (Bray *et al*., 2008; Schiaffino and Partridge, 2008). These ECM cues provide topology and mechanical properties relevant to the tissue and changes in ECM structure can affect cellular behaviour. To aid the regeneration of skeletal muscle, an oriented scaffold that provides a template for alignment could be used to encourage this organisation in myoblasts as they fuse and differentiate to form multinucleated myofibres. By electrospinning an elastomeric polymer, poly(lactide-co-glycolide), it is possible to create such a scaffold that may provide the topographical cues and contact guidance for alignment of myoblasts (Choi *et al*., 2008), while providing an elastic substrate for myotube differentiation. The technique of electrospinning is attractive to use in this application because of the amount of control available by altering various parameters. For example, the size of the fibres, from the micrometer to the nanometre range, can be controlled by changing the concentration of polymer, flow rate and the distance from needle to collector plate. A comprehensive review of the electrospinning process has been carried out by Subbiah *et al*. (2004).

Alignment of polymer nanofibres can be controlled by selecting the relevant collector plate: stationary or very slow rotation of the collector plate can be used to manufacture randomly oriented fibres, whereas a high-speed rotating mandrel can be used to create aligned fibres (Bian and Bursac, 2009; Blackwood *et al*., 2008; Courtney *et al*., 2006; Wang *et al*., 2009).

To date polyesters such as PCL (polycaprolactone), PLA (poly (lactic acid)), PGA (poly (glycolic acid)), and their co-polymer PLGA (poly (lactide-co-glycolide)) have been used in the form of foams, films, and electrospun fibres for tissue engineering applications (Huang *et al*., 2006; Huang *et al*., 2005; Singh *et al*., 2004). Levenberg *et al*. (2005) used a sponge of PLLA (poly-L-lactic acid) and PLGA to form a highly porous three-dimensional (3D)

9 References

Alberts, B., Johnson, A., Lewis, J., Raff, M., Roberts, K. and Walter, P. (2002). Molecular Biology of the Cell, (ed.: Garland Science.

Altomare, L., Gadegaard, N., Visai, L., Tanzi, M. C. and Fare, S. (2010). Biodegradable microgrooved polymeric surfaces obtained by photolithography for skeletal muscle cell orientation and myotube development. *Acta Biomaterialia* **6**, 1948-1957.

Astbury, W. T. (1947). Croonian Lecture: On the structure of biological fibres and the problem of muscle. *Proceedings of the Royal Society of London. Series B, Biological Sciences* **134**, 303-328.

Aviss, K. J., Gough, J. E. and Downes, S. (2010). Aligned electrospun polymer fibres for skeletal muscle regeneration. *European Cells and Materials* **19**, 193-204.

Baker, S. C., Rohman, G., Southgate, J. and Cameron, N. R. (2009). The relationship between the mechanical properties and cell behaviour on PLGA and PCL scaffolds for bladder tissue engineering. *Biomaterials* **30**, 1221-1328.

Bashur, C. A., Dahlgren, L. A. and Goldstein, A. S. (2006). Effect of fiber diameter and orientation on fibroblast morphology and proliferation on electrospun poly(D,L-lactic-co-glycolic acid) meshes. *Biomaterials*, 5681-5688.

Beauvais, D. M., Ell, B. J., McWhorter, A. R. and Rapraeger, A. C. (2009). Syndecan-1 regulates alphaVBeta3 and alphaVbeta5 integrin activation during angiogenesis and is blocked by synstatin, a novel peptide inhibitor. *The Journal of Experimental Medicine* **206**, 691-705.

Beckerle, M. C. (2001). Cell Adhesion. In *Frontiers in molecular biology*, (ed. B. D. Hames and D. M. Glover): Oxford University Press.

Bedair, H., Liu, T. T., Kaar, J. L., Badlani, S., Russell, A. J., Li, Y. and Huard, J. (2007). Matrix metalloproteinase-1 therapy improves muscle healing. *Journal of Applied Physiology* **102**, 2338-2345.

Bian, W. and Bursac, N. (2009). Engineered skeletal muscle tissue networks with controllable architecture. *Biomaterials* **30**, 1401-1412.

Bischoff, R. (1975). Regeneration of single skeletal muscle fibres in vitro. *The Anatomical Record* **182**, 215-236.

Bischoff, R. (1986). A satellite cell mitogen from crushed adult muscle. *Developmental Biology* **115**, 140-147.

Blackwood, K. A., McKean, R., Canton, I., Freeman, C. O., Franklin, K. L., Cole, D., Brook, I., Farthing, P., Rimmer, S., Haycock, J. W. et al. (2008). Development of biodegradable electrospun scafolds for dermal replacement. *Biomaterials*, 3091-3104.

Bossy, B., Bossy-Wetzel, E. and Reichardt, L. F. (1991). Characterisation of the integrin alpha 8 subunit: a new beta 1-associated subunit, which is prominently expressed on axons and on cells in contact with basal laminae in chick embryos. *The EMBO Journal* **10**, 2375-2385.

Callister, W. D. (2007). Materials science and engineering: an introduction. New York: John Wiley and Sons, Incorporated.

Camper, L., Holmvall, K., Wangnerud, C., Aszodi, A. and Lundgren-Akerlund, E. (2001). Distribution of the collagen-binding integrin alpha10beta1 during mouse development. *Cell and Tissue Research* **306**, 107-116.

Cao, B., Pruchnic, R., Ikezawa, M., Xiao, X., Li, J., Wickham, T. J., Kovesdi, I., Rudert, W. A. and Huard, J. (2001). The role of receptors in the maturation-dependent adenoviral transduction of myofibres. *Gene Therapy* **8**, 627-637.

Chalmers, J. M. and Everall, N. J. (1993). Vibrational Spectroscopy. In *Polymer Characterisation*, (ed. B. J. Hunt and M. I. James): Blackie Academic and Professional.

Chan, Y.-S., Li, Y., Foster, W., Horaguchi, T., Somogyi, G., Fu, F. H. and Huard, J. (2003). Antifibrotic effects of suramin in injured skeletal muscle after laceration. *Journal of Applied Physiology*, 771-780.

Charge, S. B. P. and Rudnicki, M. A. (2004). Cellular and molecular regulation of muscle regeneration. *Physiological Reviews* **84**, 209-238.

Choi, J. S., Lee, S. J., Christ, G. J., Atala, A. and Yoo, J. J. (2008). The influence of electrospun aligned poly(caprolactone)/collagen nanofiber meshes on the formation of self-aligned skeletal muscle myotubes. *Biomaterials*, 2899-2906.

Christopherson, G. T., Song, H. and Mao, H.-Q. (2009). The influence of fiber diameter of electrospun substrates on neural stem cell differentiation and proliferation. *Biomaterials*, 556-564.

Clark, P., Dunn, G. A., Knibbs, A. and Peckham, M. (2002). Alignment of myoblasts on ultrafine gratings inhibits fusion in vitro. *The International Journal of Biochemistry and Cell Biology* **34**, 816-825.

Coletti, D., Teodon, L., Albertini, M. C., Rocchi, M., Pristera, A., Fini, M., Molinaro, M. and Adamo, S. (2007). Static magnetic fields enhance skeletal muscle differentiation in Vitro by improving myoblast alignment. *Cytometry Part A* **71A**, 846-856.

Conboy, I. M., Conboy, M. J., Smythe, G. M. and Rando, T. A. (2003). Notch-mediated restoration of regenerative potential to aged muscle. *Science* **302**, 1575-1577.

Cooper, J. A., Sahota, J. S., II, W. J. G., Carter, J. and Doty, S. B. (2007). Biomimetic tissue-engineered anterior cruciate ligament replacement. *PNAS* **104**, 3049-3054.

Cooper, S. T., Maxwell, A. L., Kizana, E., Ghoddusi, M., Hardeman, E. C., Alexander, I. E., Allen, D. G. and North, K. N. (2004). C2C12 co-culture on a fibroblast substratum enables sustained survival of contractile, highly differentiated myotubes with peripheral nuclei and adult fast myosin expression. *Cell Motility and the Cytoskeleton*, 200-211.

Dalby, M. J., Childs, S., Riechle, M. O., Johnstone, H. J. H., Affrossman, S. and Curtis, A. S. G. (2003). Fibroblast reaction to island topography: changes in cytoskeleton and morphology with time. *Biomaterials* **24**, 927-935.

Dalby, M. J., Hart, A. and Yarwood, S. J. (2008). The effect of the RACK1 signalling protein on the regulation of cell adhesion and cell contact guidance on nanometric grooves. *Biomaterials*, 282-289.

Dalby, M. J., Riechle, M. O., Sutherland, D. S., Agheli, H. and Curtis, A. S. G. (2004). Use of nanotopography to study mechanotransduction in fibroblasts - methods and perspectives. *European Journal of Cell Biology*, 159-169.

Danowski, B. A., Imanaka-Yoshida, K., Sanger, J. M. and Sanger, J. W. (1992). Costameres are sites of force transmission to the substratum in adult rat cardiomyocytes. *118* **6**.

Dong, Y., Yong, T., Liao, S., Chan, C. K., Stevens, M. M. and Ramakrishna, S. (2010). Distinctive degradation behaviours of electrospun polyglycolide, poly(DL-lactide-co-glycolide), and poly(L-lactide-co-caprolactone) nanofibres cultured with/without porcine smooth muscle cells. *TIssue Engineering part A* **16**, 283-298.

Dubard, J.-L., Belkin, A. M., Syfrig, J., Thiery, J. P. and Koteliansky, V. E. (1992). Expression of alpha 1 integrin, a laminin-collagen receptor, during myogenesis and neurogenesis in the avian embryo. *Development* **116**, 585-600.

Engelmyr, G. C., Cheng, M., Bettinger, C. J., Borenstein, J. T. and Freed, L. E. (2008). Accoridan-like honeycombs for tissue engineering of cardiac anisotropy. *Nature Materials* **7**, 1003-1010.

Engler, A. J., Griffin, M. A., Sen, S., Bonnemann, C. G., Sweeny, H. L. and Discher, D. E. (2004). Myotubes differentiate optimally on substrates with tissue-like stiffness: pathological implications for soft of stiff microenvironments. *The Journal of Cell Biology* **166**, 877-887.

Geiger, B. (1979). A 130K protein from chicken gizzard: its localisation at the termini of microfilament bundles in cultured chicken cells. *Cell* **18**, 193-205.

Gilding, D. K. and Reed, A. M. (1979). Biodegradable polymers for use in surgery-polyglycolic/poly(actic acid) homo- and copolymers: 1. *Polymer* **20**, 1459-1554.

Ginde, R. M. and Gupta, R. K. (1987). In vitro chemical degradation of poly(glycolic acid) pellets and fibres. *Journal of Applied Polymer Science* **33**, 2411-2429.

Glenn, H. L., Wang, Z. and Schwartz, L. M. (2009). Acheron, a Lupus antigen family member, regulates integrin expression, adhesion, and motility in differentiating myoblasts. *Americal Journal of Cell Physiology* **298**, C46-C55.

Goldberg-Oppenheimer, P. and Steiner, U. (2010). Rapid electrohydrodynamic lithography using low viscosity polymers. *Small* **6**, 1248-1254.

Goodman, S. L., Risse, G. and Mark, K. v. d. (1989). The E8 subfragment of laminin promotes locomotion of myoblasts over extracellular matrix. *The Journal of Cell Biology* **109**, 799-809.

Graves, D. C. and Yablonka-Reuveni, Z. (2000). Vascular smooth muscle cells spontaneously adopt a skeletal muscle phenotype: A unique $Myf5^{-}/MyoD^{+}$ myogenic program. *The Journal of Histochemistry and Cytochemistry* **48**, 1173-1193.

Gullberg, D., Velling, T., Sjoberg, G. and Sejersen, T. (1995). Up-regulation of a novel integrin alpha-chain (alpha-mt) on human fetal myotubes. *Developmental Dynamics* **204**, 57-65.

Gurtner, G. C., Werner, S., Barrandon, Y. and Longtaker, M. T. (2008). Wound repair and regeneration. *Nature* **453**, 314-321.

Hartner, A., Cordasic, N., Rascher, W. and Hilgers, K. F. (2009). Deletion of the alpha 8 integrin gene does not protect mice from myocardial fibrosis in DOCA hypertension. *American Journal of Hypertension* **22**, 92-99.

Hockberger, P. E., Ahmed, M. S., Skimina, T. A., Lee, C., Hung, W.-Y. and Siddique, T. (1996). Imaging of hydrogen peroxide generation in cultured cells using dicholorofluorescein derivatives. *SPIE* **2678**, 129-140.

Holaday, D. A. and Smith, F. R. (1981). Clinical characteristics and biotransformation of sevoflurane in healthy human volunteers. *Anesthesiology* **54**, 100-106.

HPA. (2010). General cell collection: C2C12, vol. 2010 (ed., pp. Information on the murine myoblast cell line C2C12 (ECACC number: 91031101): Health Protection Agency.

Huang, N. F., Patel, S., Thakar, R. G., Wu, J., Hsiao, B. S., Chu, B., Lee, R. J. and Lee, S. (2006). Myotube assembly on nanofibrous and micropatterned polymers. *Nano Letters* **6**, 537-542.

Huang, Y.-C., Dennis, R. G., Larkin, L. and Baar, K. (2005). Rapid formation of functional muscle in vitro using fibrin gels. *Journal of Applied Physiology*, 706-713.

Huber, A., Pickett, A. and Shakesheff, K. M. (2007). Reconstruction of spatially oriented myotubes *in vitro* using electrospun, parallel microfibre arrays. *European Cells and Materials* **14**, 56-63.

Huxley, A. F. (1974). Muscular Contraction. *Journal of Physiology* **243**, 1-43.

Huxley, A. F. and Neidergerke, R. (1958). Measurement of the striations of isolated muscle fibres with interference microscopy. *Journal of Physiology* **144**, 403-425.

Hynes, R. O. (1987). Integrins: A family of cell surface receptors. *Cell* **48**, 549-554.

Hynes, R. O. (1992). Integrins: Versatility, modulation, and signaling in cell adhesion. *Cell* **69**, 11-25.

Hynes, R. O. (2002). Integrins: Bidirectional allosteric signaling molecules. *Cell* **110**, 673-687.

Jayawarna, V., Ali, M., Jowitt, T. A., Miller, A. F., Saiani, A., Gough, J. E. and Ulijn, R. V. (2006). Nanostructured hydrogels for three-dimensional cell culture through self-assembly of fluorenylethoxycarbonyl-dipeptides. *Advanced Materials* **18**, 611-614.

Jejurikar, S. S., Henkelman, E. A., Cederna, P. S., Marcelo, C. L., Urbanchek, M. G. and Juzon, W. M. (2006). Aging increases the susceptibility of skeletal muscle derived satellite cells to apoptosis. *Experimental Gerontology*, 828-836.

Kharasch, E. D., Armstrong, A. s., Gunn, K., Artru, A., Cox, K. and Karol, M. D. (1995a). Clinical sevoflurane metabolism and disposition: II. The role of cytochrome P450 in fluoride and hexafluoroisopropanol formation. *Anesthesiology* **82**, 1379-1388.

Kharasch, E. D., Karol, M. D., Lanni, C. and Sawchuk, R. (1995b). Clinical sevoflurane metabolism and disposition: I. Sevoflurane and metabolite pharmokinetics. *Anesthesiology* **82**, 1369-1378.

Kim, K., Yu, M., Zong, X., Chiu, J., Fang, D., Seo, Y.-S., Hsiao, B. S., Chu, B. and Hadjiargyrou, M. (2003). Control of degradation rate and hydrophillicity in electrospun non-woven poly(D,L-lactide) nanofiber scaffolds for biomedical applications. *Biomaterials* **24**, 4977-4985.

Kim, T. G. and Park, T. G. (2006). Surface functionalized electrospun biodegradable nanofibres for immobilisation of bioactive molecules. *Biotechnology Progress* **22**, 1108-1113.

Kumbar, S. G., Nukavarapu, S. P., James, R., Nair, L. S. and Laurencin, C. T. (2008). Electrospun poly(lactic acid - co - glycolic acid) scaffolds for skin tissue engineering. *Biomaterials* **29**, 4100-4107.

Lakhe-Reddy, S., Khan, S., Konieczkowski, M., Jared, G., Wu, K. L., Reichardt, L. F., Takai, Y., Bruggeman, L. A., Wang, B., Sedor, J. R. et al. (2006). Beta8 integrin binds rho GDP dissociation inhibitor-1 and activates rac-1 to inhibit mesangial cell myofibroblast differentiation. *The Journal of Biological Chemistry* **281**, 19688-19699.

Lam, M. T., Huang, Y.-C., Birla, R. K. and Takayama, S. (2009). Microfeature guided skeletal muscle tissue engineering for highly organised 3-dimensional free-standing constructs. *Biomaterials* **30**, 1150-1155.

Lee, M., Chen, T. T., Irvela-Arispe, M. L., Wu, B. M. and Dunn, J. C. Y. (2007). Modulation of protein delivery from modular polymer scaffolds. *Biomaterials* **28**, 1862-1870.

Lehnert, D., Wehrle-Haller, B., David, C., Weiland, U., Ballestrem, C., Imhof, B. A. and Bastmeyer, M. (2004). Cell behaviour on micropatterned substrata: limits of extracellular matrix geometry for spreading and adhesion. *Journal of Cell Science*, 41-52.

Levenberg, S., Rouwkema, J., Macdonald, M., Garfein, E. S., Kohane, D. S., Darland, D. C., Marini, R., Blitterswijk, C. A. v., Mulligan, R. C., D'Amore, P. A. et al. (2005). Engineering vascularised skeletal muscle tissue. *Nature Biotechnology* **23**, 879-884.

Levi-Mishali, M., Zoldan, J. and Levenberg, S. (2009). Effect of scaffold stiffness on myoblast differentiation. *TIssue Engineering part A* **15**, 935-944.

Li, M., Mondrinos, M. J., Chen, X., Gandhi, M. R., Ko, F. K. and Lelkes, P. I. (2006). Co-electrospun poly(lactide-co-glycolide), gelatin, and elastin blends for tissue engineering scaffolds. *Journal of Biomedical Materials Research Part A*.

Li, W.-J., Mauck, R. L., Cooper, J. A., Yuan, X. and Tuan, R. S. (2007). Engineering controllable anisotropy in electrospun biodegradable nanofibrous scaffolds for musculoskeletal tissue engineering. *Journal of Biomechanics* **40**, 1686-1693.

Lloyd, C. M., Berendse, M., Lloyd, D. G., Schevzov, G. and Grounds, M. D. (2004). A novel role for non muscle gamma-actin in skeletal muscle sarcomere assembly. *Experimental Cell Research* **297**, 82-96.

Lu, L., Garcia, C. A. and Mikos, A. G. (1999). *In vitro* degradation of thin poly(DL-lactide-co-glycolic acid) films. *Journal of Biomedical Materials Research Part A* **46**, 236-244.

Marieb, E. N. (2001). Human Anatomy and Physiology: Benjamin Cummings.

Marino, J. S., Tausch, B. J., Dearth, C. L., Manacci, M. V., McLaughlin, T. J., Rakyta, S. J., Linsenmayer, M. P. and Pizza, F. X. (2008). Beta 2 integrins contribute to skeletal muscle hypertrophy in mice. *Americal Journal of Cell Physiology* **295**, C1026-C1036.

Mauro, A. (1961). Satellite cell of skeletal muscle fibres. *Journal of Biophysical and Biochemical Cytology* **9**, 493-495.

Mayer, U. (2003). Integrins: Redundant or important players in skeletal muscle? *The Journal of Biological Chemistry* **278**, 14587-14590.

Milner, K. R. and Siedlecki, C. A. (2007). Submicron poly(L-lactic acid) pillars affect fibroblast adhesion and proliferation. *Journal of Biomedical Materials Research Part A* **82A**, 80-91.

Mobley, A. K., Tchaicha, J. H., Shin, J., Hossain, M. G. and McCarty, J. H. (2009). Beta8 integrin regulates neurogenesis and neurovascular homeostatis in the adult brain. *Journal of Cell Science* **122**, 1842-1851.

Motlagh, D., Yang, J., Antonio, K. Y., Webb, R. and Ameer, G. A. (2006). Hemocompatibility evaluation of poly(glycerol-sebacate) in vitro for vascular tissue engineering. *Biomaterials*, 4315-4324.

Nag, A. C. and Foster, J. D. (1981). Myogenesis in adult mammalian skeletal muscle *in vitro*. *Journal of Anatomy* **132**, 1-18.

Nam, J., Huang, Y., Agarwal, S. and Lannutti, J. (2008). Materials selection and residual solvent retention in biodegradable electrospun fibres. *Journal of Applied Polymer Science* **107**, 1547-1554.

Nath, D., Slocombe, P. M., Webster, A., Stephens, P. E., Docherty, A. J. P. and Murphy, G. (2000). Meltrin gamma (ADAM-9) mediates cellular adhesion through alpha6 beta1 integrin, leading to a marked induction of fibroblast cell motility. *Journal of Cell Science* **113**, 2319-2328.

Niinomi, M. (2008). Mechanical biocompatibilities of titanium alloys for biomedical applications. *Journal of the mechanical behaviour of biomedical materials* **1**, 30-42.

Nondrot, E. F., Anand, M., Sircar, M. and Finnemann, S. C. (2006). Novel role for alphaVbeta5-integrin in retinal adhesion and its durinal peak. *American Journal of Physiology and Cell Physiology* **290**, C1256-C1262.

Pan, H., Jiang, H. and Chen, W. (2008). The biodegradablilty of electrospun Dextran/PLGA scaffold in a fibroblast/macrophage co-culture. *Biomaterials*, 1583-1592.

Pardo, J. V., Siliciano, J. D. A. and Craig, S. W. (1983a). A vinculin-containing cortical lattice in skeletal muscle: transverse lattice elements ("costameres") mark sites of

attachment between myofibrils and sarolemma. *Proceedings of the National Academy of Science USA* **80**, 1008-1012.

Pardo, J. V., Siliciano, J. D. A. and Craig, S. W. (1983b). Vinculin is a component of an extensive network of myofibril-sarcolemma attachment regions in cardiac muscle fibres. *The Journal of Cell Biology* **97**, 1080-1088.

Park, H., Lee, J. W., Park, K. E., Park, W. H. and Lee, K. Y. (2010). Stress response of fibroblasts adherent to the surface of plasma-treated poly(lactic-co-glycolic acid) nanofibre matrices. *Colloids and Surfaces B: Biointerfaces* **77**, 90-95.

Peckham, M. (2008). Engineering a multinucleated myotube, the role of the actin cytoskeleton. *Journal of Microscopy* **231**, 486-493.

Ratner, B. D., Hoffman, A. S., Schoen, F. J. and Lemons, J. E. (2004). Biomaterials Science An introduction to materials in medicine, (ed. San Diego and London: Elsevier Academic Press.

Reeves, N. D., Narcini, M. V. and Maganaris, C. N. (2004). Effect of resistance training on skeletal muscle-specific force in elderly humans. *Journal of Applied Physiology* **96**, 885-892.

Ren, K., Crouzier, T., Roy, C. and Picart, C. (2008). Polyelectrolyte multilayer films of controlled stiffness modulate myoblast differentiation. *Advanced Functional Materials*, 1378-1389.

Ren, K., Fourel, L., Rouviere, C. G., Albige-Rizo, C. and Picart, C. (2010). Manipulation of the adhesive behaviour of skeletal muscle cells on soft and stiff polyelectrolyte multilayers. *Acta Biomaterialia* **Article In Press**.

Riboldi, S. A., Sampaolesi, M., Neuenschwander, P., Cossu, G. and Mantero, S. (2005). Electrospun degradable polyesterurethane membranes: potential scaffolds for skeletal muscle tissue engineering. *Biomaterials*, 4606-4615.

Rotherburger, M., Volker, W., Vischer, P., Berendes, E., Glasmacher, B., Scheld, H. H. and Derwick, M. (2002). Tissue engineering of hear valves: formation of a three-dimensional tissue using porcine heart valve cells. *ASAIO Journal* **48**, 586-591.

Sastry, S. K., Lakonishok, M., Thomas, D. A., Muschler, J. and Horwitz, A. F. (1996). Integrin alpha subunit ratios, cytoplasmic domains, and growth factor synergy regulate muscle proliferation and differentiation. *The Journal of Cell Biology* **133**, 169-184.

Schiffino, S. and Partridge, T. (2008). Skeletal Muscle Repair and Regeneration. In *Advances in Muscle Research*, vol. 3 (ed. G. J. M. Stienen): Springer.

Schnapp, L. M., Hatch, N., Ramos, D. M., Klimanskaya, I. V., Sheppard, D. and Pytela, R. (1995). The human integrin alpha 8 beta 1 functions as a receptor for tenascin, fibronectin, and vitronectin. *The Journal of Biological Chemistry* **270**, 23196-23202.

Schultz, E., Jaryszak, D. L. and Valliere, C. R. (1985). Response of satellite cells to focal skeletal muscle injury. *Muscle and Nerve* **8**, 217-222.

Senetar, M. A., Moncman, C. L. and McCann, R. O. (2007). Talin2 is induced during striated muscle differentiation and is targeted to stable adhesion complexes in mature muscle. *Cell Motility and the Cytoskeleton*, 157-173.

Shekaran, A. and Garcia, A. J. (2010). Nanoscale engineering of extracellular matrix-mimetic bioadhesive surfaces and implants for tissue engineering. *Biochimica et Biophysica Acta (BBA) - General Subjects* **In Press, Corrected Proof**.

Siegel, A. L., Atchison, K., FIsher, K. E., Davis, G. E. and Cornelison, D. D. W. (2009). 3D timelapse analysis of satellite cell motility. *Stem Cells* **27**, 2527-2538.

Sigma-Aldrich. (2010). Sigma-Aldrich Cell Culture Manual (ed.

Sinanan, A. C. M., Machell, J. R. A., Wynne-Hughes, G. T., Hunt, N. P. and Lewis, M. P. (2008). Alphavbeta3 and alphavbeta5 integrins and their role in muscle precursor cell adhesion *Biology of the Cell* **100**, 465-477.

Smit, E., Buttner, U. and Sanderson, R. D. (2005). Continuous yarns from electrospun fibres. *Polymer* **46**, 2419-2423.

Srouji, S., Kizhner, T., Suss-tobi, E., Livne, E. and Zussman, E. (2008). 3-D nanofibrous electrospun multilayered construct is an alternative ECM mimicking scaffold. *Journal of Materials Science: Materials in Medicine*, 1249-1255.

Stankus, J. J., Guan, J., Fujimoto, K. and Wagner, W. R. (2006). Microintegrating smooth muscle cells into a biodegradable, elastomeric fibre matrix. *Biomaterials* **27**, 735-744.

Subbiah, T., Bhat, G. S., Tock, R. W., Parameswaran, S. and Ramkumar, S. S. (2004). Electrospinning of nanofibres. *Journal of Applied Polymer Science* **96**, 557-569.

Sun, M.-Z. and Downes, S. (2009). Physicochemical characterisation of novel ultra-thin biodegradable scaffolds for peripheral nerve repair. *Journal of Materials Science: Materials in Medicine* **20**, 1181-1192.

Sundback, C. A., Shyu, J. Y., Wang, Y., Faquin, W. C., Langer, R. S., Vacanti, J. P. and Hadlock, T. A. (2005). Biocompatibility analysis of poly(glycerol sebacate) as a nerve guide material. *Biomaterials* **26**, 5454-5464.

Tatsumi, R. and Allen, R. E. (2004). Active hepatocyte growth factor is present in skeletal muscle extracellular matrix. *Muscle and Nerve* **30**, 654-658.

Tatsumi, R., Anderson, J. E., Nevoret, C. J., Halevy, O. and Allen, R. E. (1998). HGF/SF is present in normal adult skeletal muscle and is capable of activating satellite cells. *Developmental Biology* **194**.

Theron, A., Zussman, E. and Yarin, A. L. (2001). Electrostatic field-assisted alignment of electrospun nanofibres. *Nanotechnology* **12**, 384-390.

Tian, H., Bharadwaj, S., Liu, Y., Ma, H., Ma, P. X., Atala, A. and Zhang, Y. (2010). Myogenic differentiation of human bone marrow mesenchymal stem cells on a 3D nanofibrous scaffold for bladder tissue engineering. *Biomaterials* **31**, 870-877.

Tiger, C.-F., Fougerousse, F., Grundstrom, G., Velling, T. and Gullberg, D. (2001). Alpha11 Beta1 integrin is a receptor for interstitial collagens involved in cell migration and collagen reorganisation on mesenchymal nonmuscle cells. *Developmental Biology* **237**, 116-129.

Vandenberg, H. H., Karlisch, P. and Farr, L. (1988). Maintenance of highly contractile tissue-cultured avian skeletal muscle in collagen gel. *In Vitro Cellular and Developmental Biology* **24**, 166-174.

Vargas, C. D., Aballea, A., Rodrigues, E. C., Reilly, K. T., Mercier, C., Petruzzo, P., Dubernard, J. M. and Singu, A. (2009). Re-emergence of hand muscle representations in human motor cortex after hand allograft. *Proceedings of the National Academy of Science USA* **106**, 7197-7202.

Velling, T., Kusche-Gullberg, M., Sejersen, T. and Gullberg, D. (1999). cDNA cloning and chromosomal localization of human alpha11 integrin: A collagen-binding, I domain containing, beta1 associated integrin alpha chain present in muscle tissues. *The Journal of Biological Chemistry* **274**, 25735-25742.

Vey, E., Roger, C., Meehan, L., Booth, J., Claybourn, M., Miller, A. F. and Saiani, A. (2008). Degradation mechanism of poly(lactic-co-glycolic) acid block copolymer cast films in phosphate buffer solution. *Polymer Degradation and Stability* **93**, 1869-1876.

Vinay, D. S. and Kwon, B. S. (2010). $CD11c^{+}CD8^{+}$ T cells: Two-faced adaptive immune regulators. *Cellular Immunology* **264**, 18-22.

Vindigni, V., Mazzoleni, F., Rossini, K., Fabbian, M., Zanin, M. E., Bassetto, F. and Carraro, U. (2004). Reconstruction of ablated rat rectus abdominis by muscle regeneration. *Plastic and Reconstructive Surgery* **114**, 1509-1515.

Vorup-Jensen, T., Ostermeier, C., Shimaoka, M., Hommel, U. and Springer, T. A. (2003). Structure and allosteric regulation of the alphaXbeta2 integrin I domain. *Proceedings of the National Academy of Science USA* **100**, 1873-1878.

W. Wang, H. P., K. Murray, B. S. Jefferson, and Y. Li. (2009). Matrix Metalloproteinase-1 promotes muscle cell migration and differentiation. *The American Journal of Pathology* **174**, 541-549.

Wakelam, M. J. (1985). The fusion of myoblasts. *Biochemical Journal* **228**, 1-12.

Wang, H. and Joseph, J. A. (1999). Quantifying cellular oxidative stress by dicholorofluorescein assay using microplate reader. *Free Radical Biology and Medicine* **27**, 612-616.

Wang, H. B., Mullins, M. E., Cregg, J. M., Hurtado, A., Oudega, M., Trombley, M. T. and Gilbert, R. J. (2009). Creation of highly aligned electrospun poly-L-lactide acid fibres for nerve regeneration applications. *Journal of Neural Engineering* **6**, 016001 (15pp).

Wang, X. H., Li, D. P., Wang, W. J., Feng, Q. L., Chu, F. Z., Xu, Y. X. and Song, X. H. (2003). Covalent immobilisation of chitosan and heparin on PLGA surface. *International Journal of Biological Macromolecules* **33**, 99-100.

Wang, Y., Ameer, G. A., Sheppard, B. J. and Langer, R. (2002). A tough biodegradable elastomer. *Nature Biotechnology* **20**, 602-606.

Xin, X., Hussain, M. and Mao, J. (2006). Nanomechanical properties of electrospun PLGA nanofibres. *MCB* **3**, 187-188.

Xu, C., Yang, F., Wang, S. and Ramakrishna, S. (2004). In vitro study of human vascular endothelial cell function on materials with various surface roughness. *Journal of Biomedical Materials Research Part A* **71A**, 154-161.

Yablonka-Reuveni, Z. and Rivera, A. J. (1997). Influence of PDGF-BB on proliferation and transition through the MyoD-myogenin-MEF2A expression program during myogenesis in mouse C2 myoblasts. *Growth Factors* **15**, 1-27.

Yaffe, D. and Saxel, O. (1977). Serial passaging and differentiation of myogenic cells isolated from dystrophic mouse muscle. *Nature* **270**, 725-727.

Yamoto, D. L., Csikasz, R. I., Li, Y., Sharma, G., Hjort, K., Karlsson, R. and Bengtsson, T. (2008). Myotube formation on micropatterned glass: intracellular organisation and protein distribution in C2C12 skeletal muscle cells. *Journal of Histochemistry and Cytochemistry* **56**, 881-892.

Yao, C.-C., Ziober, B. L., Sutherland, A. E., Mendrick, D. L. and Kramer, R. H. (1996). Laminins promote the locomotion of skeletal myoblasts via the alpha 7 integrin receptor. *Journal of Cell Science* **109**, 3139-3150.

Yoon, J., Ponikau, J. U., Lawrence, C. B. and Kita, H. (2008). Innate antifungal immunity of human eosinophils mediated by beta2 integrin, CD11b. *Journal of Immunology* **181**, 2907-2915.

Zammit, P. S., Partridge, T. A. and Yablonka-Reuveni, Z. (2006). The skeletal muscle satellite cell: the stem cell that came in from the cold. *Journal of Histochemistry and Cytochemistry* **54**, 1177-1191.

Zhou, M., Smith, A. M., Das, A. K., Hodson, N. W., Collins, R. F., Ulijn, R. V. and Gough, J. E. (2009). Self-assembled peptide-based hydrogels as scaffolds for anchorage-dependent cells. *Biomaterials* **30**, 2523-2530.

Zhu, A. P., Fang, N., Chan-Park, M. B. and Chan, V. (2006). Adhesion contact dynamics of 3T3 fibroblasts on poly(lactide-co-glycolic acid) surface modified by photochemical immobilisation of biomacromolecules. *Biomaterials* **27**, 2566-2576.

Zong, X., Bien, H., Chung, C.-Y., Yin, L., Fang, D., Hsiao, B. S., Chu, B. and Entcheva, E. (2005). Electrospun fine-textured scaffolds for heart tissue constructs. *Biomaterials* **26**, 5330-5338.

Zong, X., Ran, S., Kim, K.-S., Fang, D., Hsiao, B. S. and Chu, B. (2003). Structure and morphology changes during in Vitro degradation of electrospun poly(glycolide-co-lactide) nanofibre membrane. *Biomacromolecules*, 416-423.